Calsyntenin1-Dependent Vesicular Trafficking is an Important Regulator of Axonal Behavior at Choice Points

---

Dissertation

zur

Erlangung der naturwissenschaftlichen Doktorwürde
(Dr. sc. nat.)

vorgelegt der

Mathematisch-naturwissenschaftlichen Fakultät

der

Universität Zürich

von

Tobias Andreas Alther

von

St. Gallen SG

Promotionskomitee

Prof. Dr. Esther T. Stoeckli (Vorsitz und Leitung der Dissertation)
Prof. Dr. Jean-Marc Fritschy
Prof. Dr. Dieter Zimmermann

Zürich, 2014

Table of content

1. Summary 3
2. Zusammenfassung 4
3. Introduction 5
3.1. Axon guidance 5
3.1.1. Classical axon guidance molecules 9
3.1.2. Other axon guidance molecules 12
3.2. Intracellular trafficking and axonal transport 16
3.2.1. RabGTPases and RabGDI 16
3.2.2. SNAREs 19
3.2.3. Axonal transport and kinesin motors 19
3.3. Calsyntenins 20
3.4. Chicken as a model organism and its features 23
3.4.1. Commissural neurons 24
3.4.2. The main nerves of the chicken hind limb 25
3.4.3. Motor neurons 25
3.4.4. Sensory neurons 26
3.4.5. Dermomyotome 27
3.4.6. Cerebellum 27
3.4.7. RNA interference 28
3.4.8. In ovo RNAi 29
3.5. Aim of my thesis 30
4. Manuscripts 31
4.1. Calsyntenins and APP are Expressed in a Dynamic and Similar Manner in the Chicken Embryo 31

4.2. Calsyntenin1-Mediated Trafficking of Axon Guidance Receptors Regulates the Switch in Axonal Responsiveness at Choice Points 53
5. Supplementary data 90
5.1. Supplementary results 90
5.2. Supplementary methods 104
6. Discussion and outlook 106
6.1. Calsyntenins are expressed in a distinct and partially overlapping pattern during development 106
6.2. Vesicular trafficking: a way to regulate guidance cue surface expression and a role for Cst1 in commissural axon guidance 107
6.3. A role for Calsyntenins in the floor plate? 110
6.4. Calsyntenins are required for neural circuit formation outside the CNS 111
6.5. Calsyntenin as linker protein between kinesin and vesicles and its function synaptic plasticity 112
6.6. A role for Calsyntenin in brain disorders? 113
7. References 114
8. Appendix 124
9. Acknowledgments 131
10. Curriculum vitae 132
11. Plagiarism disclaimer 133

1. Summary

During the development of the nervous system, growing axons must find their correct targets in order to form a functional neural network. If neural circuit formation is hampered, brain diseases, such as autism spectrum disorders, schizophrenia, or mental retardation can be the result. In order to understand the molecular background of these diseases, we must understand how growing nerve fibers are led to their target cells. The dorsal commissural neurons are a well-established model system to investigate the molecular mechanisms of axon guidance, as their axons always grow in a stereotypic and characteristic manner. Axons extend from the dorsal location of the cell bodies to the ventral midline, where they cross the floor plate and then, after a sharp turn, grow in rostral direction along the contralateral floor-plate border. Along their trajectory growing axons are guided by so-called guidance cues, which either attract or repel them. In order to respond to these cues, the tips of the axons, called growth cones, must carry distinct receptors on their surface.

In my thesis, I show that intracellular trafficking is a crucial regulatory mechanism for axon guidance by delivering specific receptors to the growth cone surface. Calsyntenin1, a transmembrane protein expressed in growth cones, links vesicles containing distinct cargo to kinesin motors and is thus involved in fast anterograde axonal transport. We identified Calsyntenin1 as a co-regulator of floor-plate exit and the contralateral turning decision of dorsal commissural axons. Calsyntenin1 is involved in the regulation of surface levels of two particular guidance cues, Robo1 and Fzd3.

2. Zusammenfassung

Während der Entwicklung des Nervensystems müssen die auswachsenden Axone die richtigen Zielzellen finden, um ein korrekt verbundenes Netzwerk bilden zu können. Wenn sich diese neuronalen Netzwerke nicht richtig ausbilden, kann das zu Krankheiten des Gehirns führen, wie beispielsweise zu Autismus, zu Schizophrenie oder zu geistiger Behinderung. Damit wir die molekularen Hintergründe dieser Krankheiten verstehen, ist es unabdingbar, auch zu verstehen, wie auswachsende Nervenfasern zu den richtigen Zielzellen geführt werden. Die dorsalen Kommissurualneurone sind ein etabliertes Modellsystem, um die molekularen Mechanismen der axonalen Wegfindung zu untersuchen. Kommissuralaxone wachsen entlang einem stereotypen und charakteristischen Pfad von der dorsalen Lage der Zellkörper zur ventralen Mittellinie, überqueren diese und wachsen anschliessend Richtung Kopf. Die auswachsenden Axone werden primär durch sogenannte *guidance cues* (Wegweisermoleküle) gesteuert, welche entweder attraktiv oder repulsiv auf die auswachsenden Nervenfasern wirken. Damit Axone auf diese *guidance cues* antworten können, müssen die Spitzen der Axone (sog. Wachstumskegel) bestimmte Rezeptoren auf ihrer Oberfläche tragen. Die Expression dieser Rezeptoren wiederum muss sorgfältig reguliert werden. In dieser Arbeit konnte ich zeigen, dass intrazellulärerer Vesikel-Transport ein essentieller Regulations-mechanismus für axonale Wegleitung ist, um spezifische Rezeptoren an die Oberfläche der Wachstumskegel abzuliefern. Calsyntenin1, ein Transmembran-protein, welches in Wachstumskegeln vorkommt, verbindet Vesikel, die bestimmte Fracht enthalten, mit Kinesin-Motoren. Auf diese Weise ist Calsyntenin in den schnellen anterograden Vesikeltransport in Axonen involviert. Ich konnte zeigen, dass Calsyntenin-1 eine wichtige Rolle im Transport von zwei spezifischen Rezeptoren, Robo1 und Fzd3, spielt.

3. Introduction

Our brain makes us humans what we are. It allows us to think, create and question things and therefore is probably the most important tool to do science. A decade ago, I was recovering from a serious brain surgery and ever since I have found the nervous system a most fascinating subject. It is astonishing how the several billions of neurons in our nervous system form functional units by going through a series of processes such as proliferation, differentiation, connectivity and maturation.

3.1. Axon guidance

During development, when the nervous system forms, neurons must wire up. The field that investigates these processes is called axon guidance research. As the basic principles of axon guidance are highly conserved and therefore the same in our brains as in simple neuronal circuits of certain invertebrates, neuroscientists use model organisms to study it. Axons (gr. axis) are neuronal projections that link neurons with their target cells. In the developing neuronal tissue, axons need to find their pathways and to recognize their synaptic partners in order to establish a correctly wired and functioning system. The outgrowing axons' tips are called growth cones (Figure 1). This hand-like structure steers the axons to their targets by interacting with guidance cues found in the environment, which can be attractive or repulsive and act at long or short range (Dickson, 2002). The Spanish physician Santiago Ramón y Cajal (1852–1934) was the first to describe growing axons. He already hypothesized in the late 19th century that their tips (he called them "cono de crecimiento" – growth cones) may sense chemical cues from the environment (Cajal, 1892). Technical limitations of that time did not allow him to test his hypothesis and it took another hundred years for scientists to come to a greater understanding of the underlying molecular mechanisms of axon guidance.

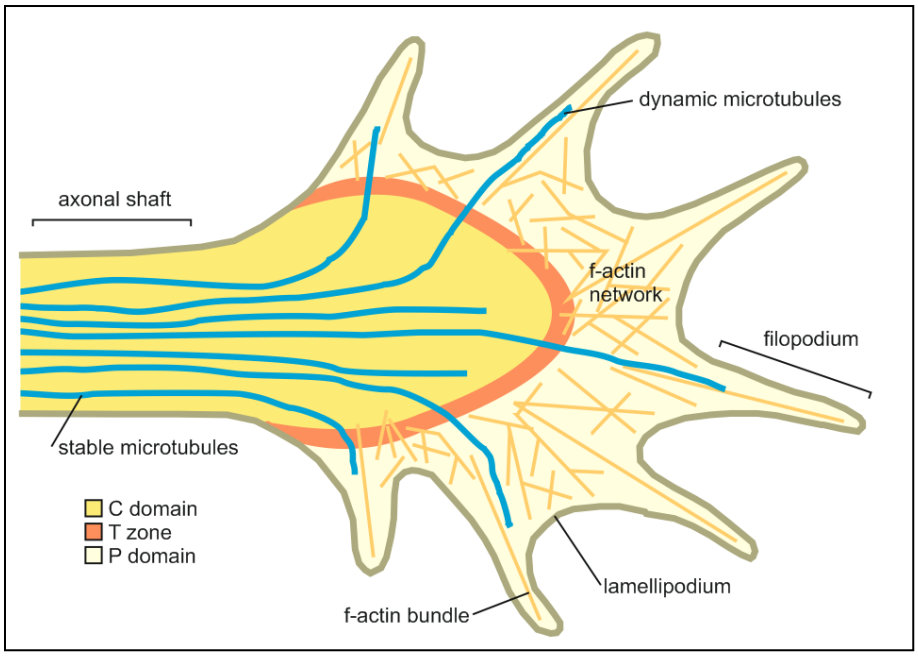

Figure 1: schematic drawing of a growth cone. Receptors on the growth cone surface probe the environment for guidance information.

The hand-like morphology of the growth cone is fundamental to its function. The fine finger-like extensions (filopodia) contain bundles of actin filaments (F-actin) and carry receptors and cell adhesion molecules on their surface. Lamellipodia contain a dense cross-linked actin meshwork. The axonal shaft is mainly composed of microtubules and intermediate filaments. A growth cone can be divided in three regions: the peripheral (P) domain, the transitional (T) domain, and the central (C) domain. The P domain is composed of highly dynamic lamellipodia and filopodia. A few microtubule bundles usually enter this zone. The C domain is mainly built by microtubules, is thicker and located in the center of the growth cone close to the axon. It also contains organelles such as mitochondria and vesicles. The zone between P and C domain is called T domain (Geraldo and Gordon-Weeks, 2009). The growth cone's actin network is constantly influenced by the environment. Surrounding guidance cues trigger the dynamic extension and retraction of filopodia by promoting polymerization or depolymerization of the cytoskeleton. A gradient of guidance cues activates asymmetrical cytoskeletal changes in the growth cone and thus triggers a turn of the navigating axon (Dickson, 2002).

Axon guidance is achieved by four different molecular mechanisms and is influenced by guidepost cells or intermediate targets and the possibility of (de)fasciculation with axon tracts. Long-range cues are secreted diffusible molecules that attract or repel

axons over distance (chemoattraction and chemorepulsion). Short-range cues directly interact with the axons by contact-mediated mechanisms which involve non-diffusible cell surface molecules. The main axon guidance molecules and their interaction partners are summarized in Figure 2. In order to be able to grow, axons need a substrate that is both adhesive and permissive for growth (Tessier-Lavigne and Goodman, 1996). Along the axon's trajectory, the growth cone faces changing environmental factors. If growth cones reach a choice point, the balance between positive and negative cues determines growth into a certain direction, stalling, or collapsing (Stoeckli and Landmesser, 1998).

Molecules involved in axon guidance can be categorized in so-called classical guidance cues which include netrins, slits, semaphorins and ephrins. Molecules such as IgCAMs are other kinds of guidance cues, which, beside their function in axon guidance, also have functions in cell adhesion. A more recently discovered group of axon guidance molecules are the morphogens. Before, they were largely thought to act during early development in patterning only. Remarkably, today, most of the morphogens have been shown to play a role in axon guidance as well.

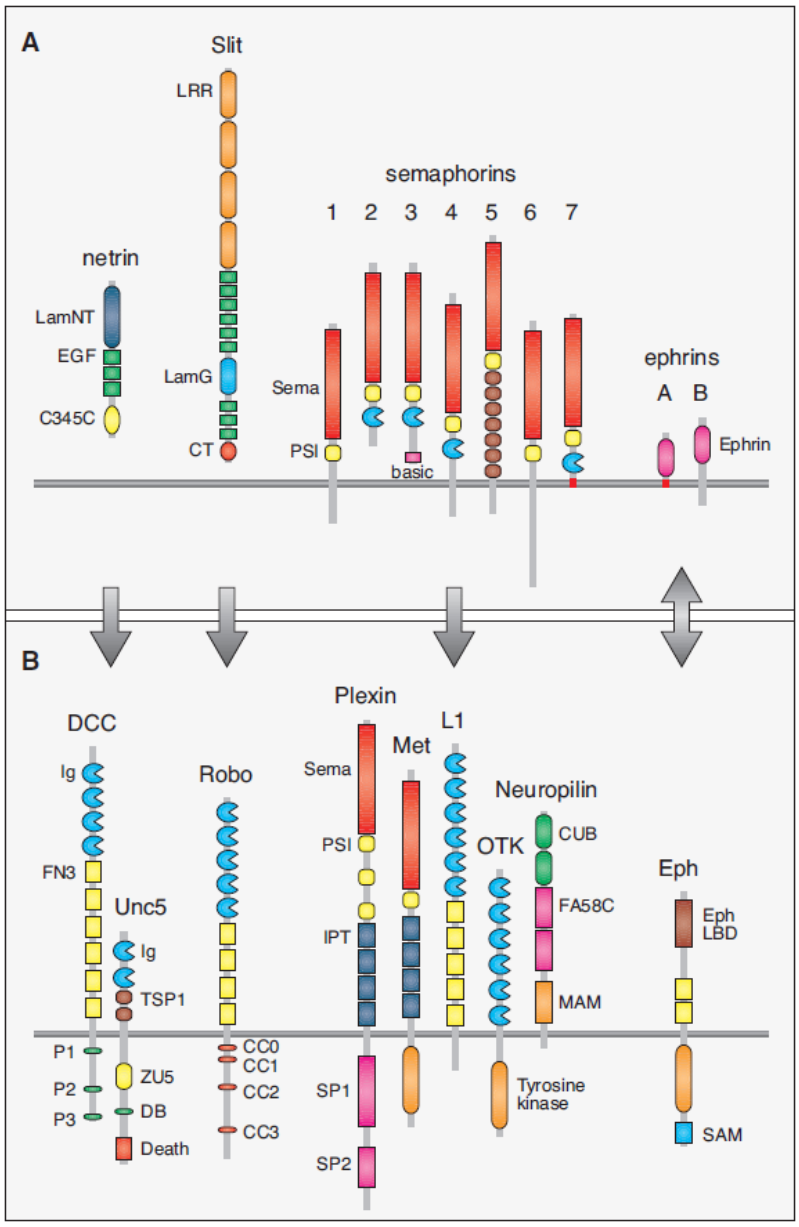

Figure 2: guidance molecules (A) and their receptors (B). A complex interaction of guidance molecules and their receptors steer the growth cone to its target. Protein domain names are from SMART (http://smart.embl-heidelberg.de). The figure is from Dickson (2002).

3.1.1. Classical axon guidance molecules

Netrin and DCC/UNC5

The first long-range attractive guidance cues that have been discovered belong to the netrin family. Netrins are secreted molecules that act as long-range cues and can act as attractant or repellent by binding to their receptors DCC or UNC5. Netrin was first identified in C. elegans and called UNC6 (Hedgecock et al., 1990). In vertebrates, they were detected as guidance cue for rodent commissural axons (Serafini et al., 1994). Up to date, four family members (Netrin-1, -3, -4 and –G1) are known in rodents and humans (Manitt and Kennedy, 2002). Depending on the receptor, Netrin acts mainly as an attractant (when interacting with DCC) or as a repellent (when interacting with UNC5 alone or with UNC5 together with DCC). In vertebrates, netrins secreted from the floor plate and the ventral spinal cord act as chemoattractants for commissural axons (Kennedy et al., 1994). However, studies in COS cells showed that netrin also acts a chemorepellent for trochlear motor axons (Colamarino and Tessier-Lavigne, 1995). Interestingly, mice lacking netrin do not display obvious defects in the trochelar motor axon guidance. These facts cliearly confirm the bifunctionality of netrin as both attractive and repulsive cue.

Slit and Robo

In contrast to netrins, the Slits/Robos were the first long-range axon guidance cues that have been discovered and identified as axonal repellents. Robos (roundabouts) are transmembrane proteins and act as receptors for Slits. They were first identified in Drosophila as regulators for midline crossing (Seeger et al., 1993). During neuronal development, Slit/Robo signaling is repulsive and determines the direction of pioneer axons in both invertebrates and vertebrates (Kidd et al., 1998; Brose et al., 1999). In vertebrates, three Slits (Holmes et al., 1998; Itoh et al., 1998; Yuan et al., 1999) and four Robos (Robo1, 2, Rig1/Robo3, Robo4) have been identified (Sundaresan et al., 2004). Except for Robo4, they are all expressed in the developing nervous system (Huminiecki et al., 2002). Robo1 and 2 consist of five immunoglobulin-like domains (binding sites for Slits), three fibronectin-like domains, a transmembrane domain and four C-terminal intracellular domains (Kidd et al., 1998; Vargesson et al., 2001). They are expressed in dorsal commissural axons and

transiently located at the growth-cones surface in order to mediate the repulsive effects of the Slits, which are expressed by the floor plate. Commissural growth cones express only very low levels of Robo protein as they grow towards the midline, but they dramatically upregulate their Robo levels once they cross and reach the opposite side. Ipsilateral projecting axons, in contrast, express high levels of Robo from the beginning on (Seeger et al., 1993; Kidd et al., 1999). Ipsilaterally projecting axons are inhibited from crossing, and post-crossing commissural axons from re-crossing the midline (Kidd et al., 1999). In Drosophila, comm (commissureless) was found to regulate Robo surface expression (Keleman et al., 2005). Comm is transiently expressed in contralaterally projecting neurons and its presence prevents the delivery of Robo to the growth cone surface. Only during floor-plate crossing, comm expression stops and Robo is no longer diverted to the late endocytic pathway. Thus, Robo is inserted into the growth-cone membrane and the floor-plate derived Slits force the axons out of the midline. Vertebrates do not have a comm ortholog (Guthrie, 2004). Instead, it was shown in chicken embryos that RabGDI has a similar function to comm as regulator of Robo1 surface levels (Philipp et al., 2012). RabGDI expression is in line with a role as regulator of Robo1: only when the axons enter and cross the floor plate, RabGDI is rapidly upregulated. Its downregulation mimicked the effects caused by the absence of Robo1 or negative cues associated to the floor plate. In vitro assays confirmed the role of RabGDI as a regulator of Robo1 surface expression and showed that Robo1 associates to Rab11-positive vesicles. The low amounts of Robo1 on the growth-cone surface before midline crossing (Mambetisaeva et al., 2005; Tamada et al., 2008) are inhibited by the Robo3 subtype Rig-1/Robo3.1. When commissural growth cones have crossed the floor plate, a switch in subtype expression from Rig-1/Robo3.1 to Rig-1/Robo3.2 abrogates the inhibition of Robo1 (Sabatier et al., 2004). Interestingly, recent studies showed that in flies, the comm-mediated regulation of axon outgrowth across the midline is independent of Rab function (Van den Brink et al., 2013).

Semaphorin and plexin/neuropilin

Another important group of axon guidance cues are the semaphorins. They are a large family of cell surface and secreted guidance molecules that function primarily

as axonal repellents. The first semaphorins were identified in grasshopper as guidance cue for Ti1 axons (Kolodkin et al., 1992) and as inducer of vertebrate sensory growth cone collapse (Luo et al., 1993). They are defined by a conserved Sema domain at the N-termini of the proteins and their structure allows dividing them into eight classes. Class 1 (transmembrane) and 2 (secreted) are found in invertebrates, classes 3 to 7 are vertebrate specific. Class 3 semaphorins encode secreted, class 4-6 transmembrane and class 7 GPI-anchored semaphorins. Semaphorins encoded by viruses are termed class V (Raper, 2000). Semaphorins signal by binding and activating complexes of cell-surface receptors. Transmembrane semaphorins (class 1 and 4-6) bind specifically to plexins, another large family of transmembrane molecules. Secreted semaphorins interact with receptor complexes including plexins and neuropilins, as neuropilins lack a signaling-competent cytoplasmic domain (Tamagnone and Comoglio, 2000; Dickson, 2002). Thus, plexins are receptors for multiple classes of semaphorins, either alone or in combination with neuropilins. According to their sequence similarity, plexins can be divided into four groups and include two members in invertebrate species (PlexA and PlexB) and nine members in vertebrates (plexinA1–plexinA4, plexinB1–plexinB3, plexinC1 and plexinD1) (Tamagnone et al., 1999). Receptor complexes can include additional components, such as members of the immunoglobulin superfamily of cell adhesion molecules (Zhou et al., 2008).

Eph and ephrin

Ephs are tyrosine kinase receptors and bind cell-surface tethered ephrin ligands in trans on opposing cells (Kullander and Klein, 2002). Sperry proposed in 1963 in his chemoaffinity hypothesis that vertebrate retinal axons are guided to their targets in the optic tectum by molecular gradients (Sperry, 1963). Only in the nineties, the search for these cues resulted in the identification of ephrins and Eph receptors (Cheng and Flanagan, 1994; Müller et al., 1996). There are two classes of ephrin proteins and they are defined by the way of membrane attachment. Ephrin-As are linked through a GPI anchor whereas ephrin-Bs have a transmembrane domain (Gale et al., 1996). Ephrin-As bind to EphA receptors and ephrin-Bs to EphB receptors. The only exception is EphA4 which can also bind ephrin-Bs (Wilkinson,

2001). Unlike most receptor tyrosine kinases, both ephrins and Eph receptors can transmit a signal. Bidirectional signaling by ephrins and Ephs is an important signaling contribution to cell-cell communication where each component can act as ligand and receptor (Holland et al., 1998). Up to date, several biological functions have been identified for ephrins and Eph receptors. In addition to axon guidance (Nakamoto et al., 1996), they have been shown to play roles in vascular development, boundary formation (Adams et al., 1999), and synaptic plasticity (Gao et al., 1998).

3.1.2. Other axon guidance molecules

IgCAM

Immunoglobulin cell adhesion molecules (IgCAMs) form a large group of membrane proteins that mediate adhesion between axons and thus induce axonal fasciculation. Their characteristic extracellular immunoglobulin-like domain consists of one or more folds of 60 – 80 specific amino acids. They can interact with each other in a homophilic or heterophilic manner, depending on the type of IgCAM. Many studies have demonstrated their capacity as promoter of fasciculation and neurite outgrowth (Payne and Lemmon, 1993; Burden-Gulley et al., 1995). The role of the IgCAMs has been investigated intensively in the chicken hind limb by Lynn Landmesser and colleagues (Landmesser et al., 1990), where they showed the importance of the polysialic acid component of NCAM. Later, Stoeckli and Landmesser found a role for NrCAM and NgCAM in neural circuit formation in the spinal cord. They could show that the interaction between axonin-1 and NrCAM induces commissural axons to enter the floor plate whereas in the absence of either one of them, the floor plate is less attractive. NgCAM was found to have no major role in guidance, but was shown to have an important role in maintaining the fasciculation of commissural axons (Stoeckli and Landmesser, 1995; Stoeckli et al., 1997).

Morphogens

Definitely no classical axon guidance molecules are the morphogens. Morphogen represent special signaling molecules that determine the pattern of tissue during

development and the positions of the various specialized cell types within a tissue. They are produced and secreted by particular sources and thus form concentration gradients. Depending on their local concentration, morphogens act directly on cells to induce specific cellular responses (Wolpert, 1989). Interestingly, developmental morphogens such as BMPs, Wnts and Hedgehogs turned all out to play a role in axon guidance.

BMP

Bone morphogenetic proteins (BMPs) are members of the transforming growth factors-β (TGFβ) superfamily and also known as cytokines and as metabologens (Reddi and Reddi, 2009). They were originally discovered as inducer of bone and cartilage formation and were shown to have a role in the patterning of the dorsal spinal cord as they are expressed in the roof plate (Lee and Jessell, 1999). Nowadays, they are known to orchestrate tissue architecture in the entire body (Bleuming et al., 2007). Besides these roles, BMPs act as repulsive guidance cues for commissural axons by repelling them from the dorsal spinal cord towards the floor plate (Augsburger et al., 1999). In mice, three BMPs are expressed in the roof plate: BMP7, BMP6 and GDF7. Butler and Dodd showed that the expression of both BMP7 and GDF7 by the roof plate is required for proper commissural axon growth. They also demonstrated that BMP7 and GDF7 heterodimerize in vitro and suggested that they have to work in common to act as repellent to push commissural axons ventrally (Butler and Dodd, 2003). The BMP signal is transduced by receptor complexes of type I and type II receptor serine/threonine kinases. After the binding of BMP, distinct proteins of the Smad family are phosphorylated and form heteromeric complexes. These complexes translocate to the nucleus and regulate specific target genes (Attisano and Wrana, 2002). In axon guidance, it remains unclear which intracellular pathways are regulated by BMP ligands. Sanchez and Bovolenta reported that type II BMP receptors regulate the actin cytoskeleton (Sánchez-Camacho and Bovolenta, 2009). Recent work of Zhou and colleagues showed that BMP2 induction of Smad1/5/8 phosphorylation was reduced in chondrocytes from neogenin mutant mice (Zhou et al., 2010).

Wnts and Fzd

The first Wnt has been discovered in Drosophila as a segment polarity gene involved in the formation of the body axis and was called wingless (Nüsslein-Volhard and Wieschaus, 1980). In parallel, a gene called Int1 was characterized from mouse tumor cells (Nusse and Varmus, 1982). When researchers realized that int and wingless refer to the same genes, the family was renamed and int1 became Wnt1. Up to date, many more components of the Wnt pathways have been identified and investigated (Klaus and Birchmeier, 2008). Wnts transmit signals via frizzled receptors (Fzd) to the inside of cells via mainly three different pathways: the canonical Wnt pathway, the non-canonical planar cell polarity (PCP) pathway, and the non-canonical Wnt/calcium pathway. All these pathways activate dishevelled (Dvl) in order to regulate gene transcription, cytoskeletal dynamics or calcium levels inside the cell (Gordon, 2006). Wnts were detected to be involved in post-crossing commissural axon guidance (Lyuksyutova et al., 2003). In the murine floor plate, Wnt4 is expressed in an anterior^{high} to posterior^{low} gradient and thus attracts post-crossing axons. As the downregulation of Fzd3 resulted in complete randomization of commissural axons after floor-plate crossing, Fzd3 and Wnt4 were suggested to interact, although no direct physical interaction between them has been shown (Lyuksyutova et al., 2003). Similarly, in the chicken embryo, Wnts were shown to influence the commissural axons' behavior after floor-plate crossing (Domanitskaya et al., 2010). Wnt5a and Wnt7a act as attractive cues in vivo, but unlike Wnt4 in mice, they are not expressed in a gradient along the floor plate. In the chicken, sonic hedgehog (shh), which is expressed in a gradient in the floor plate, induces an sfrp gradient that in turn blocks Wnt activity. Thus, an activity gradient of Wnt5a/7a (posterior^{low} to anterior^{high}) is formed that guides post-crossing axons rostrally (Domanitskaya et al., 2010). Wnt-induced axon guidance is promoted by the activation of the PI3K-atypical PKCζ and the PCP pathway that results in attraction (Avilés et al., 2013). When Fzd3 is phosphorylated by Dvl, the PCP pathway is inhibited and Fzd3 remains in the plasma membrane. Local Vangl2 expression in the filopodia of the growth cones inhibits Dvl, which as a result no longer phosphorylates Fzd3. Fzd3 is thus internalized and activates the PCP pathway (Wolf et al., 2008).

Sonic Hedgehog

The hedgehog gene was also identified in Drosophila as patterning controller of the body axis (Nüsslein-Volhard and Wieschaus, 1980). Besides desert hedgehog and Indian hedgehog, sonic hedgehog (Shh) is one of the three mammalian hedgehog family members (Pan et al., 2013). During patterning of the neural tube, Shh and Wnts act in an antagonistic manner: Shh is secreted from the floor plate and induces ventral cell fates, whereas Wnts (and BMPs) are expressed in the roof plate and determine dorsal cell fates (Dessaud et al., 2008; Ulloa and Martí, 2010). Like for the Wnts, a role for Shh in commissural axon guidance was found, too (Bourikas et al., 2005). Charron and colleagues demonstrated the chemoattractant activity of shh in parallel to netrin-1. Cyclopamine-mediated inhibition of the Shh signaling mediator smoothened (Smo) as well as the conditional knock out of Smo in commissural neurons confirmed that Shh, acting via Smo, is a midline-derived chemoattractant for commissural axons (Charron et al., 2003). Later Boc was identified as a co-receptor for Shh for attractive axon guidance effects (Okada et al., 2006). Interestingly, Shh was additionally shown to act as repulsive guidance cue for post-crossing commissural axons (Bourikas et al., 2005; Yam et al., 2012). Commissural axons must change their responsiveness to Shh when they cross the midline, which is achieved by the rapid change of distinct growth cone receptors. Pre-crossing commissural axons express Smo and Boc that mediate the attractive effect of Shh derived from the floor plate. Upon floor-plate contact, the transient expression of Hhip, which is induced by glypican-1 (Wilson and Stoeckli, 2013), mediates the repulsive response to Shh, probably together with a yet unknown co-receptor. As Shh is expressed in an anterior^{low} to posterior^{high} gradient, Shh pushes the commissural axons rostrally. This is supported by the Wnt5a/7a activity gradient that attracts them rostrally.

3.2. Intracellular trafficking and axonal transport

Intracellular protein and membrane trafficking is a basic process contributing to cellular communication and survival of every eukaryotic cell. It is required for proper organelle formation and maintenance. One way of communication between organelles or between organelles and the plasma membrane is through vesicular transport. This multi-step process includes vesicle budding, transport and fusion with the target. It requires the cooperation of a large number of different regulatory and motor proteins. Among those I would like to point out especially the Rab proteins. Other molecules that are critical for intracellular trafficking are the SNAREs and kinesin motor proteins which are also briefly discussed.

3.2.1. RabGTPases and RabGDI

Rab proteins form a large family of monomeric GTPases which operate as molecular switches. In the GTP-bound form, the Rab proteins act as effectors. Thereby GTP is hydrolyzed by the GTPase activating protein (GAP). In the GDP-bound form, they are inactive. Guanosin exchange factors (GEFs) catalyze the replacement of GDP by GTP, thus recycling the active form (Stenmark, 2009). There are more than 60 different RabGTPases in humans. They regulate membrane traffic, vesicle formation and membrane fusion by vesicular trafficking. In order to do so, they are localized to distinct intracellular compartments and are anchored to the membranes via a prenyl group linked to an amino acid (Zerial and McBride, 2001; Pfeffer and Aivazian, 2004). Rab4 is thought to be restricted to a role in sorting and recycling early endosomes (Van der Sluijs et al., 1992; Seabra et al., 2002) whereas Rab5 is shown to have a function in ligand sequestration (Zerial and McBride, 2001), early endosome motility and fusion (Nielsen et al., 1999). Rab11 is involved in recycling through perinuclear recycling endosomes and in the traffic from the plasma membrane to the Golgi apparatus (Ullrich et al., 1996; Trischler et al., 1999).

RabGDP-dissociation inhibitors (GDI) are evolutionarily conserved cytosolic proteins that bind prenylated GTPases in their inactive, GDP bound state, with high affinity. Thereby they extract RabGDP from the plasma membrane and deliver it back to its origin for recycling (Pfeffer et al., 1995; Pfeffer, 2001). RabGDI was first discovered

and characterized in the bovine brain (Sasaki et al., 1990). In the mammalian brain, two GDI isoforms (α and β) have been identified, in which GDI-β is ubiquitously expressed in contrast to GDI-α, that is predominantly found in neuronal tissue (Nishimura et al., 1994). In birds, only one isoform of the GDI gene, genetically similar to the mammalian GDI-α form, is known. It is expressed in a highly regulated manner in distinct neurons (Sedlacek et al., 1999; Philipp et al., 2012). It remains unclear how the recycling of Rab proteins for the constitutive vesicle formation and fusion is managed. At the donor membrane, RabGDI complexes are recognized by a Rab-specific GDI displacement factor (GDF). RabGDI releases the Rab protein for reactivation by GEF (Pfeffer et al., 1995). Suppression of RabGDI expression was associated with inhibited axonal outgrowth during embryonic development and mutations in the GDI1 gene (that encodes GDI-α) were found to be responsible for X-linked mental retardation (D'Adamo et al., 1998; Strobl-Wildemann et al., 2011). Furthermore, studies in GDI1-null mice revealed short-term memory deficits in adult mice that are thought to be causes by alterations of different synaptic vesicle recycling pathways (Bianchi et al., 2012). In the chicken embryo, RabGDI was shown to regulate Robo1-surface expression in dorsal commissural axons. The temporal expression is consistent with its role as a regulator of Robo1 expression as it appears at HH22, when the first dorsal commissural axons grow into the floor plate. Only in the presence of RabGDI, Robo1-positive vesicles are delivered to the growth cone surface. Thus, after RabGDI silencing, dorsal commissural axons stall in the floor plate (Philipp et al., 2012). The Rab- and RabGDI cycle is summarized in Figure 3.

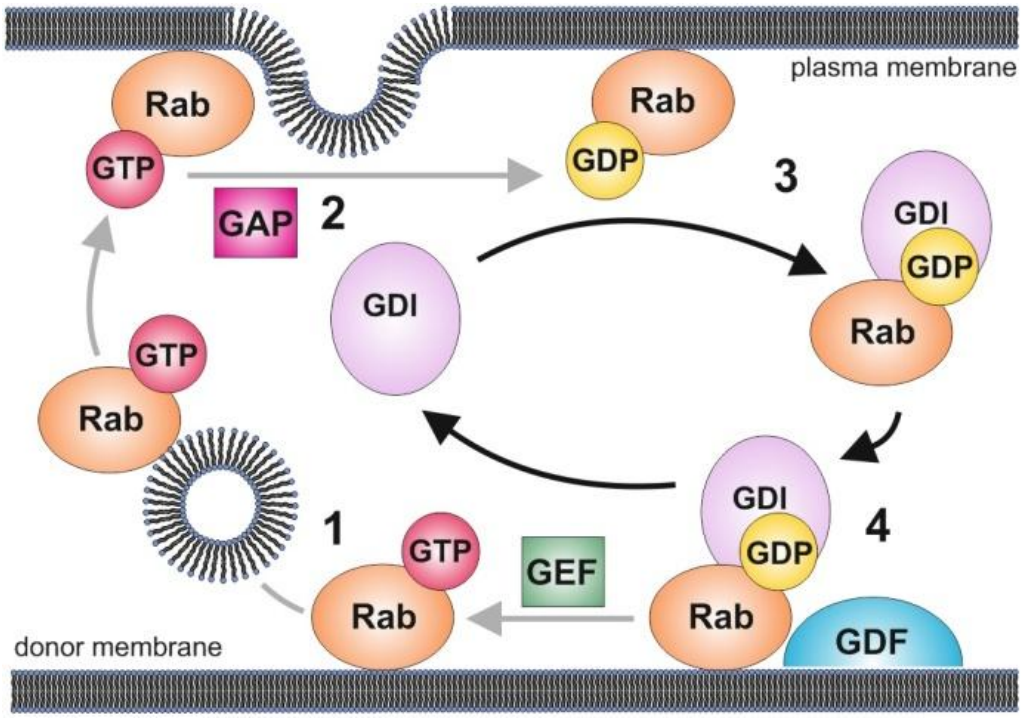

Figure 3: RabGTPase and RabGDI cycles.

1. Activated, GTP-bound Rab proteins are recognized by multiple effector proteins (here: a RabGTPase accompanies a vesicle to the plasma membrane).
2. Through hydrolysis of GTP which is stimulated by a GTPase-activating protein (GAP), the RabGTPase acts as effector and and is converted to the GDP-bound, inactive conformation.
3. Unoccupied, cytosolic GDI removes prenyltated RabGDP from the plasma membrane.
4. The GDP-bound, prenylated Rab proteins are presented to the donor membranes, where Rab-specific GDI displacement factors (GDFs) make GDI release RabGDP. The conversion of the GDP-bound Rab to its active, GTP-bound conformation is catalyzed by a guanine nucleotide exchange factor (GEF) (after Pfeffer et al., 1995 and Stenmark, 2009).

3.2.2. SNAREs

The evolutionarily conserved SNARE proteins and their complexes are required for the docking and fusion of vesicles with their target membranes. In yeast and mammalian cells, more than 60 SNARE members are known. They interact with SNAP (soluble NSF (N-ethylmaleimide-sensitive factor) attachment proteins where the acronym SNARE comes from (SNAP Receptor). SNAREs can be divided into two categories defined by their localization: vesicle or v-SNAREs are incorporated into the membranes of transport vesicles during budding, and target or t-SNAREs are located in the membranes of target compartments (Hanson et al., 1997). SNAREs vary in structure and size, but all share a conserved SNARE motif in the cytosolic domain that consists of about 70 amino acids, which are critical for SNARE complex formation (Paumet et al., 2004). In neurons, syntaxin and synaptobrevin (vesicle-associated membrane protein; VAMP) are anchored by their C-terminal domains in the cell and vesicular membranes. SNAP-25 is attached to the plasma membrane via several cysteine-linked palmitoyl chains. These SNARE proteins can form a macromolecular complex that spans the two membranes, bringing them into close apposition and finally to fusion (Brunger, 2005).

3.2.3. Axonal transport and kinesin motors

Axonal transport is the lifeline of axons and growth cones. It keeps the soma and the distal tips connected, delivers various cargo and clears recycled or misfolded proteins. Proteins that are synthesized in the soma are delivered to the axon's tips via slow and fast anterograde axonal transport (Lasek et al., 1984). Slow axonal transport delivers cytoskeletal and soluble cytosolic proteins; fast transport supplies the growth cone with vesicles with distinct cargo and is kinesin (anterograde transport) or dynein (retrograde transport) dependent (Roy et al., 2005). Adaptors are required to dock particular vesicles to motor proteins. The number of such motor protein receptors is large. Cst1 is one of these linker proteins as it docks vesicular cargo to kinesin-1 (Konecna et al., 2006). The Calsyntenin family is introduced in detail in paragraph 3.3.

Kinesins are mechanochemical motor proteins that move along microtubule filaments by hydrolyzing ATP (Schnitzer and Block, 1997). Most kinesins walk towards the plus end, and thus contribute to fast anterograde axonal transport, whereas dynein motor

proteins move toward the microtubules' minus ends. By their movement, kinesins are involved in several cellular processes such as mitosis, meiosis and intracellular transport of cargo (Mallik et al., 2013). The first kinesin, kinesin-1, was discovered and described by Vale and colleagues (Vale et al., 1985) as a heterotetrameric fast axonal transport motor consisting of 2 light chains (KLC) and 2 heavy chains (KHC) that function as motor subunits. Up to date, more than 40 kinesin proteins have been identified that are organized into at least 14 families termed kinesin-1 to kinesin-14 (Lawrence, 2004).

3.3. Calsyntenins

Calsyntenins (CLSTN, Cst) are type-I transmembrane proteins that belong to the cadherin superfamily (Vogt et al., 2001). Beside the classic, fat-like and flamingo cadherins, Calsyntenins belong to the major cadherin subtypes that are conserved between insects and vertebrates (Pettitt, 2005). Calsyntenins obtained their name due to the ability of their cytoplasmic domains to bind synaptic calcium. In human, mice and chicken, the Calsyntenin family consists of three members (Cst1, 2 and 3), in nematodes and flies, one ortholog (CASY-1, CDH-11) is known (Ikeda et al., 2008). CASY-1 is most similar to Cst2 (Hoerndli et al., 2009). All Calsyntenins have the same domain structure, consisting of an extracellular signal peptide, two cadherin-like domains, a long segment with a strongly conserved cleavage site (Vogt et al., 2001; Hintsch et al., 2002), a transmembrane part and a conserved acidic cytoplasmic segment. Cst1 and 2 have a similar acidic cytoplasmic domain. In contrast, Cst3 lacks a part of the acidic stretch. Calsyntenins are located in various tissues primarily inside, but also outside the nervous system. They were first detected at the postsynaptic membranes of excitatory synapses in the central nervous system (CNS) of chicken embryos (Vogt et al., 2001). Later, they were found in vesicles in transit to growth cones (Konecna et al., 2006) and associated with the ER and the trans-Golgi network (TGN) in hippocampal neurons (Ludwig et al., 2009). Cst3 was most strongly expressed in interneurons (Pettem et al., 2013). Cst1 and 3 were also detected in endocrine glands inside and outside the nervous system (Rindler et al., 2008).

The function of Calsyntenins varies along with the tissue-specific expression pattern. In postsynaptic membranes of excitatory CNS neurons, Calsyntenins are putative modulators for postsynaptic calcium signaling and cell adhesion. When Cst1 is proteolytically cleaved, its ectodomain is released and accumulates in the cerebrospinal fluid. The transmembrane intracellular stump is internalized and translocated to the cytoplasmic surface of the spine apparatus, thereby transporting calcium away from the surface (Vogt et al., 2001). The detailed physiological function of this calcium modulation is not completely understood.

Another important feature of Calsyntenins is their binding to kinesin. The intracellular tetratricopeptides of Cst1 dock distinct vesicular cargo to kinesin-1 that accomplishes anterograde axonal transport (Vale et al., 1985). Mutations in this domain slow down fast anterograde axonal transport (Konecna et al., 2006). So far, Cst1 and 3 have been shown to directly interact with kinesin-1 light chain (KLC1). The particular binding and trafficking of Cst1 is dependent on conserved WDDS motifs (kinesin binding site KBS1 and KBS2) (Ludwig et al., 2009) and can be modulated by the phosphorylation of KLC1 at Ser460 (Vagnoni et al., 2011).

Cst1-positve vesicles are found in two distinct and non-overlapping trans-Golgi network-derived pathways. On the one hand, Cst1 is found on early endosomes containing the amyloid β-precursor protein (APP), together with the GTPases Rab4 or 5. On the other hand, Cst1 is also detected in the recycling endosomal pathway associated with Rab11 and its interacting protein Rip11 (Steuble et al., 2010). Overexpression of any Calsyntenin in cultured cells results in rapid shedding of the full-length protein similar to the proteolytic cleavage of APP (Vogt et al., 2001; Araki et al., 2004). All Calsyntenins are subject to primary membrane-proximal proteolytic cleavage resulting in ectodomain shedding which is followed by intramembranous cleavage by a presenilin-dependent γ-secretase (Araki et al., 2004; Hata et al., 2009).This constitutive cleavage was investigated in CAD cells and shown to prevent aberrant peripheral kinesin-1 retention (Maruta et al., 2012). Cst1 also associates with the adaptor proteins Mint2/X11L and FE65 which are involved in APP processing (Araki et al., 2003; Araki et al., 2004). Furthermore, the up-regulation of Cst3 in cultured neurons by amyloid-β precursors was shown to result in an increased vulnerability of cortical neurons and neuronal death (Uchida et al., 2011). Recent studies confirm its neurotoxic role (Uchida et al., 2013). Intriguingly, Cst3 was

also shown to promote excitatory and inhibitory synapse development (Pettem et al., 2013). Cst3$^{-/-}$ mice showed deficits in synaptic development. In addition, siRNA-mediated loss of Cst1 was shown to increase APP processing at the BACE1 site and thus amyloid-β production in neurons (Vagnoni et al., 2012).

Different studies reported altered Calsyntenin levels in the cerebrospinal fluid of patients suffering from neurodegenerative diseases, such as Alzheimer's disease (AD), Parkinson's disease (PD) or dementia with Lewy bodies (Yin et al., 2009; Ringman et al., 2012; Dieks et al., 2013). Furthermore, fMRI studies showed that allelic variations of Cst2 have an influence on learning (Jacobsen et al., 2009; Preuschhof et al., 2010). Also studies in C. elegans demonstrated a role for Calsyntenins in memory, as it was shown that the Cst2 ortholog CASY-1 is essential for learning in C. elegans (Ikeda et al., 2008). CASY-1 mutants have defects in salt chemotaxis and temperature learning, in olfactory adaptation and integration of sensory signals. Due to these effects on synaptic plasticity, it is likely that Calsyntenins may have a function in neural circuit formation and as Cst1 is expressed in growth cones, they may also contribute to axon guidance. During mouse development, Calsyntenin expression has not been investigated in detail (Vogt et al., 2001). Calsyntenin mRNA expression in the adult mouse brain was investigated by Hintsch and colleagues (Hintsch et al., 2002) using the in situ hybridization technique. Cst1 was found to be abundant in most neurons of the CNS, with relatively little variation in its expression level. Cst2 and 3 expressions were lower in glutamatergic neurons, but strong in GABAergic cells such as interneurons of the cerebral cortex, the basal ganglia, the thalamic nuclei, and Purkinje cells of the cerebellum. The variations within the Cst1, 2 and 3 expression patterns suggest different functional roles of the three family members (Hintsch et al., 2002).

3.4. Chicken as a model organism and its features

To study axon guidance, in vitro experiments are of very limited value because they only reflect poorly the developmental features that exist in vivo. Organisms as Drosophila melanogaster or Caenorhabditis elegans have a simpler nervous system and we can learn a lot by studying them, but some features are vertebrate specific and cannot be assessed in invertebrates. Rodents are well-established model organisms to study a variety of neurobiological questions, especially due to sophisticated genetic tools available in mice. For developmental studies though, the accessibility to the embryo is difficult and both high costs as well as ethical constraints may favor another organism for embryonic studies: the chick. The chicken embryo (Gallus gallus domesticus) is an ideal model organism for developmental biological and biochemical investigations. Due to the simple access through the eggshell it can easily be observed and manipulated. Already Cajal used the chicken embryo for his studies and drawings. Throughout the entire 20th century, the chicken embryo has been used as a model organism not only for neuroscientific research, but also for many other developmental studies (Wolpert, 2004). Viktor Hamburger and Howard Hamilton precisely described the developmental stages of the chicken embryo (Hamburger and Hamilton, 1951). Precise timing of experimental approaches contributed to the success of the chicken embryo as model organism. Since the chicken genome has been sequenced and genomic resources have become available, many more questions were addressed using the chicken embryo as a model organism (Davey and Tickle, 2007). Although no genetic knock-out chickens are available, the in ovo RNAi technique allows silencing particular genes of interest at the mRNA level (Pekarik et al., 2003; Wilson and Stoeckli, 2011). Different cell types have been meticulously investigated in the chicken embryo. Besides the brain, both chick motor neurons of the spinal cord and sensory neurons in the dorsal root ganglia (DRGs) are commonly used as models for research in neural circuit formation. Another well established system for studying axon guidance display the commissural axons. In the following six paragraphs, certain neuronal populations and distinct structures of the chicken embryo that are important for the understanding of my work are briefly discussed.

3.4.1. Commissural neurons

Commissural neurons link the two halves of the CNS and thus ensure the transfer of information. In vertebrates, insects and nematodes, commissural axons are attracted to the ventral midline (floor plate) by the chemoattractant netrin, which signals attraction by activating the DCC receptors on growth cones (Serafini et al., 1994; Stein and Tessier-Lavigne, 2001). Additionally, the roof plate repels commissural axons by expressing BMP (Augsburger et al., 1999). It has been shown that BMP7 and GDF7 heterodimerize in vitro to work together as repellent and push commissural axons ventrally (Butler and Dodd, 2003). In addition, it was shown that the morphogen Sonic hedgehog (Shh) contributes to the chemoattractant activity of the floor plate. Its effect is mediated by Smo and Boc (Charron et al., 2003; Okada et al., 2006). Futhermore, the roof-plate derived axon guidance molecule Draxin (dorsal repulsive axon guidance protein) was shown to repel dI1 axons (Islam et al., 2009). Once the commissural growth cones have reached the floor plate, short-range cues based on direct cell-cell interactions become relevant. Stoeckli and Landmesser demonstrated with in vivo studies that the interactions of axonin-1 on commissural growth cones and NrCAM on floor-plate cells are required for accurate pathfinding in and through the midline (Stoeckli and Landmesser, 1995). In invertebrates and vertebrates, the direct interaction of Robo on commissural growth cones with Slits derived from the floor plate leads to repulsion of the commissural growth cones and prevents them from re-crossing (Kidd et al., 1998; Sabatier et al., 2004). In chicken, the regulation of Robo1 in commissural growth cones is mediated by RabGDI (Philipp et al., 2012). Thus, RabGDI takes over a function similar to comm in Drosophila (Keleman et al., 2005). Post-commissural longitudinal axon guidance was shown to be determined by the morphogen Shh (Bourikas et al., 2005; Yam et al., 2012) and Wnts (Lyuksyutova et al., 2003). In chicken, Wnt5a and Wnt7a are, unlike Wnt4 in mice, not expressed in a gradient in the floor plate. In the chicken, Shh induces an sfrp gradient that blocks Wnt5a and Wnt7a to form an activity gradient (posterior^{low} to anterior^{high}) (Domanitskaya et al., 2010). At the lumbar level in the chicken embryo, dorsal commissural neurons start to grow towards the floor plate around Hamburger and Hamilton stage 18/19 (HH18/19) (Hamburger and Hamilton, 1951). They reach the floor plate around HH21/22, cross the midline at HH23 reach the contralateral site at HH24.

3.4.2. The main nerves of the chicken hind limb

Investigating axon guidance in the chicken embryo is not restricted to the CNS. The nerves that grow into the chicken hind limb are well described (Landmesser and Morris, 1975) and represent a good model to study axon guidance in the PNS. Innervation of the chicken extremities is mediated by several nerves originating in the motor columns and/or the sensory DRGs. In the hind limb, the most prominent nerve branches form the crural nerve, the lateral femoral cutaneous nerve (LFCt) and the sciatic nerve. Except from the LFCt, they all consist of a mixture of motor and sensory axons. The cell bodies of the crural and the sciatic nerves are localized in the motor columns. The crural nerve is divided into a ventral and dorsal part and grows rostally of the sciatic nerve to innervate thigh musculature. The sciatic nerve grows to the lower leg to innervate muscles around the knee and foot (Landmesser and Morris, 1975). The further away a motor neuron is located to the central canal the more distal its axon projects. A motor neuron that locates closer to the central canal projects to more proximal targets (Shirasaki and Pfaff, 2002).

3.4.3. Motor neurons

Motor neurons form efferent nerves that carry signals from the spinal cord to the periphery to control muscles directly or indirectly. Cell bodies of motor neurons are located in the CNS but they project their axons outside the CNS. Depending on the target, they form pools that locate to distinct positions in the ventral spinal cord. Within the spinal cord they can be subdivided in five columnar groups: The median motor column (MMC) with its medial and lateral part, pre-ganglionic autonomic motor neurons (CT; column of Terni in chicken, only at the thoracic level of the spinal cord) and the lateral motor column (LMC) with its medial and lateral part at the limb levels of the spinal cord. The MMC neurons innervate the trunk musculature, the CT neurons project to sympathetic neuronal targets and the LMC neurons project axons to ventral (medial) and dorsal (lateral) limb muscles (Landmesser, 1978; William et al., 2003). Many motor neurons express the homeodomain transcription factors Islet and HB9 which can be used for specific staining (Vult von Steyern et al., 1999). In the chicken spinal cord, the first motor neurons are born in the LMC at HH17. Soon after motor neurons have extended their axons, they stall for roughly 24 h in the plexus region to wait for limb maturation. At HH23 they start to grow into the distal limb and

at HH26, they form dorsal and ventral nerve trunks towards the premuscle masses in the limbs (Krull and Koblar, 2000). The correct growth and formation of the limbs are required to guide the motor axons to their appropriate targets (Lance-Jones and Landmesser, 1980a; Lance-Jones and Landmesser, 1980b). Medial MMC neurons project dorsally and form the epaxial nerves which innervate the epaxial muscles. In the chicken embryo they reach the epaxial muscle precursor around HH25 and start to defasciculate around HH27 (Eberhart, 2004).

3.4.4. Sensory neurons

Sensory neurons of the dorsal root ganglia (DRGs) belong to the peripheral nervous system (PNS) and send projections into the CNS where sensory information is processed. They develop from neural crest cells that migrate away from the neural tube during neurogenesis. The DRGs contain three main classes of bipolar sensory neurons with bifurcating axons: noci/thermoceptive, mechanoreceptive and proprioceptive neurons. Their axons transfer sensory inputs from the periphery to the cell bodies that are located to particular parts of the DRG. Their collaterals project into distinct layers (laminae) in the spinal cord via the dorsal root entry zone (DREZ). Nociceptive neurites project to the very dorsal layers (laminae I-II), mechanoreceptive neurites to laminae III to VI and proprioceptive neurites to the ventral horn (Snider, 1994). The laminae in the spinal cord are arranged differently in chicken compared to humans. In birds, lamina I, II and III are arranged from lateral to medial whereas in humans these laminae are arranged dorso-ventrally (Brinkman and Martin, 1973; Martin, 1979). For growth and survival DRG neurons need neurotrophins, including nerve growth factor (NGF), brain-derived neurotrophic factor (BDNF) and neurotrophin-3 and 4 (NT-3 and NT-4). The receptors for the neurotrophins are the tyrosin receptor kinases (TrkA, B and C). Different DRG neurons express different combinations of Trks at the cell surface and thus determine their fate (Bartkowska et al., 2007). In the chicken embryo, neural crest cells start delaminating around HH12. DRGs form around HH18. Their four to five parallel axon bundles extend and reach the spinal cord at HH19. All major nerves that grow into the chicken limb are composed of both sensory and motor axons except for the lateral femoral cutaneous (LFCt) nerve, that is composed of only sensory axons (Honig et al., 2002).

3.4.5. Dermomyotome

In vertebrates, the segmentally arranged somites give rise to all body muscles. During their maturation, the ventral half divides into the so-called sclerotome, whereas the dorsal half forms the dermomyotome (dorsal somite epithelium) (Christ and Scaal, 2008). The dermomyotome is a transitory epithelial sheet and lies in between the sclerotome and the surface ectoderm and gives rise to most mesodermal structures such as muscles, connective tissue, endothelium and cartilage (Ben-Yair and Kalcheim, 2008). Cells at the border of the dermomyotome generate myocytes (Cinnamon, 2006). The central dermomyotome dissociates and produces dermis as well as Pax3- and Pax7-positive myoblasts that divide further (Buckingham and Montarras, 2008).

3.4.6. Cerebellum

The cerebellum is involved in the integration of sensory perception, coordination and motor control. It does not initiate movements but contributes to the fine tuning and timing of motor activity. Sensory systems of the spinal cord and other units of the brain send inputs to the cerebellum (Pascuzzi et al., 2002). It develops from the rhombencephalon and forms characteristic cell layers that are similar in all vertebrate embryos (Wang and Zoghbi, 2001). Granule cell precursors of the external granule cell layer (EGL) originate from the rostral metencephalon and undergo extensive tangential migration (Hallonet and Le Douarin, 1993). The Purkinje, Golgi, stellate and basket cells all arise from the ventricular neuroepithelium (Hatten and Heintz, 1995), whereby the Purkinje cells develop first. The inhibitory Purkinje neurons later receive signals from the cerebrum. Between the EGL and the Purkinje cell layer, the molecular layer forms from axons of granule cells. The molecular layer contains also Golgi, stellate and basket cells that have a modulatory action on the Purkinje cells and granule neurons (Wang and Zoghbi, 2001). The inner granule cell layer (IGL) is formed of granule neurons precursors that migrate inwards. The neurons of the deep cerebellar nuclei receive signal input from the Purkinje neurons and finally project to the cerebral cortex. They are located at the cerebellar ventral basis (Voogd and Glickstein, 1998).

3.4.7. RNA interference

To study molecules and their effect on axon guidance, we need to interfere with their function. In principle, the most powerful way to understand a gene function is a genetic knock out. Up to date, knock out technologies allow conditional or inducible removal of genes. But besides the high costs and often early embryonic lethality, the temporal resolution for developmental studies is not given (Baeriswyl and Stoeckli, 2006). As mentioned above, the chicken embryo cannot be manipulated with genetic approaches. However, RNA interference (RNAi) allows silencing of genes at mRNA level with high spatial and temporal control. RNAi represents an evolutionarily conserved mechanism, which protect organisms from invasion by both exogenous (e.g., viruses) and endogenous (e.g., mobile genetic elements) genetic parasites (Almeida and Allshire, 2005). First observations of RNAi were made in plants as post-transcriptional gene silencing (Napoli et al., 1990). The standard RNAi technique using double-stranded RNA (dsRNA) was finally described in C. elegans by Fire and Mello (Fire et al., 1998). The RNAi pathway (Figure 4) is initiated by the helicase/RNase III-like enzyme called Dicer, which cleaves long dsRNA or double stranded micro RNA (miRNA) molecules into short fragments of about 23 nucleotides (small-interfering RNAs; siRNAs). The sense strands of these siRNAs are then incorporated into the RNA-induced silencing complex (RISC) which unwinds the double-stranded siRNAs. These strands pair with complementary sequences of mRNA molecules available in the cell and argonaute, the catalytic component of the RISC complex, induces further cleavage of the new double stranded siRNA. As a result, the mRNA is degraded and no protein is produced (Bernstein et al., 2001).

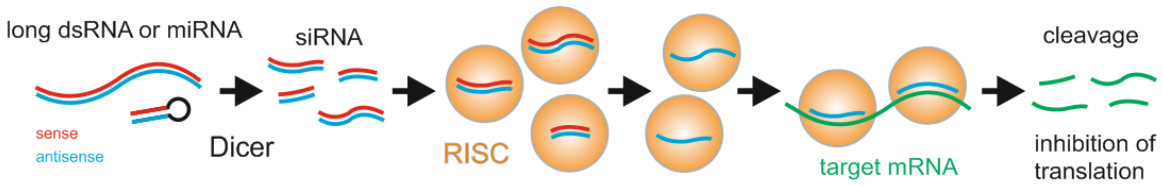

Figure 4: RNAi pathway. RNAi allows for spatial and temporal control of gene expression.

3.4.8. In ovo RNAi

One application of RNAi in the chicken embryo is the in ovo RNAi technique developed in our lab (Pekarik et al., 2003; Wilson and Stoeckli, 2011). It induces loss of gene function in vivo during development of the chicken embryo. DsRNA in combination with a plasmid encoding a reporter protein, or plasmids encoding miRNAs plus a reporter protein is injected into the central canal of the neural tube. The application of a small electrical field around the spinal cord allows the mix to be taken up by the cells on the plus side of the electrode through electroporation. Depending on the position of the electrodes or the promoter in the plasmid encoding the miRNA, specific cells can be targeted (Pekarik et al., 2003), such as the commissural neurons (Math1 enhancer) or the floor plate (Hoxa1 enhancer) (Wilson and Stoeckli, 2011). From embryonic day 2 (E2) to E4, the chicken embryo is accessible in ovo for injection into the central canal of the spinal cord. Using ex ovo cultures, the in ovo RNAi technique can even be applied on older embryos (Baeriswyl and Stoeckli, 2006). After re-incubating the embryo for a defined time, the fluorescent reporter protein indicates where RNAi has taken place. Using this method, genes can be silenced in a spatially and temporally controlled manner. RNAi in chicken embryo can also be used for gene silencing in other tissues than the spinal cord such as the limbs or in the cerebellum (Baeriswyl et al., 2008).

3.5. Aim of my thesis

This thesis aims at analyzing the importance of Calsyntenin1-mediated vesicular trafficking during neural circuit formation. In particular, I want to test if the specific delivery of guidance receptors to the growth cone is Calsyntenin1 dependent.

4. Manuscripts

4.1. Calsyntenins and APP are Expressed in a Dynamic and Similar Manner in the Chicken Embryo

Tobias Alther, Diego Geering and Esther T. Stoeckli
Institute of Molecular Life Sciences

Corresponding author: Esther T. Stoeckli
e-mail: esther.stoeckli@imls.uzh.ch

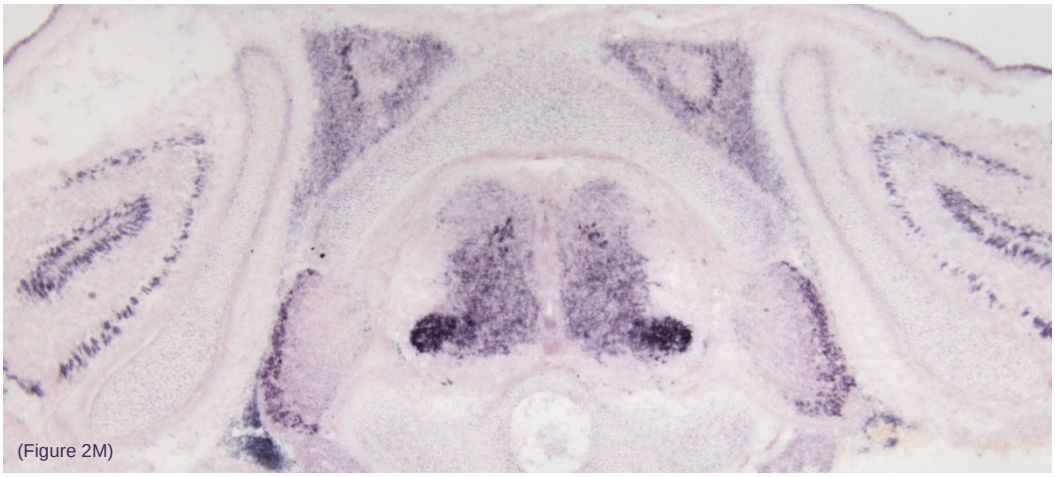
(Figure 2M)

My contributions to this manuscript were all the experiments with the exception of the APP analysis in the cerebellum and I have written the manuscript.

Abstract

Calsyntenins form a family of linker proteins between distinct vesicles and kinesin motors for axonal transport. A detailed biochemical analysis of Calsyntenin-positive vesicles indicated that there are at least two subpopulations of vesicles, one containing amyloid precursor protein (APP), the other devoid of APP. APP transported by Calsyntenin-positive vesicles was protected from cleavage by ADAM10. Calsyntenins were implicated in synaptic plasticity by findings in human and worms. Despite the fact that Calsyntenins were discovered originally from developing chicken motor neurons, their distribution in the developing nervous system has not been analyzed so far. In adult mouse brain, Calsyntenins are expressed in most brain regions. During development, Calsyntenins are expressed in both the peripheral and the central nervous system. Their expression patterns are highly dynamic and partially overlapping.

Introduction

Delivery of proteins to specific cellular destinations is crucial for neural circuit formation and synaptic plasticity. Thus, transport of vesicular cargo needs to be precisely regulated both temporally and spatially. Calsyntenins, a family of three transmembrane proteins, have been identified as cargo-docking proteins in vesicular transport along axons (Vogt et al., 2001; Hintsch et al., 2002, Konecna et al., 2006). In its cytoplasmic domain Calsyntenin1 was shown to contain two binding sites for the interaction with the tetratricopeptide repeats of kinesin-1, the motor for anterograde axonal transport (Vale et al., 1985). Mutations in the kinesin-binding domains of Calsyntenin1 significantly reduced fast anterograde axonal transport of vesicles (Konecna et al., 2006). The interaction of Calsyntenin1 with the kinesin light chain1 (KLC1) subunit was shown to be regulated by phosphorylation of Ser460 of KLC1 (Vagnoni et al., 2011).

A role for Calsyntenins in synaptic plasticity is in line with findings in human, where specific alleles of Calsyntenin2 have been linked to episodic memory performance

(Zhang et al., 2009; Preuschof et al., 2010). These findings have been supported by functional analyses in C. elegans. CASY-1, the worm ortholog of Calsyntenin2, was shown to be required for associative learning. Learning deficits in CASY-1-deficient worms could be rescued by neuronal expression of human Calsyntenin2 (Hoerndli et al., 2009, Ikeda et al., 2008).

A link between Calsyntenin and memory is also provided by a study addressing the differences between normal aged brains and brains from patients diagnosed with Alzheimer's disease (Ringman et al., 2012). This finding is interesting in the context of cell biological and biochemical analyses that link Calsyntenins to neuronal APP transport (Araki et al., 2003; Ludwig et al., 2009; Steuble et al., 2010 and 2012; Vagnoni et al., 2012). Axons were shown to contain two non-overlapping populations of Calsyntenin-positive vesicles: one population with APP, the other one without APP immunoreactivity. By sheltering APP from cleavage by the α-secretase ADAM10, Calsyntenin1 was suggested to contribute to the transport of full-length APP to the cell surface. In the absence of Calsyntenin1, increased co-localization of APP and ADAM10 in axons resulted in increased levels of Aβ-production (Steuble et al., 2012; Vagnoni et al., 2012).

Northern blot analysis of Calsyntenins localized Calsyntenin2 and -3 mRNAs exclusively to brain tissue in adult mice. Calsyntenin1 was also found predominantly in the brain, but also in non-neuronal tissues, such as kidney, lung, skeletal muscles, and heart. A more detailed analysis of Calsyntenins in the adult mouse brain revealed Calsyntenin mRNA expression in the majority of neurons (Hintsch et al., 2002). Calsyntenin1 was found at high levels in most neurons. In contrast, Calsyntenin2 levels were low with only few exceptions. Higher levels were found in a subpopulation of pyramidal neurons in layer 5/6 of the cortex, in regions CA2/CA3 in the hippocampus, and in some Purkinje cells of the cerebellum. Calsyntenin3 expression was more similar to Calsyntenin2 than Calsyntenin1, as it was also mainly found at low levels in most neurons, with the exceptions of GABAergic neurons. At the electron microscopic level, Calsyntenin1 was found in the post-synaptic membrane and in the spine apparatus of dendritic spines. The distinct localization of Calsyntenin1 fragments is consistent with proteolytic cleavage of full-length Calsyntenin in the synaptic cleft resulting in the release of the N-terminal fragment

and followed by the internalization of the transmembrane stump into the spine apparatus (Vogt et al., 2001). The cleavage site of Calsyntenin1 is strongly conserved in all three Calsyntenins (Hintsch et al., 2002). Overall human, murine and chicken Calsyntenins are highly conserved, with amino acid identities ranging from 75 to 95 % (Table 1).

Although Calsyntenin1 was initially identified in cultures of motor neurons taken from embryonic chicken spinal cords, very little is known about the temporal and spatial expression of Calsyntenins in the developing nervous system. Here, we compare the temporal and spatial expression pattern of all three Calsyntenins and compare them with the expression of APP in selected neuronal populations.

Results

Calsyntenins are expressed in the developing neural tube and in the dermomyotome at early developmental stages

Calsyntenin1 mRNA was detected as early as HH12 (E2) at the lumbar level of the chicken neural tube (Figure 1). Between HH12 and HH20, Calsyntenin1 was expressed in the ventricular zone and in the floor plate. Expression of Calsyntenin3 in the ventricular zone and in the floor plate was detectable starting at HH16 (Figure 1F). By HH20, both Calsyntenin1 and -3 were expressed in the ventricular zone of the neural tube and in the floor plate. Calsyntenin2 was expressed mainly in somites, but not in the neural tube with the exception of very few motor neurons starting at HH16 (Fig 1B,E,H). Calsyntenin2 is never expressed in the floor plate. In contrast to Calsyntenin2, Calsyntenin1 and -3 are expressed only weakly in somites (HH14 and HH16, respectively) and in the dermomyotome at HH20.

At HH22, the expression patterns of all Calsyntenins were very similar (Figure 1J-L). They were all expressed in motor neurons of the developing spinal cord. Moreover, they were all expressed in sensory neurons of the dorsal root ganglia (DRG). Calsyntenin1 and -3, but not Calsyntenin2, were still expressed in the floor plate and in interneurons. Calsyntenin2 differed from the other two family members by its

strong expression in the dermomyotome during the first five days of development (Figure 1E,H,K and Figure 2). At HH14, Calsyntenin2 expression overlapped clearly with Pax3, a marker for somites and early dermomyotome cells. At both HH16 and HH19, Calsyntenin2 expression overlapped both with cells derived from the somites (Figure 2D-F) and with neural crest cells (Figure 2G-I).

Calsyntenins are differentially expressed in motor and sensory neurons

At E5 (HH26) the expression pattern of the three Calsyntenins started to diverge compared to HH22 (Figure 3A-C). Calsyntenin1 and -3 were expressed in all neurons of the spinal cord. Only Calsyntenin1 expression was maintained in the floor plate (Figure 3A). Calsyntenin2 was expressed in motor neurons of the lateral motor column (Figure 3B). All Calsyntenins were expressed in DRGs at HH26. Calsyntenin2 expression in the dermomyotome was maintained (Figure 3B).

After one week, at HH33, both Calsyntenin1 and -3 were expressed throughout the gray matter of the spinal cord (Figure 3D and F). Calsyntenin2 expression was more sparse than that of the other two family members and not found in the dorsal horn. Strongest expression was still found in the lateral motor columns (Figure 3E). All Calsyntenins were expressed in DRGs and Calsyntenin1 and -3 also in sympathetic ganglia.

In the mature spinal cord, at the time of hatching (HH45), the expression of all Calsyntenins was maintained. Calsyntenin1 was still expressed in individual cells throughout the gray matter of the spinal cord (Figure 3G). In contrast, Calsyntenin2 and -3 expression was restricted to motor neurons in the ventral spinal cord (Figure 3H and I). All three Calsyntenins were still found in the DRGs. Expression levels of Calsyntenin1 and -3 were now higher in sympathetic ganglia compared to DRGs. Calsyntenin2 was only found very transiently in sympathetic ganglia at HH41 (Figure 3H’’).

Expression patterns of Calsyntenin1 and -3 were very similar to each other, whereas Calsyntenin2 differed by its expression in the dermomyotome and in the cartilage surrounding the notochord (Figure 2N-Q). Myoblasts generating hypaxial muscles

delaminating from the ventrolateral dermomyotome still expressed Calsyntenin2 (Figure 2M). Similarly Calsyntenin2 was also found in epaxial muscles at HH33.

Calsyntenins are expressed in the developing forebrain and eye

To distinguish the different brain areas, we used anti-SV2 antibodies to visualize synaptic layers and anti-Pax6 antibodies to identify precursor cells (Figure 4). At HH30 Pax6 staining covered the ventricular half of the wall of the tectum, overlapping only little with the pial layer of SV2 staining (Figure 4A). By HH38 SV2 staining was not found throughout the tectal layers, overlapping with Pax6 still expressed in the ventricular zone (Figure 4B). In addition, Pax6 was now found expressed very strongly in the dorsal most layer of the tectum, the stratum opticum (SO). At HH44, the dorsal expression of Pax6 has expanded beyond the stratum opticum. The ventricular expression has retracted more compared to HH38 (Figure 4C). Expression of SV2 at HH44 does not differ significantly from HH38.

In the early tectum (HH30), Calsyntenin1 expression was found in the dorsal half (Figure 4D). Calsyntenin3 was found at low levels throughout the tectum. Calsyntenin2 was only found at HH38 (Figure 4E). At this stage, Calsyntenin1 levels were reduced. Calsyntenin2 and -3 were found in a similar pattern. At HH44, both Calsyntenin1 and Calsyntenin2 were expressed at low levels, only Calsyntenin3 was maintained in different layers. Strongest expression was now found in the dorsal-most layer, the stratum opticum (Figure 4F). Expression of all Calsyntenins was also found in the projection neurons targeting the tectum, the retinal ganglion cells (Figure 4G-I). At HH30, when the first axons have reached the tectum, Calsyntenin1 and Calsyntenin2 were expressed in retinal ganglion cells. No changes were seen at HH38 in the retinal ganglion cell layer. However, Calsyntenin1 was now also found in the future photoreceptor layer (Figure 4H). By HH44, Calsyntenin1 was also found in the inner nuclear layer. Calsyntenin2 and Calsyntenin3 were expressed in a salt-and-pepper- like manner in the inner nuclear layer, but only weakly. By HH44, Calsyntenin3 was expressed in some but not all retinal ganglion cells.

We found Calsyntenins expressed diffusely throughout the entire telencephalon between stages HH30 and HH44. Higher levels were found in pial layers. An example is shown for Calsyntenin1 at HH36 (Figure 4B').

Calsyntenins are dynamically expressed in the cerebellum

All Calsyntenins were expressed in the developing cerebellum (Figure 5). We already observed Calyntenin1 and -3 in some cells of the cerebellar anlage at HH32, before foliation starts (Figure 5A,C). In contrast, Calsyntenin2 was expressed strongly in the caudal ventricular zone and in the roof of the cerebellar anlage (Figure 5B). By HH35, Calsyntenin2 expression was more or less restricted to the trigone area, the precursor area in the caudal cerebellum (Figure 5E). Calsyntenin1 and -3 were found in the deep cerebellar nuclei (Figure 5D,F). After the initiation of foliation, at HH36, the expression patterns of Calsyntenin2 and -3 were similar (Figure 5H,I). Both were found to be expressed in migrating Purkinje cells. In addition, Calsyntenin2 but not Calsyntenin3, was also found in the external granule cell layer. Calsyntenin1 was rather not found in Purkinje cells but maybe in migrating glia cells (Figure 5G). Expression patterns of Calsyntenin2 and -3 were very similar at HH38 and HH40. Expression in migrating Purkinje cells was maintained for both. In addition, Calsyntenin2 expression persisted in the external granule cell layer, as indicated by Pax6 staining (Figure 5M). In contrast to the other Calsyntenins, Calsyntenin1 was not expressed in Purkinje cells at HH38 or HH40 (identified with Calbindin staining, Figure 5Q). Rather it was found in the inner granule cell layer. Calsyntenin1 and -3 but not Calsyntenin2 were expressed in deep cerebellar nuclei throughout development (HH35 to HH44). Calsyntenin2 expression was not seen consistently in deep cerebellar nuclei.

In the mature cerebellum, the expression patterns of all three family members differed considerably. Calsyntenin1 was found at high levels in the inner granule cell layer (Figure 5R). Low levels of Calsyntenin2 were expressed in the inner granule cell layer but only in the distal tips of the folia (Figure 5S). Expression was still seen in the external granule cell layer and in some Purkinje cells. Calsyntenin3 was more or less restricted to Purkinje cells (Figure 5T).

The expression of APP largely overlaps with the Calsyntenins

Consistent with findings in the mature mouse brain, where Calsyntenin1 and APP were found in the same vesicles, we observed a strong overlap between APP and Calsyntenin1 expression in the developing neural tube and in somites (Figure 6). APP was found in the ventricular zone and the floor plate of the early spinal cord. At HH20, APP was found in dorsal commissural neurons (dI1 neurons) as well as more ventrally located interneurons. Motor neurons also expressed APP. At HH26, APP expression was similar to the sum of all Calsyntenins. It was expressed in all cells of the gray matter with higher levels in the motor neurons. APP was also found in dorsal root ganglia, similar to the Calsyntenins.

Cst1 and APP were shown to interact directly (Ludwig et al., 2009) and localize to the same vesicles (Steuble et al., 2010). As the expression of APP in the chicken embryo has not been analyzed in detail (Carrodeguas et al., 2005), we analyzed its expression also in the chicken brain (Figure 6E,G). At HH38, we also found APP in the tectum. However, the layers expressing APP did fully overlap with the Calsyntenin-positive layers (Figure 6E). In the retina at HH44, APP expression was most similar to Calsyntenin1, although APP was expressed in a non-homogenous way in retinal ganglion cells (Figure 6F). In the cerebellum at HH40 (Figure 6G), APP expression appeared to be the sum of all Calsyntenins, as it was expressed in the inner granule cell layer (like Calsyntenin1), the Purkinje cell layer (like Calsyntenin3), and in the external granule cell layer (like Calsyntenin2).

Discussion

The expression patterns of Calsyntenins are highly dynamic throughout neural development. Whereas Calsyntenin1 and -3 were mainly found in neurons after the first three days of development, Calsyntenin2 was always found in non-neuronal cell types as well. Particularly prominent were expression in dermomyotome and in the cartilage around the notochord. In general, the expression patterns of Calsyntenins were overlapping but never really identical. Mostly, expression of Calsyntenin1 and -3 were more similar to each other than to Calsyntenin2 in the spinal cord. In contrast, during brain development Calsyntenin2 and -3 were more similar to each other than to Calsyntenin1. However, at the end of development, at HH44, shortly before hatching, the expression patterns of all three Calsyntenins were distinct in all areas of the nervous system that we tested.

In hippocampal cultures, Calsyntenin1 was found to link vesicles to the kinesin motors transporting them along the axons in anterograde direction (Konecna et al., 2006). In addition, a role of Calsyntenin1 in vesicular cargo selection was found in the Golgi apparatus (Ludwig et al., 2009). In line with these functions, Calsyntenins were expressed in neurons during neural development, at the time of axonal pathfinding and synaptogenesis. With few exceptions, Calsyntenins were not expressed in proliferating precursor cells but rather after they started to differentiate and migrate to their destination.

Taken together, our results suggest that Calsyntenins are involved in trafficking of specific vesicles during development. As their expression patterns are only partially overlapping the functions of the Calsyntenin family members do not seem to be redundant. Interestingly, also during development, APP expression partially overlaps with Calsyntenin expression. It will be interesting to see what the contribution of Calsyntenin-mediated vesicular trafficking to neural circuit formation is. Based on the expression patterns, one would expect to see specific deficits in axon guidance and synaptogenesis.

Material and Methods

Comparison of murine, human and chicken Calsyntenin protein sequences

Sequences were obtained from Pubmed (http://www.ncbi.nlm.nih.gov/pubmed/) and the following protein IDs were used: mmCst1, CAC17788.1; mmCst2, CAC14887.1; mmCst3, NP_705728.1; ggCst1, CAC17757.1; ggCst2, XP_422633.2; ggCst3, XP_416520.2; hsCst1, NP_001009566.1; hsCst2, NP_071414.2; hsCst3, NP_055533.2. We performed a pairwise comparison including gaps, differences, distances, similarities and identities using the CLC main workbench (v5).

Probe preparation for in situ hybridization

Plasmids containing Calsyntenin or APP cDNA fragments were linearized by digestion with the appropriate restriction enzymes to produce templates for the synthesis of antisense and sense probes. For linearization of 10 µg plasmid DNA, 20 U restriction enzyme were incubated in the appropriate buffer for 2-4 h at 37°C. After phenol/chloroform extraction and acetate/ethanol precipitation, DIG-labeled sense and anti-sense probes were synthesized by in vitro transcription. Two µg linearized plasmid DNA, 2 µl of 10x concentrated DIG RNA Labeling Mix (Roche), 2 µl 100 mM DTT (Promega), 4 µl 5x concentrated transcription buffer (Promega), 1 µl RNasin (40 U/µl; Promega), 2 µl of T3 or T7 RNA polymerase (Roche) and DEPC-treated H2O were mixed to a final volume of 20 µl and incubated at 37°C for 2 h. The DIG-labeled RNA probes were extracted by lithium chloride precipitation and dissolved in 100 µl DEPC-treated H2O.

Cloning an alternative Cst2 probe

Because only a single EST for Calsyntenin2 (1538 bp) was commercially available, we generated two non-overlapping fragments for in situ probe synthesis for this EST. To this end, we excised a 783-bp-long fragment from the ChEST 1002C5 with XbaI (Roche). The plasmid backbone with the remaining 755 bp of Calsyntenin2 were ligated. In situ probes generated from the two Cst2 fragments generated identical results.

Embryo preparation for cryostat sections

Fertilized chicken eggs obtained from a local hatchery (Brueterei Stoeckli, Ohmstal, Switzerland) were stored at 16°C for a maximum of 7 days until incubation at 39°C. Throughout all our procedures, we staged embryos according to Hamburger and Hamilton (Hamburger and Hamilton, 1951). When the desired stage was reached, embryos were sacrificed and the entire embryos or dissected brains were fixed in 4% paraformaldehyde (PFA) in PBS. Depending on the stage, the tissue was kept in 4% PFA for 30 min (HH14-18), 1 h (HH19-24) or 2 h (HH25 and older). After fixation, the tissue was rinsed in PBS and infiltrated with 25% sucrose in PBS overnight at 4°C before embedding in Tissue-Tek O.C.T. Compound. Tissue was frozen in isopentane at -80°C and stored at -20°C until sectioning. Transverse cryostat sections of 25 µm (spinal cord) or 30 µm thickness (brain and retina) were cut using a Leica cryostat, and collected on SuperFrost Plus glass slides (Menzel Glaeser). Sections were dried overnight at room temperature and then stored at -20°C.

In situ hybridization of cryostat sections

In situ hybridization was performed as described earlier (Mauti et al., 2006). The in situ pictures from the eye were taken at an area adjacent to the pecten.

Immunohistochemistry of cryostat sections

Antibodies recognizing Pax3 and Pax6 were obtained from Developmental Studies Hybridoma Bank (University of Iowa, Iowa City, USA). The antibody against Calbindin D28k was obtained from Swant (Bellizona, Switzerland). The secondary antibodies donkey anti-rabbit Cy3 and goat anti-mouse Cy3 were from Jackson ImmunoResearch. The protocol for immunohistochemistry was described earlier (Perrin et al., 2000).

References

Araki Y, Tomita S, Yamaguchi H, Miyagi N, Sumioka A, Kirino Y, Suzuki T. 2003. Novel cadherin-related membrane proteins, Alcadeins, enhance the X11-like protein-mediated stabilization of amyloid beta-protein precursor metabolism. J. Biol. Chem 278:49448–49458.

Carrodeguas JA, Rodolosse A, Garza MV, Sanz-Clemente A, Pérez-Pé R, Lacosta AM, Domínguez L, Monleón I, Sánchez-Díaz R, Sorribas V, Sarasa M. 2005. The chick embryo appears as a natural model for research in beta-amyloid precursor protein processing. Neuroscience 134:1285–1300.

Hamburger V and Hamilton HL. 1951. A series of normal stages in the development of the chick embryo. J. Morph. 88:49–92.

Hintsch G, Zurlinden A, Meskenaite V, Steuble M, Fink-Widmer K, Kinter J, Sonderegger P. 2002. The calsyntenins--a family of postsynaptic membrane proteins with distinct neuronal expression patterns. Mol. Cell. Neurosci 21:393–409.

Hoerndli FJ, Walser M, Fröhli Hoier E, Quervain D de, Papassotiropoulos A, Hajnal A. 2009. A conserved function of C. elegans CASY-1 calsyntenin in associative learning. PLoS ONE 4:e4880.

Ikeda DD, Duan Y, Matsuki M, Kunitomo H, Hutter H, Hedgecock EM, Iino Y. 2008. CASY-1, an ortholog of calsyntenins/alcadeins, is essential for learning in Caenorhabditis elegans. Proc. Natl. Acad. Sci. U.S.A 105:5260–5265.

Konecna A, Frischknecht R, Kinter J, Ludwig A, Steuble M, Meskenaite V, Indermühle M, Engel M, Cen C, Mateos J, Streit P, Sonderegger P. 2006. Calsyntenin-1 docks vesicular cargo to kinesin-1. Mol. Biol. Cell 17:3651–3663.

Ludwig A, Blume J, Diep T, Yuan J, Mateos JM, Leuthäuser K, Steuble M, Streit P, Sonderegger P. 2009. Calsyntenins mediate TGN exit of APP in a kinesin-1-dependent manner. Traffic 10:572–589.

Mauti O, Sadhu R, Gemayel J, Gesemann M, Stoeckli ET. 2006. Expression patterns of plexins and neuropilins are consistent with cooperative and separate functions during neural development. BMC Dev. Biol 6:32.

Perrin FE, Stoeckli ET. 2000. Use of lipophilic dyes in studies of axonal pathfinding in vivo. Microsc. Res. Tech 48:25–31.

Preuschhof C, Heekeren HR, Li S, Sander T, Lindenberger U, Bäckman L. 2010. KIBRA and CLSTN2 polymorphisms exert interactive effects on human episodic memory. Neuropsychologia 48:402–408.

Ringman JM, Schulman H, Becker C, Jones T, Bai Y, Immermann F, Cole G, Sokolow S, Gylys K, Geschwind DH, Cummings JL, Wan HI. 2012. Proteomic changes in cerebrospinal fluid of presymptomatic and affected persons carrying familial Alzheimer disease mutations. Arch. Neurol. 69:96–104.

Steuble M, Diep T, Schätzle P, Ludwig A, Tagaya M, Kunz B, Sonderegger P. 2012. Calsyntenin-1 shelters APP from proteolytic processing during anterograde axonal transport. Biol Open 1:761–774.

Steuble M, Gerrits B, Ludwig A, Mateos JM, Diep T, Tagaya M, Stephan A, Schätzle P, Kunz B, Streit P, Sonderegger P. 2010. Molecular characterization of a trafficking organelle: dissecting the axonal paths of calsyntenin-1 transport vesicles. Proteomics 10:3775–3788.

Vagnoni A, Perkinton MS, Gray EH, Francis PT, Noble W, Miller CCJ. 2012. Calsyntenin-1 mediates axonal transport of the amyloid precursor protein and regulates Aβ production. Hum. Mol. Genet 21:2845–2854.

Vagnoni A, Rodriguez L, Manser C, Vos KJ de, Miller CCJ. 2011. Phosphorylation of kinesin light chain 1 at serine 460 modulates binding and trafficking of calsyntenin-1. J. Cell. Sci 124:1032–1042.

Vale RD, Schnapp BJ, Mitchison T, Steuer E, Reese TS, Sheetz MP. 1985. fferent axoplasmic proteins generate movement in opposite directions along microtubules in vitro. Cell 43:623–632.

Vogt L, Schrimpf SP, Meskenaite V, Frischknecht R, Kinter J, Leone DP, Ziegler U, Sonderegger P. 2001. Calsyntenin-1, a proteolytically processed postsynaptic membrane protein with a cytoplasmic calcium-binding domain. Mol. Cell. Neurosci 17:151–166.

Zhang H, Kranzler HR, Poling J, Gruen JR, Gelernter J. 2009. Cognitive flexibility is associated with KIBRA variant and modulated by recent tobacco use. Neuropsychopharmacology 34:2508–2516.

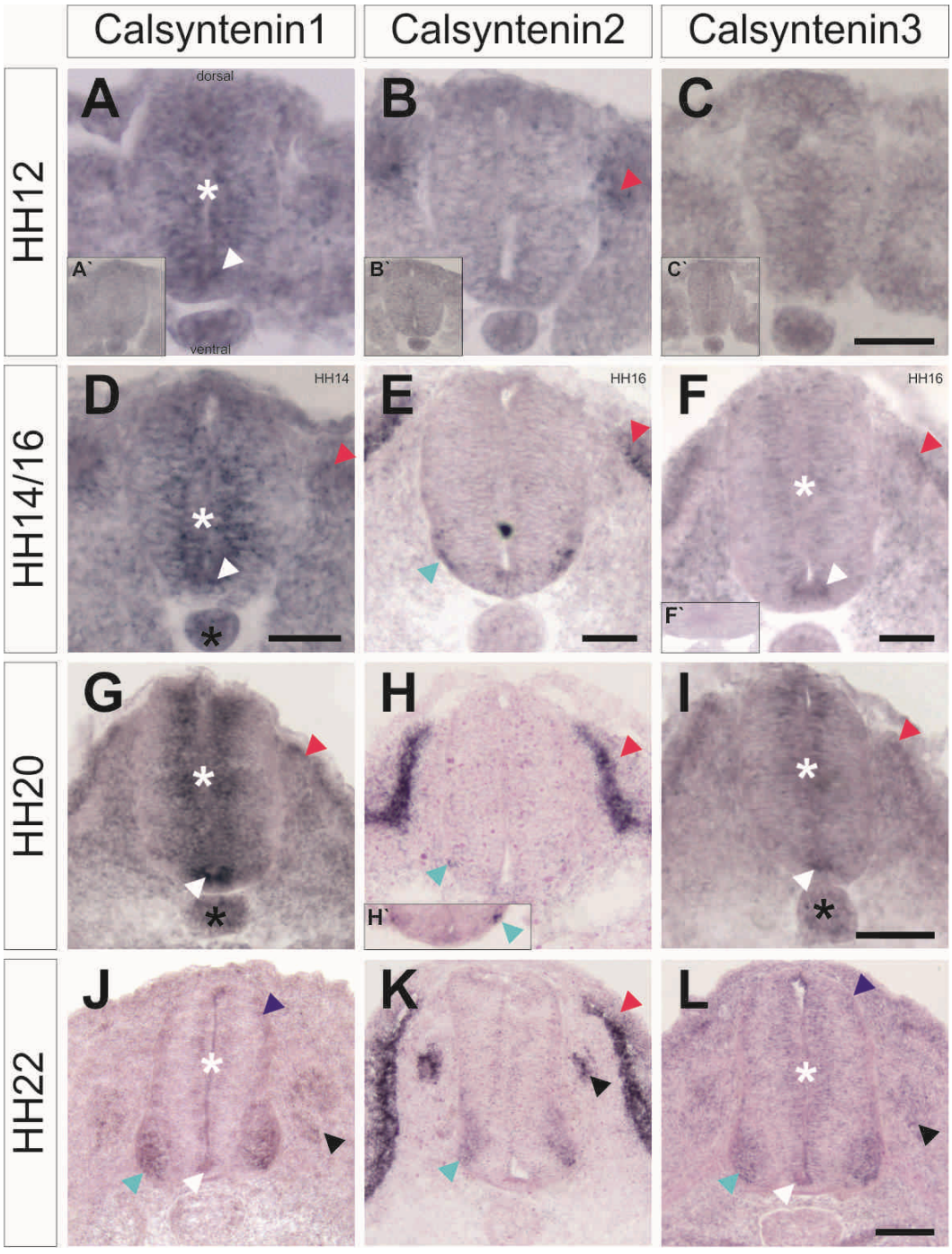

Figure 1: Calsyntenins are expressed in the lumbosacral spinal cord and dermomyotome at early stages. At HH12, Calsyntenin1 is expressed in neuronal precursors in the ventricular zone (A; white asterisk) and in the floor plate (white arrowhead). In contrast, Calsyntenin2 is not expressed in the spinal cord. Expression is only found in the somites (B; red arrowhead). Calsyntenin3 is not expressed at HH12 (C). At HH14, Calsyntenin1 is now also detected in the somites (D; red arrowhead) and in the notochord (black asterisk). At HH16, Calsyntenin2 is now detectable in a few motor neurons (E; light blue arrowhead). Calsyntenin3 is now

expressed similarly to Calsyntenin1, but without expression in the notochord (F). Starting at HH20, both Calsyntenin1 (G) and Calsyntenin3 (I) are expressed in the notochord (black asterisk). Calsyntenin2 is strongly expressed in the dermomyotome (H; red arrowhead) and some motor neurons (H,H'; light blue arrowhead). At HH22, all Calsyntenins are expressed in the DRGs (J-L; black arrowheads) and Calsyntenin1 and -3 are now also found in dorsal commissural neurons (dark blue arrowhead) and motor neurons (J,L; light blue arrowhead). Calsyntenins are no longer found in the notochord. (A'-C' and F') are sections hybridized with sense probes. Bar: 50 µm for (A-F) and 100 µm for (G-L).

Figure 2 (next page)**: Calsyntenin2 expression in the embryonic spinal cord is different from the other family members.** Expression of Calsyntenin2 (A-C) is compared to Pax-3 (D-F) and HNK1 (G-I) staining in the embryonic lumbosacral chicken spinal cord. Calsyntenin2 mRNA initially partially overlaps with Pax-3 (indicating the somites) (A,D). Later, we found overlap with some HNK1-positive cells which indicate neural crest cells (B,C,H and I). This is illustrated by the merged pictures (F,I), where Calsyntenin2 is shown in pink. (F',I') show antibody staining. From HH21 to HH28 (J-L), Calsyntenin2 is expressed in the dermomyotome (black arrowheads). At HH33 (M), Calsyntenin2 is expressed in epaxial (red arrowhead) and hypaxial muscles (blue arrowhead). Calsyntenin2 expression in cells surrounding the notochord is weak between HH33 (N) and HH36 (O), and increases at HH38 (P). At HH41 (Q), the signal in cells surrounding the notochord decreases. Bar: 50 µm for (A,B,D,E,G and H), 100 µm for (C,F,I,P and Q). 200 µm for (J,K,N and O), 500 µm for (L,M).

Figure 2

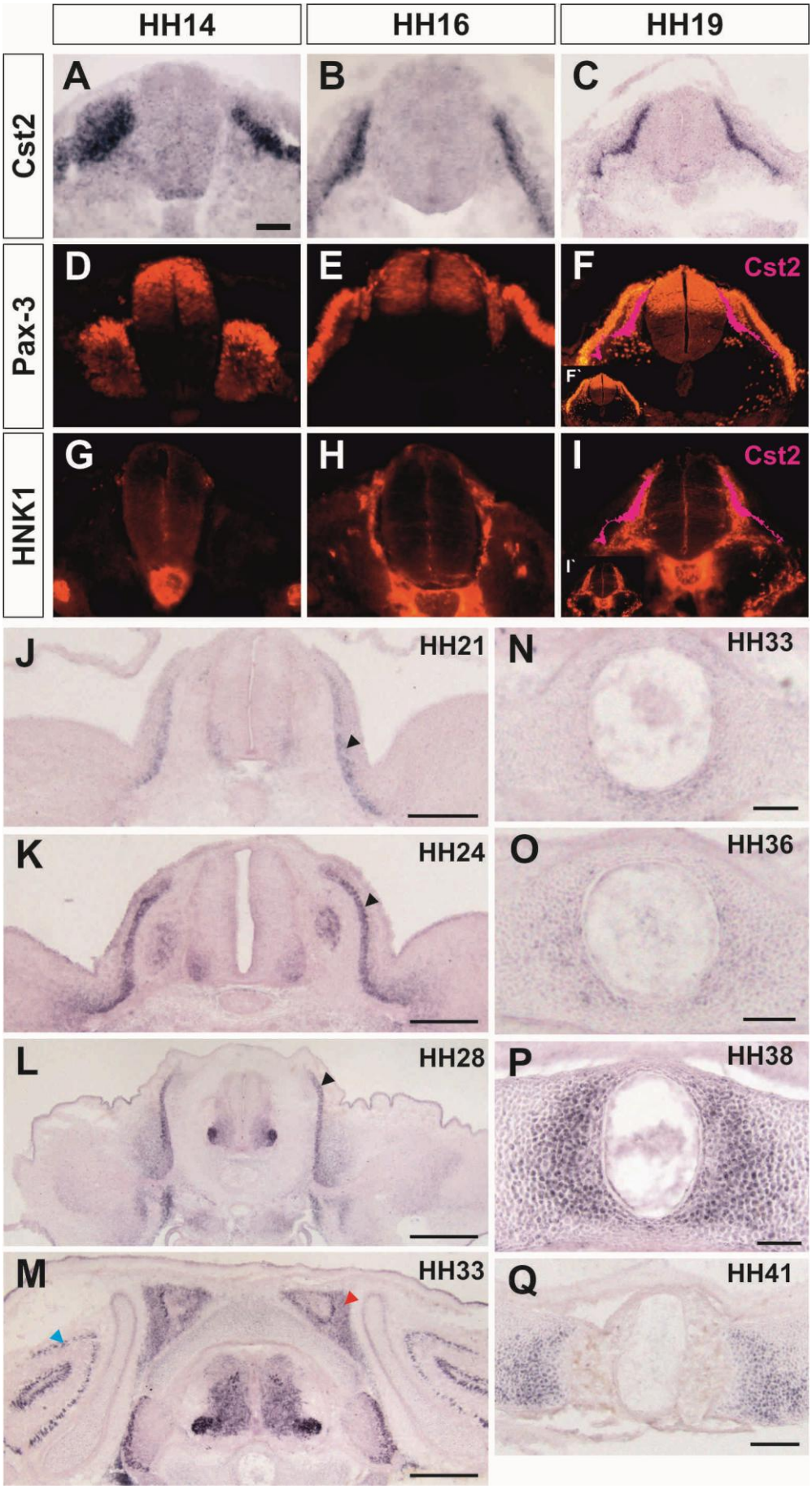
HH14
HH16
HH19
Cst2
Pax-3
HNK1
A
B
C
D
E
F
Cst2
F`
G
H
I
Cst2
I`
J
HH21
N
HH33
K
HH24
O
HH36
L
HH28
P
HH38
M
HH33
Q
HH41

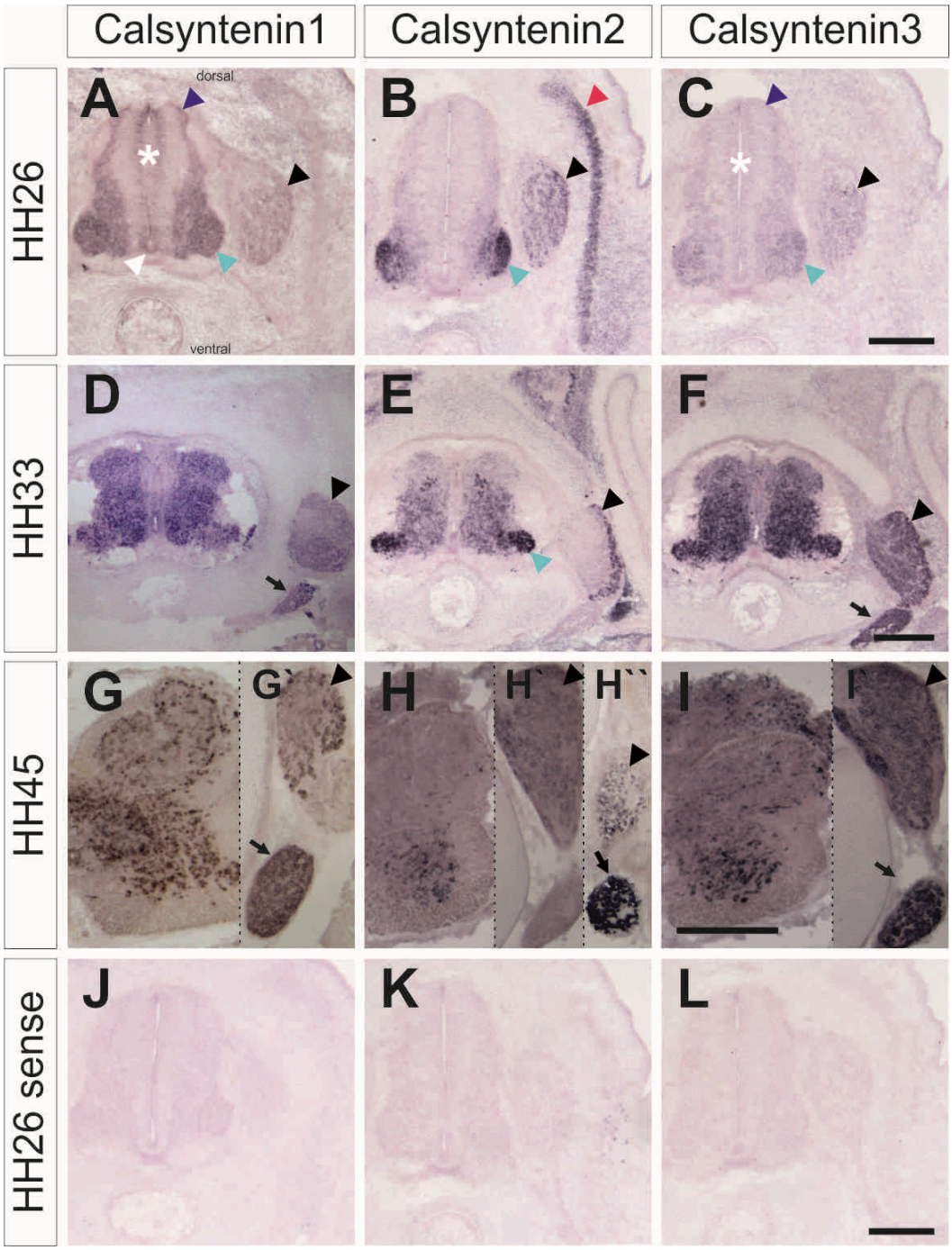

Figure 3: Calsyntenin expression in the lumbosacral chicken spinal cord persists between HH26 and HH45. At HH26, Calsyntenin1 (A) is expressed similarly as at HH22. Calsyntenin1 is still expressed in the ventricular zone (white asterisk), in DRGs (black arrowhead), in motor neurons (light blue arrowhead), in the floor plate (white arrowhead) and in dorsal commissural neurons (dark blue arrowhead). Similarly, Calsyntenin2 (B) and Calsyntenin3 (C) expression remains unchanged (see Figure 1K,L). At HH33 (D-F) Calsyntenins are expressed throughout the gray matter of the spinal cord, in the DRGs (black arrowhead), and in sympathetic

ganglia (arrow; except Calsyntenin2). Calsyntenin2 expression (E) is absent from the dorsal horn and strongest in the lateral motor columns (light blue arrowhead). At HH45, Calsyntenin1 (G) is still expressed throughout the gray matter of the spinal cord, in contrast to Calsyntenin2 (H) and -3 (I), which become restricted to the ventral spinal cord. All Calsyntenins are still expressed in the DRGs (G'-I'; black arrowheads) and Calsyntenin1 and -3 in the sympathetic ganglia (arrow). Calsyntenin2 is also expressed in the sympathetic ganglia, but only transiently around HH41 (H''; arrow). HH26 sense controls are shown in (J-L). Bar: 200 µm for (A-C) and (J-L), 500 µm for (D-I).

Figure 4

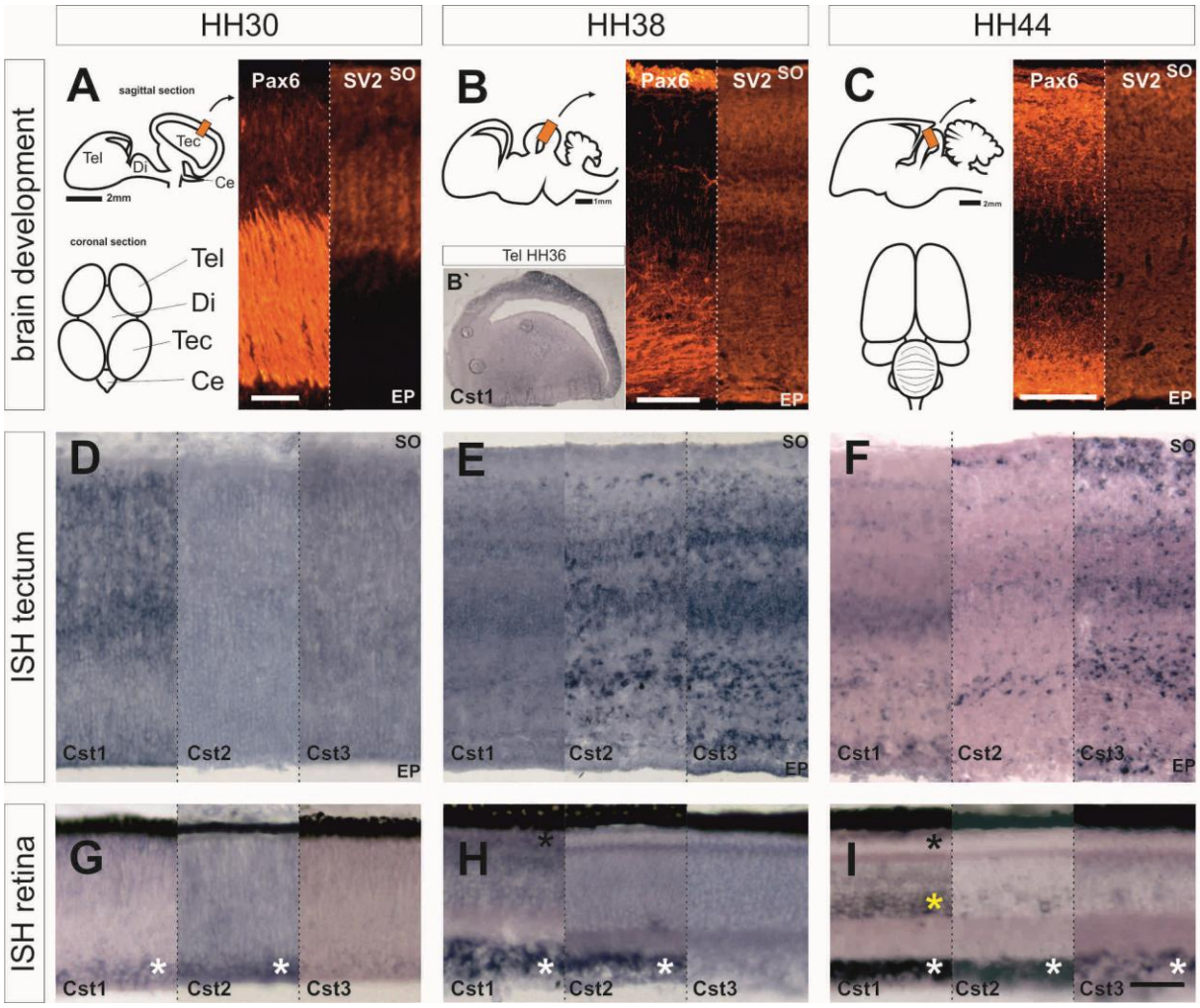

Figure 4 (previous page)**: All Calsyntenins are expressed in the developing brain in a dynamic manner.** Schematic development of the embryonic chicken brain and expression of Pax6 (indicating proliferating precursor cells) and SV2 (indicating synapses) in the embryonic tectum (A,B,C). (B') shows Calsyntenin1 expression in the telencephalon at HH36, which is similar for Calsyntenin2 and 3 (not shown). Calsyntenin expression in the tectum (D-F) and in the retina (G-I) indicate the dynamic expression of these genes during development. SO, stratum opticum; EP, ependymal layer; Tel, telencephalon; Di, diencephalon; Tec, tectum; Ce, cerebellum; future photoreceptor layer, black asterisk; inner nuclear layer, yellow asterisk; ganglion cell layer, white asterisk. Bar: 50 µm for HH30 (A and D) and all retina sections (G-I), 100 µm for HH38 (B and E), and 200 µm for HH44 (C and F).

Figure 5 (next page)**: Calsyntenins are dynamically expressed in the embryonic cerebellum.** At HH32, Calsyntenin1 (A) and -3 (C) are expressed in some cells of the cerebellar anlage. Calsyntenin2 (B) is detected in the roof of the cerebellar anlage (yellow arrowhead) and in the caudal ventricular zone (red arrowhead). At HH35, Calsyntenin1 (D) and -3 (F) are expressed in the deep cerebellar nuclei (red asterisks) and Calsyntenin2 (E) in the trigone area (red arrowhead). At HH36, Calsyntenin1 (G) is expressed in putative migrating glia cells (yellow asterisk) and in deep cerebellar nuclei (G'; red asterisk). Calsyntenin2 (H) and -3 (I) are expressed in the Purkinje cell layer (black arrowheads). In addition, Calsyntenin2 is expressed in the external granule cell layer (blue arrowhead) and Calsyntenin3 in deep cerebellar nuclei (I';red asterisk). At HH38 and HH40, Calsyntenin1 (J,N) is primarily expressed in the inner granule cell layer (black asterisks) and deep cerebellar nuclei (J',N'; red asterisks). Calsyntenin2 (K,O) and -3 (L,P) are still expressed in the Purkinje cell layer (black arrowhead). Calsyntenin2 is still found in the external granule cell layer (blue arrowhead) and Calsyntenin3 in deep cerebellar nuclei (L',P'; red asterisks). At HH44, Calsyntenin1 (R) and -2 (S) expressions become stronger in the inner granule

cell layer (black asterisks), whereas Calsyntenin3 expression (T) becomes restricted to some Purkinje cells (black arrowhead). No signals are detected when sections are processed with sense probes (U-W; HH44). Pax6 (M) was used as a marker for external germinal layer and calbindin (Q) was used as a marker for Purkinje cells. The inserts (G'-T') show the entire cerebellum. Bar: 100 µm for (A-C) and (J-M), 200 µm for (D-I) and (N-T).

Figure 5

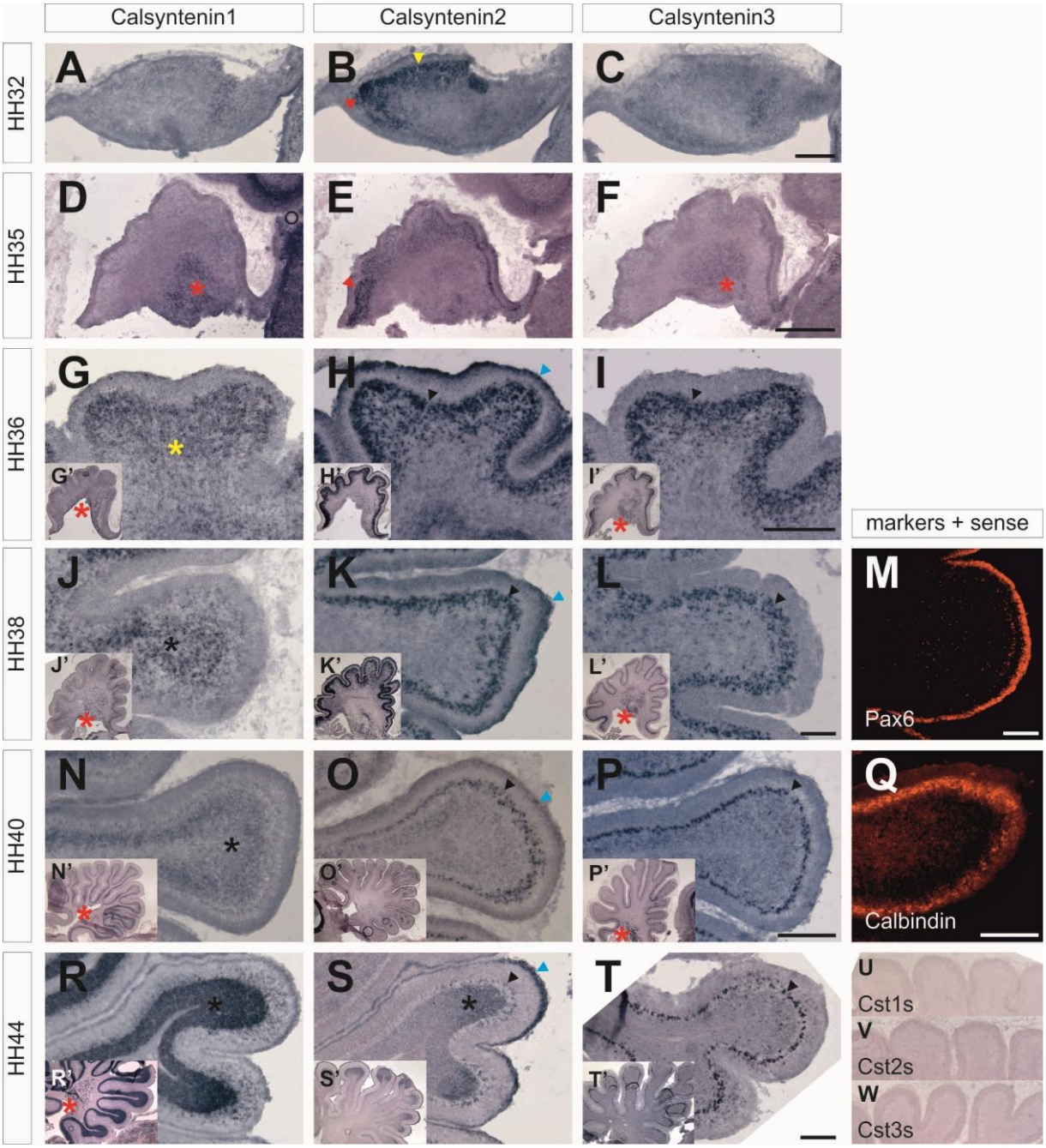

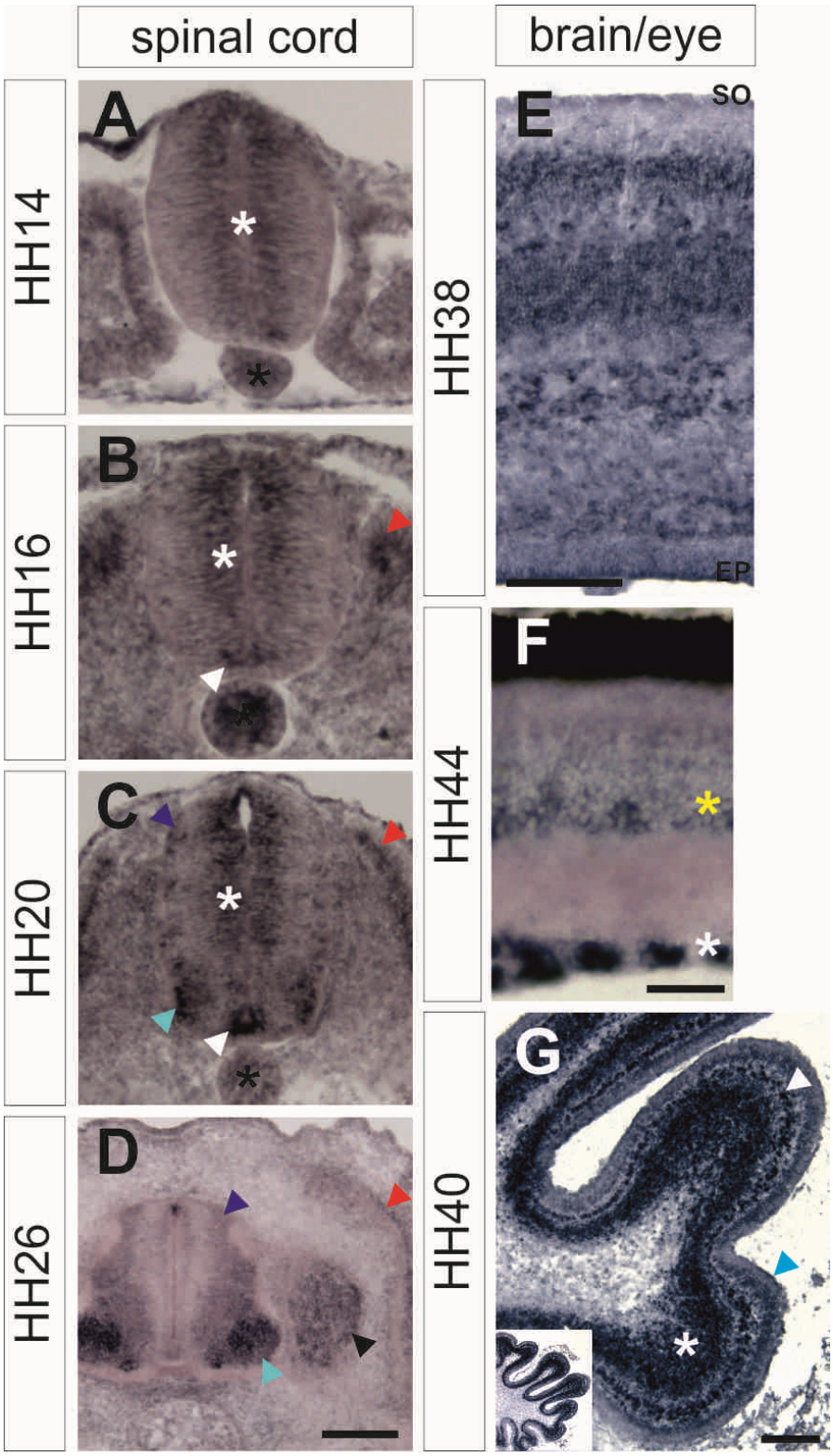

Figure 6: APP is expressed in a similar manner as Calsyntenins in and around the lumbosacral spinal cord and in the brain. Like Calsyntenin1 and -3, APP is also expressed in the early spinal cord in the ventricular zone (A-C; white asterisks). Similar to Calsyntenin2, APP is expressed in somites and their derivatives (B-D; red arrowheads). APP is also found in the notochord (A-C; black asterisks), in

commissural and motor neurons (C,D; dark and light blue arrowheads, respectively), in the floor plate (B,C; white arrowheads) and in the DRGs (D; black arrowheads). In the tectum at HH38 (E), APP and Calsyntenin expression patterns do not fully overlap (compare to Figure 4E). In the eye at HH44 (F), APP expression is found in retinal ganglion cells (white asterisk) and inner nuclear layer (yellow asterisk). APP is also expressed in the cerebellum at HH40 (G) in a Calsyntenin-like manner. APP is found in the inner granule cell layer (white asterisk), in the Purkinje cell layer (white arrowhead), and in the external granule cell layer (blue arrowhead). SO, stratum opticum; EP, ependymal layer. Bar: 50 µm for (A, B, and F), 100 µm for (C), and 200 µm for (D, E and G).

Table 1: Comparison of protein identities of Calsyntenin1, -2 and -3 from different species (hs, Homo sapiens; mm, Mus musculus; gg, Gallus gallus).

mmCst1	ggCst1	hsCst2	mmCst2	ggCst2	hsCst3	mmCst3	ggCst3	identities [%]
92.46	83.3	51.78	50.24	55.22	48.37	48.96	46.64	hsCst1
	81.67	51.38	49.85	54.22	48.27	48.66	46.34	mmCst1
		54.66	53.18	58.96	49.95	50.05	47.06	ggCst1
			92.76	75.35	44.54	44.54	42.16	hsCst2
				73.08	44.69	44.39	41.94	mmCst2
					44.58	44.28	41.89	ggCst2
						95.71	77.04	hsCst3
							77.04	mmCst3

4.2. Calsyntenin1-Mediated Trafficking of Axon Guidance Receptors Regulates the Switch in Axonal Responsiveness at Choice Points

Tobias Alther, Elena Domanitskaya and Esther T. Stoeckli
Institute of Molecular Life Sciences

Corresponding author: Esther T. Stoeckli
e-mail: esther.stoeckli@imls.uzh.ch

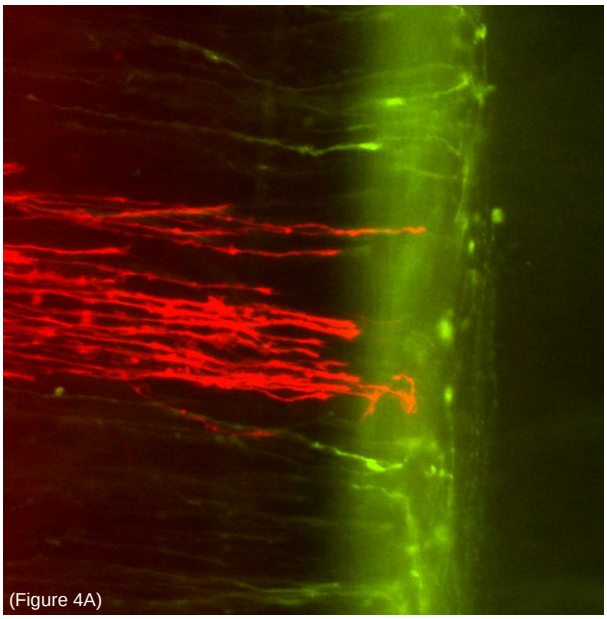

Key words: Commissural Axon Guidance, Frizzled3, RabGDI, Robo1, Wnt signaling, midline crossing

Highligts: specific trafficking of vesicles regulates receptor expression at choice points
Robo1 expression is regulated by both Calsyntenin1 and RabGDI
Frizzled3 expression is regulated by Calsyntenin1 but independent of RabGDI

I have carried out all the experiments except for the analysis of Frizzled3 function by in ovo RNAi with dsRNA. I have written the draft of the manuscript.

Abstract

Axon guidance at choice points depends on the precise regulation of guidance receptors on the growth cone surface. Upon arrival at the intermediate target or choice point, attraction needs to be switched to repulsion in order for the axon to move on. Dorsal commissural (dI1) axons crossing the ventral midline of the spinal cord in the floor plate represent a model for such a switch in axonal behavior.

Calsyntenin1 is involved in the regulation of vesicular trafficking of guidance receptors in dI1 axons and, thus, contributing to the switch in axonal responsiveness at the midline. In cooperation with RabGDI, Calsyntenin1 shuttles Rab11-positive vesicles containing Robo1 to the growth cone surface. In contrast, Calsyntenin1-mediated trafficking of Fzd3 is independent of RabGDI. Thus, tightly regulated insertion of these guidance receptors, which is required for midline crossing and the subsequent turn into the longitudinal axis, is achieved by specific trafficking.

Introduction

Correct wiring of the nervous system provides the basis for neural function. Attractive and repulsive cues cooperate to guide growing neurites to their correct targets. On their way to the final target, axons contact one or several intermediate targets. At each one of them, growth cones need to change their surface receptors in order to overcome the attraction derived from the cues associated with the intermediate target in order to continue their journey.

The dI1 population of commissural neurons has been widely used to study molecular mechanisms of axon guidance (Chédotal, 2011; Nawabi and Castellani, 2011). They extend their axons ventrally towards the floor plate, the structure that forms the midline of the neural tube. Thereby, axons are repelled by BMPs (Augsburger et al., 1999) and Draxin (Islam et al., 2009), the chemorepellents derived from the roof plate. At the same time, axons are attracted by the floor-plate derived chemoattractants Netrin (Kennedy et al., 1994) and Shh (Charron et al., 2003). Along their ventral pathway commissural axons are fasciculated due to the interaction of Axonin1/Contactin2 and NgCAM/L1, whereas the interaction between axonal

Axonin1 and floor plate NrCAM is responsible for floor-plate entry (Stoeckli and Landmesser, 1995; Stoeckli et al., 1997). RabGDI-dependent insertion of Robo1 into the growth cone membrane triggers sensitivity to the midline-associated repellent Slit (Philipp et al., 2012). Upon exit from the floor plate, post-crossing commissural axons turn rostrally guided by two opposing morphogen gradients (Stoeckli, 2006). A Wnt4 expression gradient in mouse (Lyuksyutova et al., 2003) or activity gradients of Wnt5a and Wnt7a in chick (Domanitskaya et al., 2010) were shown to attract post-crossing axons. At the same time, axons were repelled by a rostral^{low}-caudal^{high} gradient of Shh (Bourikas et al., 2005). In chick, Shh was shown to shape the Wnt gradient by inducing the expression of the endogenous Wnt antagonists Sfrp1 and Sfrp2 in a rostral^{low}-caudal^{high} gradient (Domanitskaya et al., 2010). Thus, Shh has multiple roles in commissural axon guidance: It attracts pre-crossing axons to the intermediate target in a Boc- and Smo-dependent manner (Charron et al., 2003; Okada et al., 2006). Then, it affects post-crossing axons both directly and indirectly by shaping the Wnt activity gradient. The direct repulsive effect on post-crossing axons is mediated by Hhip (Hedgehog-interacting protein; Bourikas et al., 2005). Recently, we demonstrated that Shh itself regulates the expression of Hhip in a Glypican1-dependent manner (Wilson and Stoeckli, 2013). The transcriptional regulation of Hhip by Shh, its own ligand, represents one mechanism explaining the switch in axonal responsiveness at the intermediate target. Another mechanism was described for the same axonal population by Nawabi and colleagues (Nawabi et al., 2010). NrCAM-dependent inhibition of the protease calpain upon midline contact stabilized PlexinA1 on axons and, thus, triggered a negative response to midline-derived Sema3B. In the visual system responsiveness to Sema3A was shown to be regulated at the posttranslational level by miR124 (Baudet et al., 2012). Our observation of the regulation of Robo1 surface expression at the posttranslational level by RabGDI suggested trafficking as yet another mechanism to switch axonal responsiveness at choice points (Philipp et al., 2012).

RabGDI, a gene linked to human mental retardation (D'Adamo et al. 1998), is an essential component of the vesicle fusion machinery (Seabra et al., 2002; Pfeffer and Aivazian, 2004). RabGDI associates with Rab11-positive vesicles (Philipp et al., 2012). Likewise, an association of Rab11-positive vesicles and Calsyntenin1 was found in kinesin-1-dependent axonal transport (Konecna et al., 2006; Steuble et al.,

2010). Calsyntenin1 is a member of a family of three transmembrane proteins (Vogt et al. 2001; Hintsch et al. 2002). They act as linkers between vesicular cargo and kinesin-1 (Konecna et al. 2006). Calsyntenin1 consists of an N-terminal signal peptide, two cadherin domains, an extracellular part with a conserved cleavage site (Hintsch et al. 2002), a transmembrane domain and an intracellular part containing two kinesin-1 binding sites (Konecna et al. 2006). Kinesin-1, the motor for anterograde axonal transport (Vale et al. 1985) interacts via its tetratricopeptides with the cytoplasmic domain of Calsyntenin1. Mutations in this domain result in reduced fast anterograde axonal transport (Konecna et al. 2006). The interaction between Calsyntenin1 and kinesin light chain1 (KLC1) was shown to be regulated by phosphorylation of Ser460 of KLC1 (Vagnoni et al. 2011).

Several studies reported that mutated calsyntenins result in memory impairment. CASY-1, the worm ortholog of Calsyntenin2, was shown to be essential for learning in Caenorhabditis elegans (Ikeda et al. 2008). Learning deficits in worms could be rescued by neuronal expression of human Calsyntenin2 (Hoerndli et al. 2009). Furthermore, human fMRI studies showed that allelic variations of Calsyntenin2 have an influence on learning (Jacobsen et al. 2009; Preuschhof et al. 2010). Another link to memory was provided by studies in Alzheimer research where lower levels of Calsyntenin3 were found in the cerebrospinal fluid of patients suffering from a familial form of Alzheimer's disease (Ringman et al. 2012). A study by Vagnoni and colleagues reported an association between the extent of Calsyntenin1 reduction in patients suffering from Alzheimer's disease and the levels of Aβ (Vagnoni et al. 2011). These results are in line with previous findings which link Calsyntenins to neuronal APP transport (Araki et al. 2003; Ludwig et al. 2009). Calsyntenin1 has been found in two non-overlapping trans-Golgi network-derived pathways (Steuble et al. 2010; Steuble et al. 2012). On the one hand, Calsyntenin1 was found in early endosomes together with APP, and on the other hand, Calsyntenin1 was found in recycling endosomes.

We have investigated the expression of Calsyntenins in the chicken embryo (Alther et al., submitted) and found them to be expressed in a dynamic, partially overlapping pattern in the developing spinal cord. In particular, we found Calsyntenin1 to be expressed in commissural neurons at the time when their axons reach and cross the

midline. Because Calsyntenin1 was found associated with Rab11-positive vesicles (Steuble et al. 2010; Steuble et al. 2012) and because RabGDI-positive vesicles which contained Robo1 were also positive for Rab11 immunoreactivity, we used heterologous expression in COS7 cells to test whether RabGDI co-localized with Calsyntenin1. Indeed, we found a partial overlap of Calsyntenin1 with Robo1, Rab11 and RabGDI-positive vesicles both in COS7 cells and in growth cones of commissural axons. Furthermore, in embryos lacking Calsyntenin1 many commissural axons were found to stall in the floor plate, thus, exhibiting the same phenotype as observed after knockdown of Robo1 or RabGDI. In addition, combinatorial knockdown of Calsyntenin1, Robo1 or RabGDI, indicated that commissural axons need all three proteins for proper midline crossing.

However, when Calsyntenin1 was silenced, we did not only observe commissural axons stalling in the floor plate but also found a large number of axons stalling at the contralateral floor-plate exit site, suggesting that Calsyntenin1 was also involved in an additional step of axonal navigation at the midline. Our previous studies indicated a role for the synaptic cell adhesion molecules SynCAMs (Niederkofler et al., 2010) and the morphogen Shh and Wnts in post-crossing axon guidance (Bourikas et al., 2005; Wilson and Stoeckli, 2013; Domanitskaya et al., 2010). Therefore, we investigated a role for Calsyntenin1-dependent trafficking in the regulation of SynCAM and Wnt/Shh signaling. Consistent with the co-localization studies, we found a role for Calsyntenin1-mediated trafficking in the regulation of Robo/Slit and Fzd/Wnt signaling.

Results

Commissural axons lacking Calsyntenin1 stall at the midline and fail to turn into the longitudinal axis

We found Calsyntenin1 to be expressed in dorsal commissural (dI1) neurons during the time of midline crossing (HH22-24) (Hamburger and Hamilton 1951; Alther et al., submitted). Calsyntenin1 mRNA was detected in lumbar dI1 commissural neurons

starting at HH21, that is, when the first axons have reached the ipsilateral floor-plate border and are ready for midline crossing (Supplementary Figure 1A-E). To investigate a potential function of the Calsyntenins in commissural axon guidance, we used in ovo RNAi and analyzed the consequences of Calsyntenin1 downregulation in open-book preparations of spinal cords collected from embryos at HH25-26 (Fig. 1A). In untreated (Fig. 1B) and in control-injected embryos (Fig. 1C) dI1 axons had crossed the midline and turned rostrally along the contralateral floor-plate border. After downregulation of Calsyntenin1 in dI1 neurons with a miR-based construct driven by the Math1 enhancer (Fig. 1D) or after Calsyntenin1 silencing by electroporation of dsRNA (Fig. 1E) axon guidance was severely perturbed (Fig. 1F). Both methods of Calsyntenin1 perturbation resulted in axonal stalling in the floor plate and in the failure of axonal turning into the longitudinal axis. On average, only 22.5±5.2% of the injection sites showed normal axonal navigation after injection and electroporation of a Math1-driven miR construct targeting Calsyntenin1. After injection and electroporation of dsRNA targeting Calsyntenin1, only 27.7±2.8% of the injection sites were found to show normal axon guidance. No, or only minor effects were observed when Calsyntenin2 or 3 were silenced, as 72.0±4.4% (miCst2) or 56.2±9.3% (dsCst2), and 46.7±4.0% (miCst3) or 63.0±8.4% (dsCst3), respectively, of the injection sites were normal (not shown; Table 1). Calsyntenin2, which is not expressed in dI1 neurons served as a negative control, demonstrating specificity of our approach. Although Calsyntenin3 is expressed in dI1 neurons during their navigation towards the floor plate and across the midline, its downregulation did not affect commissural axon guidance (Table 1). Efficiency of downregulation was demonstrated by in situ hybridization (Supplementary Fig. 1F,G; Supplementary Table 1).

Calsyntenin1 had a direct effect on axonal navigation, as it did not affect spinal cord patterning. After silencing calsyntenin1 during commissural axon guidance, expression of cell type-specific marker proteins did not differ between experimental and untreated control embryos (not shown). Furthermore, the phenotype was not due to a delay in axon outgrowth or a slower growth rate, as axons reached the floor plate at the appropriate stage and axons in embryos sacrificed one day later (at HH28/E6) had not grown any further and still failed to turn into the longitudinal axis (Supplementary Figure 1H-K). Similarly, neurite length was not different when

control-treated commissural neurons were compared to neurons lacking Calsyntenins grown on laminin (Figure 1G-K).

Taken together, our in vitro and in vivo experiments demonstrate a role for Calsyntenin1 in commissural axon guidance during floor-plate crossing and in the subsequent turning decision.

Calsyntenin1 partially overlaps with Robo1, RabGDI and Rab11 in COS7 cells and in commissural neurons

The aberrant axon guidance phenotype observed in the absence of Calsyntenin1 strongly resembled the phenotype observed in the absence of RabGDI (Philipp et al., 2012). In biochemical studies, Calsyntenin1 was shown to be associated with Rab11-positive vesicles (Steuble et al. 2010; Steuble et al. 2012). Since our previous in vivo studies indicated that RabGDI-dependent vesicular trafficking of Robo1 was also linked to Rab11-positive vesicles (Philipp et al., 2012), we tested for a role of Calsyntenin1 in the regulation of Robo1 surface expression. As a first step, we carried out co-localization studies with Calsyntenin1, Robo1, RabGDI and Rab11 using heterologous expression in COS7 cells. We also included Calsyntenin2 and -3, as well as Robo2. As described by others (Ludwig et al. 2009), we found Calsyntenins in the perinuclear area in the endoplasmatic reticulum, the Golgi apparatus and in the cytoplasm but rarely on the cell surface. Robo1 and 2 were localized to the same structures but also on the cell surface (Supplementary Figure 2). The analysis of ectopic expression of Robo1 and Robo2 with RabGDI, Rab11 and the Calsyntenins indicated their partial co-localization. The only exception was Calsyntenin2 which did not overlap with Rab11. The co-localization coefficient (Pearson's coefficient) in combination with scatter plots confirmed that Calsyntenin1 indeed partially co-localized with Robo1, Rab11 and RabGDI.

We verified these co-localizations in commissural neurons (Figure 2). To this end, we overexpressed Calsyntenin1, Robo1, RabGDI or Rab11 in commissural neurons in vivo at HH17. After two day, we sacrificed the embryos and dissected commissural neuron explants to visualize individual growth cones. We did not include Robo2 in these analyses because the lack of Robo2 was shown to result primarily in ipsilateral

turns and, thus, a phenotype different from the one obtained after downregulation of Calsyntenin1, Robo1, or RabGDI (Philipp et al. 2012). For the same reason, we also excluded Calsyntenin2 and -3. We found partial overlap between Calsyntenin1 and Robo1 (Figure 2A), RabGDI (Figure 2D), and Rab11 (Figure 2F). We confirmed our previous observations of a co-localization of Robo1 and Rab11 (Figure 2B) and RabGDI and Robo1 (Figure 2C), as well as RabGDI and Rab11 (Figure 2E; Philipp et al., 2012). The Pearson's coefficients of the double-stained axons are given in Figure 2H. The values from both the positive and negative control (Figure 2G,H) are significantly different from the other conditions (ANOVA, $p<0.05$). As positive control, we used an HA-Robo1-myc construct that was stained for both tags (HA in green, myc in red). As a negative control, we stained growth cones for γ-tubulin (green) and neurofilament (red). We also used triple staining to confirm co-localization of Calsyntenin1, Robo1, RabGDI, and Rab11 (Supplementary Figure 3).

Our co-localization studies confirm the existence of Calsyntenin1-positive vesicles containing Robo1 as cargo. In agreement with previous studies, Robo1-containing vesicles are associated with RabGDI and Rab11, suggesting that they are also associated with Calsyntenin1.

Calsyntenin1 and RabGDI are required for Robo1 insertion in commissural growth cones during floor-plate crossing

To get functional evidence for the cooperation between Calsyntenin1 and RabGDI in the regulation of Robo1 surface expression, we injected and electroporated miR-based constructs at hypomorphic doses. If Calsyntenin1 and RabGDI would act in the same pathway, the use of low doses should reproduce the phenotypes observed after efficient downregulation of RabGDI or Robo1. For a direct comparison we repeated the silencing of RabGDI and Robo1 obtained previously with dsRNA (Philipp et al., 2012) with miR constructs (Figure 3; see Experimental Procedures for details).

As expected, downregulation of Robo1 (Figure 3A) or RabGDI (Figure 3B) with 700 ng/µl of the Math1-driven miR constructs resulted in axonal stalling in the floor plate as seen previously, when we injected and electroporated dsRNA derived from Robo1

or RabGDI (Philipp et al., 2012). Downregulation of Robo1 (Figure 3C), RabGDI (Figure 3D), or Calsyntenin1 (Figure 3E) with low doses of miR constructs (300 and 350 ng/µl, respectively; see Experimental Procedures for details) did not result in axonal pathfinding errors (Figure 3F).

However, co-injection of all these miRs (against Calsyntenin1, Robo1, and RabGDI) at low concentrations did result in the expected phenotype, that is, axons were stalling in the floor plate and those that did reach the contralateral floor-plate border failed to turn rostrally along the longitudinal axis (Figure 4A,E). Similarly, reducing both Calsyntenin1 and RabGDI with hypomorphic doses was sufficient to induce floor-plate stalling (Figure 4B,E). The combination of low doses of Calsyntenin1 and Robo1 was less efficient in inducing floor-plate stalling (30.7±7.0% of the injection sites per embryo) but still interfered with correct axon guidance in comparison to control-treated embryos (Figure 4C,E). At HH18 Robo1 mRNA is already detected in dI1 neurons (Philipp et al., 2012). Thus, we reasoned that the weaker effect might be due to the presence of Robo1 protein in vesicles already at the time of electroporation at HH18. Thus, we repeated the injection and electroporation of the miCst1 together with the miRobo1 at HH15. In agreement with our hypothesis, we now found floor-plate stalling at 55.6±3.3% of the injection sites.

Taken together, the in ovo perturbation experiments indicate a role for Calsyntenin1 and RabGDI in the regulation of Robo1 trafficking to the growth cone surface.

Calsyntenin1 co-localizes with Fzd3 in COS7 cells and in commissural explants

In comparison with Calsyntenin1 silencing, RabGDI had a weaker effect on axonal turning into the longitudinal axis, although the strong effect on midline crossing did to some extent prevent the analysis of post-crossing axon guidance. Still, the qualitative difference between the RabGDI and the Calsyntenin1 phenotype prompted us to analyze the role of Calsyntenin1 in post-crossing commissural axon guidance in more detail.

In a previous study we had shown an effect of the synaptic cell adhesion molecules SynCAM1 and SynCAM2 on post-crossing commissural turning into the longitudinal

axis (Niederkofler et al., 2010). After silencing SynCAM1 in commissural neurons and SynCAM2 in neurons or the floor plate, axons crossed the midline successfully but failed to turn into the longitudinal axis at the contralateral floor-plate border. Because the observed phenotypes were similar to the aberrant turning seen in the absence of Calsyntenin1, we analyzed the distribution of SynCAMs in COS7 cells and in commissural axons (Figure 5). No significant overlap was found in COS7 cell expressing Calsyntenin1 and SynCAM1 (Figure 5A), SynCAM2 (Figure 5B), or SynCAM3 (Figure 5C). Similarly, no overlap was found between Calsyntenin1 and SynCAMs when overexpressed in commissural neurons (Figure 5D-F).

An alternative guidance receptor that might be trafficked to the growth cone membrane in a RabGDI and Calsyntenin-dependent manner was suggested by our studies on the role of morphogens, Shh and Wnts, in post-crossing commissural axon guidance (Bourikas et al., 2005; Domanitskaya et al., 2010; Wilson and Stoeckli, 2013). Shh, Wnt5a, and Wnt7a form gradients along the longitudinal axis of the spinal cord and steer growth cones of post-crossing commissural axons rostrally. Pre-crossing axons are not sensitive to these gradients. Therefore, the expression of surface receptors needs to be regulated in a temporally precisely controlled manner.

We showed earlier that the switch in responsiveness to Shh from attraction of pre-crossing axons to repulsion of post-crossing axons was due to the expression of a different receptor. While pre-crossing axons were attracted to Shh due to the expression of Boc and Smo (Charron et al., 2003; Okada et al., 2006), post-crossing axons were repelled by Shh due to the expression of Hhip (Bourikas et al., 2005). Recently, we showed that the expression of Hhip is controlled at the transcriptional level by Shh itself in a Glypican-1-dependent manner (Wilson and Stoeckli, 2013). Therefore, Hhip was unlikely to be trafficked by Calsyntenin1 or RabGDI. Indeed, we did not find any overlap between Hhip and Calsyntenin1 (Supplementary Figure 4A-D).

In contrast, immunoreactivities of Calsyntenin1 and Fzd3, the receptor for Wnts, strongly overlapped in commissural axons (Figure 6A,B). The divergent expression patterns of Hhip and Fzd3 were in line with the results of our in vivo analyses. Downregulation of Hhip at HH18/19 (E3) effectively interfered with the rostral turn of post-crossing commissural axons (Bourikas et al., 2005). In contrast, downregulation

of Fzd3 at HH18/19 did not effectively prevent the rostral turn of post-crossing commissural axons (Figure 6C). In agreement with the hypothesis that Fzd3 expression was regulated by selective trafficking, we found a robust interference with rostral turning of post-crossing commissural axons when the downregulation was done earlier, that is by injection and electroporation of a miR directed against Fzd3 at HH14/15 (Figure 6D). Fzd3 mRNA was already detected at HH18 (Figure 6E), thus, suggesting a regulation at the post-transcriptional or post-translational level.

Calsyntenin1 regulates Fzd3 expression on commissural axons independently of RabGDI

In embryos lacking Fzd3, 69.3±6.2% (Fzd3miR) of all injection sites displayed axons that failed to turn rostrally along the contralateral floor-plate border (Figure 6G,J). Similar findings have been published earlier in Fzd3 knockout mice, where post-crossing axons turned randomly anteriorly or posteriorly (Lyuksyutova et al. 2003). To assess a potential cooperation of Calsyntenin1 and Fzd3 in post-crossing commissural axon guidance, we again used a hypomorphic approach (Figure 6H-J). To this end, we decreased the amount of miRNA so that the injection of either the miR targeting Fzd3 (67.0±8.5% of the injection sites with normal axon guidance) or the one targeting Calsyntenin1 alone (67.0±5.2% of the injection sites with normal axon guidance) did not significantly interfere with post-crossing commissural axon guidance (Figure 6H,J). However, when we co-injected the low levels of miRs against Calsyntenin1 and Fzd3 most axons reached the contralateral border of the floor plate but did not turn rostrally at 70.6±5.5% of the injection sites.

Taken together, these results indicate a Calsyntenin1-dependent regulation of Fzd3 surface expression to ensure that dI1 axons respond to the Wnt activity gradient only after midline crossing.

Calsyntenin1 regulates Fzd3 expression independently of RabGDI

As a next step, we tested whether Fzd3 expression was regulated by vesicle trafficking involving both Calsyntenin1 and RabGDI, similar to Robo1. Using a similar

approach as detailed above, we injected and electroporated low amounts of miR constructs targeting Fzd3 and RabGDI. Again, the analysis of post-crossing axon navigation in open-book preparation of spinal cords dissected from embryos injected with a low dose of either miR alone did not reveal a significant perturbation of rostral turning (Figure 7A-C). We found normal axon pathfinding at 67.0±8.5% of the injection sites after electroporation of miFzd3 at low concentration, and at 60.2±5.6% after perturbation of RabGDI function with miRabGDI. This time, co-injection of both miRs did not increase the percentage of injection sites with aberrant axon pathfinding (65.9±1.5% injection sites with normal pathfinding; Figure 7C). Thus, we concluded that RabGDI is not required for Fzd3 trafficking to the growth cone surface.

Next, we analyzed the co-localization of Robo1 and Fzd3. Although both Robo1 and Fzd3 were mostly positive for Calsyntenin1 immunoreactivity, Robo1 and Fzd3 barely overlapped (Figure 7D-L). These findings support our in vivo data implicating Calsyntenin1 in both Robo1 and Fzd3 trafficking. However, in contrast to Robo1, Fzd3 trafficking is independent of RabGDI. Most likely, Calsyntenin1 is also required for the trafficking of additional vesicles containing yet unknown cargos, as many vesicles that were Calsyntenin-positive were not associated with either Fzd3 or Robo1 (Figure 7D-L).

Discussion

Midline crossing by dI1 commissural axons represents an easily accessible model to study the molecular mechanisms underlying the required switch in axonal responsiveness at a choice point. Axons are attracted towards the floor plate by chemoattractants. Entry into the floor plate is achieved by a predominance of positive signals derived from the growth cone's interaction with guidance cues expressed by floor-plate cells. However, in order to leave the floor plate and move on along the trajectory to the final target, axons need to overcome this attraction. Thus, the growth cone needs to change its surface receptors to recognize previously undetectable negative cues associated with the intermediate target. At the floor plate, these negative cues have been identified as Slits (Brose et al., 1999; Yuan et al., 1999) and class-3 semaphorins (Nawabi et al., 2010; Zou et al., 2000). Furthermore, axons need to ignore the guidance cues directing them along the longitudinal axis on the ipsilateral floor-plate border but readily detect them upon floor-plate exit. Both floor-plate crossing and turning into the longitudinal axis therefore depend on precisely regulated expression of guidance receptors on the growth cone surface.

Responsiveness to Semaphorin3B was shown to depend on stabilization of the surface receptor component PlexinA1 (Nawabi et al., 2010) and involve Shh-dependent sensitization (Parra and Zou, 2010). The sensitivity to Slit1 was triggered by the RabGDI-dependent trafficking of Robo1 to the growth cone surface (Philipp et al., 2012). In mouse, a switch in Robo3 isoform expression seems to contribute to regulate Robo1 sensitivity to Slit on pre- versus post-crossing commissural axons (Chen et al., 2008). Thus, different mechanisms are used to regulate midline crossing of commissural axons.

Similarly, the regulation of responsiveness to guidance cues for the longitudinal axis depends on changes in gene transcription and specific trafficking of guidance receptors. An example for regulation at the transcriptional level is provided by our findings that Shh induces the expression of its own receptor Hhip for the guidance of post-crossing axons in a Glypican1-dependent manner (Wilson and Stoeckli, 2013; Bourikas et al., 2005). In contrast, responsiveness of post-crossing axons to Wnts is regulated by trafficking of Fzd3 to the growth cone surface (this study). The specificity of vesicle trafficking and insertion of cargo proteins into the growth cone membrane is

supported by our findings that the regulatory mechanisms of Robo1 and Fzd3 surface expression differ. Robo1 surface expression depends on both RabGDI (Figure 4; Philipp et al., 2012) and Calsyntenin1 (Figure 4). In contrast, RabGDI was not required for the regulation of Fzd3 surface expression on post- versus pre-crossing axons (Figure 7).

Both, our previous in vivo studies characterizing the role of RabGDI in Robo1 regulation (Philipp et al., 2012) and the studies characterizing the role of Calsyntenin1 in Robo1 and Fzd3 regulation reported here, indicate that RabGDI and Calsyntenin1 are not required for axonal growth but specifically for axon guidance.

Material and Methods

In situ hybridization and immunohistochemistry of cryostat sections

Tissue preparation and sectioning for in situ hybridization and immunohistochemistry was described previously (Perrin and Stoeckli 2000). For in situ hybridization, we used the protocol described earlier (Mauti et al., 2006). Spinal cord patterning was assessed using antibodies against Nkx2.2, Isl1, and Pax6 (all from the Developmental Studies Hybridoma Bank). Commissural axons were stained with a rabbit anti-Axonin-1 antibody. As secondary antibodies, we used donkey anti-rabbit Alexa488 and goat anti-mouse Cy3 (both Jackson ImmunoResearch).

In ovo RNAi and open-book preparation

Fertilized chicken eggs obtained from a local hatchery were windowed after incubation at 38.5°C for 2-3 days. At the appropriate stage of development, we removed the extra-embryonic membranes to inject plasmids or dsRNA into the central canal of the embryo (Wilson and Stoeckli, 2012). We either used a miR-based

construct encoding GFP and the shRNA (Wilson and Stoeckli, 2011; see Supplementary Table 2 for sequences of the miR construct) at a concentration of 250 ng/µl for β-actin-driven constructs or 700 ng/µl for Math1-driven constructs. Alternatively, we used a combination of dsRNA (300 ng/µl) and a plasmid encoding GFP (25 ng/µl) in PBS with 0.02 % Fast Green (AppliChem). For electroporation, we used the same settings as described previously (Pekarik et al. 2003). After incubation for 2 to 3 days, embryos were sacrificed at the desired Hamburger and Hamilton (HH) stage (Hamburger V and Hamilton HL 1951) and their spinal cord were analyzed as open-book preparations as described earlier (Perrin and Stoeckli 2000). Open-book preparations were imaged using an OLYMPUS BX61 spinning disc microscope.

The polymerase-II-driven miRNA constructs were cloned as described previously (Wilson and Stoeckli 2011). We inserted the miR hairpin-loop structure using NheI and MluI (both NEB) to create either β-actin- or Math1-driven plasmids (see Supplementary Table 2 for sequences). We used bp 4283-4995 of the 3' UTR of chicken Calsyntenin1 (NM_001197050.1) to produce dsRNA according to our previously published protocol (Bourikas et al. 2005).

Hypomorphic dosages

To mimic double heterozygous approaches, which are often used in genetic analyses, we lowered the injected amount of each construct to levels which did not effectively interfere with axon guidance. The co-injection of two miR constructs targeting different genes was expected to interfere with axonal navigation, if the two target genes were working in the same pathway. The feasibility of this approach has been demonstrated previously in our analyses of Shh's role in post-crossing commissural axon guidance (Wilson and Stoeckli, 2013). To determine the hypomorphic amounts of the injected miR constructs, we typically used half the concentration (350 ng/µl) that was used for effective gene silencing. An exception was Math1-miRobo1, where we had to lower the concentration to 300 ng/µl.

Quantification of open-book phenotypes

For each group, a person blind to the experimental condition analyzed 10 to 15 open-book preparations with 11±3 injection sites per spinal cord. Only injection sites with GFP expression were included. We distinguished between three phenotypes: ipsilateral errors, which included either ipsilateral turns or stalling at the ipsilateral floor-plate border, floor-plate stalling, and no axonal turns at the contralateral floor-plate border. Because it is impossible to count individual axons, we scored an injection site as showing floor-plate stalling only when at least 50% of the DiI-labeled axons failed to reach the contralateral floor-plate border. Similarly, for the 'no turning' phenotype at least 50% of the axons reaching the floor-plate exit site had to fail to turn rostrally. Obviously, these two phenotypes are not completely independent of each other, as stalling of all axons in the floor plate would prevent the analysis of their turning behavior at the floor-plate exit site. Therefore, we compared the percentages of injection sites per embryo exhibiting normal axon guidance in our quantitative analyses. Statistical analysis of the data was done with SPSS. Normal distribution of the values was verified with the Shapiro-Wilk test ($p \leq 0.01$). P values were calculated with one-way ANOVA and Tukey's post-hoc tests (*$p \leq 0.05$ **$p \leq 0.001$ ***$p \leq 0.0001$). The p-values are given in the appendix.

COS7 cell cultures

COS-7 cells grown in Dulbecco's Modified Eagle Medium (DMEM, Invitrogen) supplemented with 2 % FCS were regularly passaged to avoid a confluent state. For transfection, cells were incubated in 150 µl DMEM with 10 % FCS and 50 µl transfection solution containing 250-400 ng DNA (for single transfection), 2x 200 ng DNA (for co-transfection) or 3x 200 ng DNA (for triple-transfection) and 1.25% Lipofectamine (Invitrogen) in Opti-MEM (GIBCO). A list of the transfected plasmids is given in Supplementary Table 3. Cells were incubated for 24-36 h. Cultures were washed, fixed and permeabilized for immunohistochemistry using rabbit anti-HA (Rockland) and mouse anti-myc (9E10; Developmental Studies Hybridoma Bank). We used goat anti-mouse Cy3 and donkey-anti rabbit Cy3 (ImmunoResearch), goat-anti mouseAlexa488 (MolecularProbes) and donkey anti-rabbitAlexa488.

Immunolabelled cells were imaged with a Leica SP2 confocal microscope using a 63x oil-immersion objective (NA=1.4) and an OLYMPUS BX61 spinning disc microscope with a 60x oil-immersion objective (NA=1.42). Image stacks (at least 20 stacks/cell, embracing the Nyquist criterion) were deconvolved using 3D Huygens Deconvolution & Analysis Software. Image analysis was done with Imaris (Bitplane).

Cultures of commissural neural explants and dissociated DRG neurons

Explants of commissural neurons or dissociated DRG neurons were dissected from untreated, control-treated or experimental embryos at HH25. Gene silencing (as described above) was carried out at HH18 for commissural neuron targeting and at HH15 for targeting DRG neurons. Neurons were plated in 8-well Lab-Tek dishes coated with polylysine and laminin (20 ng/ml). Dissociated DRG neurons were cultured for 24-36 h at a density of 10'000 cells/cm^2 as described previously (Stoeckli et al., 1996). Commissural explants were cultured as described previously (Stoeckli et al., 1997). Staining was done essentially as described above for COS7 cells, except that we also use goat-anti mouseAlex350 (Molecular Probes) and goat-anti rabbitAlexa350 (Invitrogen). Commissural growth cones were imaged using an OLYMPUS BX61 spinning disc microscope (NA=1.42). Image stacks were analyzed as described for the COS7 cells. For the co-localization assays, we compared scatter plots and the values of the Pearson's coefficient. Normal distribution of the values was verified with the Shapiro-Wilk test ($p \leq 0.01$). P values were calculated with one-way ANOVA and Tukey's post-hoc tests. The p-values of the comparison of the Pearson's coefficients are given in the appendix.

References

Araki, Yoichi; Tomita, Susumu; Yamaguchi, Haruyasu; Miyagi, Naomi; Sumioka, Akio; Kirino, Yutaka; Suzuki, Toshiharu (2003): Novel cadherin-related membrane proteins, Alcadeins, enhance the X11-like protein-mediated stabilization of amyloid beta-protein precursor metabolism. In *J. Biol. Chem.* 278 (49), pp. 49448–49458.

Augsburger, A.; Schuchardt, A.; Hoskins, S.; Dodd, J.; Butler, S. (1999): BMPs as mediators of roof plate repulsion of commissural neurons. In *Neuron* 24 (1), pp. 127–141.

Baudet, Marie-Laure; Zivraj, Krishna H.; Abreu-Goodger, Cei; Muldal, Alistair; Armisen, Javier; Blenkiron, Cherie et al. (2012): miR-124 acts through CoREST to control onset of Sema3A sensitivity in navigating retinal growth cones. In *Nat. Neurosci* 15 (1), pp. 29–38.

Bourikas, Dimitris; Pekarik, Vladimir; Baeriswyl, Thomas; Grunditz, Asa; Sadhu, Rejina; Nardó, Michele; Stoeckli, Esther T. (2005): Sonic hedgehog guides commissural axons along the longitudinal axis of the spinal cord. In *Nat. Neurosci* 8 (3), pp. 297–304.

Charron, Frédéric; Stein, Elke; Jeong, Juhee; McMahon, Andrew P.; Tessier-Lavigne, Marc (2003): The morphogen sonic hedgehog is an axonal chemoattractant that collaborates with netrin-1 in midline axon guidance. In *Cell* 113 (1), pp. 11–23.

Chédotal, Alain (2011): Further tales of the midline. In *Curr. Opin. Neurobiol.* 21 (1), pp. 68–75.

Chen, Zhe; Gore, Bryan B.; Long, Hua; Le Ma; Tessier-Lavigne, Marc (2008): Alternative splicing of the Robo3 axon guidance receptor governs the midline switch from attraction to repulsion. In *Neuron* 58 (3), pp. 325–332.

D'Adamo, P.; Menegon, A.; Lo Nigro, C.; Grasso, M.; Gulisano, M.; Tamanini, F. et al. (1998): Mutations in GDI1 are responsible for X-linked non-specific mental retardation. In *Nat. Genet.* 19 (2), pp. 134–139.

Domanitskaya, Elena; Wacker, Andrin; Mauti, Olivier; Baeriswyl, Thomas; Esteve, Pilar; Bovolenta, Paola; Stoeckli, Esther T. (2010): Sonic hedgehog guides post-crossing commissural axons both directly and indirectly by regulating Wnt activity. In *J. Neurosci.* 30 (33), pp. 11167–11176.

Hamburger V and Hamilton HL (1951): A series of normal stages in the development of the chick embryo. J. Morph. 8 (8), pp. 49-92.

Hintsch, G.; Zurlinden, A.; Meskenaite, V.; Steuble, M.; Fink-Widmer, K.; Kinter, J.; Sonderegger, P. (2002): The calsyntenins--a family of postsynaptic membrane proteins with distinct neuronal expression patterns. In *Mol. Cell. Neurosci* 21 (3), pp. 393–409.

Hoerndli, Frédéric J.; Walser, Michael; Fröhli Hoier, Erika; Quervain, Dominique de; Papassotiropoulos, Andreas; Hajnal, Alex (2009): A conserved function of C. elegans CASY-1 calsyntenin in associative learning. In *PLoS ONE* 4 (3), pp. e4880.

Ikeda, Daisuke D.; Duan, Yukan; Matsuki, Masahiro; Kunitomo, Hirofumi; Hutter, Harald; Hedgecock, Edward M.; Iino, Yuichi (2008): CASY-1, an ortholog of calsyntenins/alcadeins, is essential for learning in Caenorhabditis elegans. In *Proc. Natl. Acad. Sci. U.S.A.* 105 (13), pp. 5260–5265.

Islam, Shahidul M.; Shinmyo, Yohei; Okafuji, Tatsuya; Su, Yuhong; Naser, Iftekhar Bin; Ahmed, Giasuddin et al. (2009): Draxin, a repulsive guidance protein for spinal cord and forebrain commissures. In *Science* 323 (5912), pp. 388–393.

Jacobsen, Leslie K.; Picciotto, Marina R.; Heath, Christopher J.; Mencl, W. Einar; Gelernter, Joel (2009): Allelic variation of calsyntenin 2 (CLSTN2) modulates the impact of developmental tobacco smoke exposure on mnemonic processing in adolescents. In *Biol. Psychiatry* 65 (8), pp. 671–679.

Kennedy, T. E.; Serafini, T.; La Torre, J. R. de; Tessier-Lavigne, M. (1994): Netrins are diffusible chemotropic factors for commissural axons in the embryonic spinal cord. In *Cell* 78 (3), pp. 425–435.

Konecna, Anetta; Frischknecht, Renato; Kinter, Jochen; Ludwig, Alexander; Steuble, Martin; Meskenaite, Virginia et al. (2006): Calsyntenin-1 docks vesicular cargo to kinesin-1. In *Mol. Biol. Cell* 17 (8), pp. 3651–3663.

Ludwig, Alexander; Blume, Jessica; Diep, Tu-My; Yuan, Ju; Mateos, José María; Leuthäuser, Kerstin et al. (2009): Calsyntenins mediate TGN exit of APP in a kinesin-1-dependent manner. In *Traffic* 10 (5), pp. 572–589.

Lyuksyutova, Anna I.; Lu, Chin-Chun; Milanesio, Nancy; King, Leslie A.; Guo, Nini; Wang, Yanshu et al. (2003): Anterior-posterior guidance of commissural axons by Wnt-frizzled signaling. In *Science* 302 (5652), pp. 1984–1988.

Mauti, Olivier; Sadhu, Rejina; Gemayel, Joelle; Gesemann, Matthias; Stoeckli, Esther T. (2006): Expression patterns of plexins and neuropilins are consistent with cooperative and separate functions during neural development. In *BMC Dev. Biol.* 6, p. 32.

Nawabi, Homaira; Briançon-Marjollet, Anne; Clark, Christopher; Sanyas, Isabelle; Takamatsu, Hyota; Okuno, Tatsusada et al. (2010): A midline switch of receptor processing regulates commissural axon guidance in vertebrates. In *Genes Dev* 24 (4), pp. 396–410.

Nawabi, Homaira; Castellani, Valérie (2011): Axonal commissures in the central nervous system: how to cross the midline? In *Cell. Mol. Life Sci.* 68 (15), pp. 2539–2553.

Niederkofler, Vera; Baeriswyl, Thomas; Ott, Regula; Stoeckli, Esther T. (2010): Nectin-like molecules/SynCAMs are required for post-crossing commissural axon guidance. In *Development* 137 (3), pp. 427–435.

Okada, Ami; Charron, Frédéric; Morin, Steves; Shin, David S.; Wong, Karen; Fabre, Pierre J. et al. (2006): Boc is a receptor for sonic hedgehog in the guidance of commissural axons. In *Nature* 444 (7117), pp. 369–373.

Pekarik, Vladimir; Bourikas, Dimitris; Miglino, Nicola; Joset, Pascal; Preiswerk, Stephan; Stoeckli, Esther T. (2003): Screening for gene function in chicken embryo using RNAi and electroporation. In *Nat. Biotechnol* 21 (1), pp. 93–96.

Perrin, F. E.; Stoeckli, E. T. (2000): Use of lipophilic dyes in studies of axonal pathfinding in vivo. In *Microsc. Res. Tech.* 48 (1), pp. 25–31.

Pfeffer, Suzanne; Aivazian, Dikran (2004): Targeting Rab GTPases to distinct membrane compartments. In *Nat. Rev. Mol. Cell Biol.* 5 (11), pp. 886–896.

Philipp, Melanie; Niederkofler, Vera; Debrunner, Marc; Alther, Tobias; Kunz, Beat; Stoeckli, Esther T. (2012): RabGDI controls axonal midline crossing by regulating Robo1 surface expression. In *Neural Dev* 7 (1), p. 36.

Preuschhof, Claudia; Heekeren, Hauke R.; Li, Shu-Chen; Sander, Thomas; Lindenberger, Ulman; Bäckman, Lars (2010): KIBRA and CLSTN2 polymorphisms exert interactive effects on human episodic memory. In *Neuropsychologia* 48 (2), pp. 402–408.

Ringman, John M.; Schulman, Howard; Becker, Chris; Jones, Ted; Bai, Yuchen; Immermann, Fred et al. (2012): Proteomic changes in cerebrospinal fluid of presymptomatic and affected persons carrying familial Alzheimer disease mutations. In Arch. Neurol. 69 (1), pp. 96–104.

Seabra, Miguel C.; Mules, Emilie H.; Hume, Alistair N. (2002): Rab GTPases, intracellular traffic and disease. In *Trends Mol Med* 8 (1), pp. 23–30.

Steuble, Martin; Diep, Tu-My; Schätzle, Philipp; Ludwig, Alexander; Tagaya, Mitsuo; Kunz, Beat; Sonderegger, Peter (2012): Calsyntenin-1 shelters APP from proteolytic processing during anterograde axonal transport. In *Biol Open* 1 (8), pp. 761–774.

Steuble, Martin; Gerrits, Bertran; Ludwig, Alexander; Mateos, José María; Diep, Tu-My; Tagaya, Mitsuo et al. (2010): Molecular characterization of a trafficking organelle: dissecting the axonal paths of calsyntenin-1 transport vesicles. In *Proteomics* 10 (21), pp. 3775–3788.

Stoeckli, E. T.; Landmesser, L. T. (1995): Axonin-1, Nr-CAM, and Ng-CAM play different roles in the in vivo guidance of chick commissural neurons. In *Neuron* 14 (6), pp. 1165–1179.

Stoeckli, E. T.; Sonderegger, P.; Pollerberg, G. E.; Landmesser, L. T. (1997): Interference with axonin-1 and NrCAM interactions unmasks a floor-plate activity inhibitory for commissural axons. In *Neuron* 18 (2), pp. 209–221.

Stoeckli, E. T.; Ziegler, U.; Bleiker, A. J.; Groscurth, P.; Sonderegger, P. (1996): Clustering and functional cooperation of Ng-CAM and axonin-1 in the substratum-contact area of growth cones. In *Dev. Biol.* 177 (1), pp. 15–29.

Stoeckli, Esther T. (2006): Dissection of Spinal Cords for Analysis of Axonal Pathfinding in dsRNA-Treated Avian Embryos. In *CSH Protoc* 2006 (4).

Vagnoni, Alessio; Rodriguez, Lilia; Manser, Catherine; Vos, Kurt J. de; Miller, Christopher C. J. (2011): Phosphorylation of kinesin light chain 1 at serine 460 modulates binding and trafficking of calsyntenin-1. In *J. Cell. Sci.* 124 (Pt 7), pp. 1032–1042.

Vale, R. D.; Schnapp, B. J.; Mitchison, T.; Steuer, E.; Reese, T. S.; Sheetz, M. P. (1985): Different axoplasmic proteins generate movement in opposite directions along microtubules in vitro. In *Cell* 43 (3 Pt 2), pp. 623–632.

Vogt, L.; Schrimpf, S. P.; Meskenaite, V.; Frischknecht, R.; Kinter, J.; Leone, D. P. et al. (2001): Calsyntenin-1, a proteolytically processed postsynaptic membrane protein with a cytoplasmic calcium-binding domain. In *Mol. Cell. Neurosci* 17 (1), pp. 151–166.

Wilson, Nicole H.; Stoeckli, Esther T. (2011): Cell type specific, traceable gene silencing for functional gene analysis during vertebrate neural development. In *Nucleic Acids Res* 39 (20), pp. e133.

Wilson, Nicole H.; Stoeckli, Esther T. (2012): In ovo Electroporation of miRNA-based Plasmids in the Developing Neural Tube and Assessment of Phenotypes by DiI Injection in Open-book Preparations. In *J Vis Exp* (68).

Wilson, Nicole H.; Stoeckli, Esther T. (2013): Sonic hedgehog regulates its own receptor on postcrossing commissural axons in a glypican1-dependent manner. In *Neuron* 79 (3), pp. 478–491.

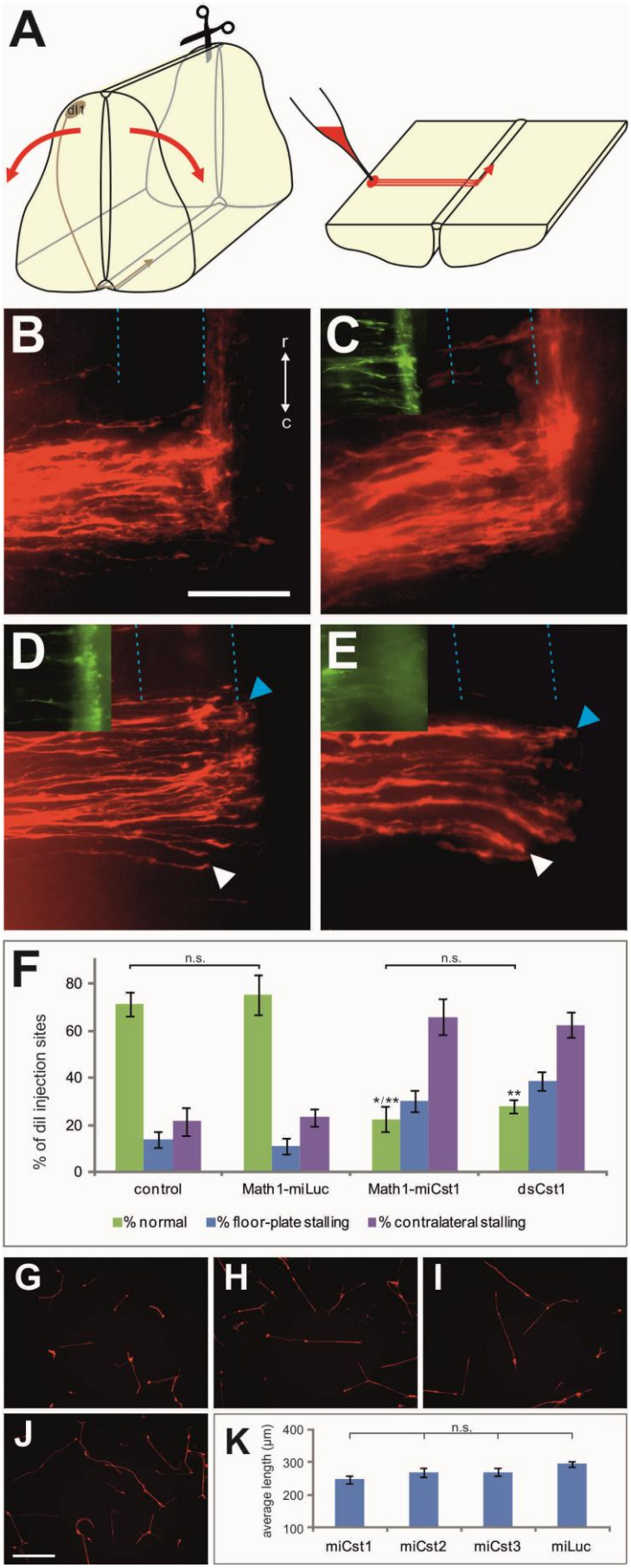
A
dil
B
r
c
C
D
E
F
n.s.
n.s.
80
60
40
20
0
% of dil injection sites
*/**
**
control
Math1-miLuc
Math1-miCst1
dsCst1
% normal
% floor-plate stalling
% contralateral stalling
G
H
I
J
K
n.s.
400
300
200
100
average length (µm)
miCst1
miCst2
miCst3
miLuc

Figure 1

Figure 1 (previous page)**: Silencing calsyntenin1 prevents commissural axons from crossing the floor plate and turning rostrally along the contralateral border.** (A) Spinal cords were dissected from embryos at HH25/26 and prepared as open-book preparations to visualize commissural axons labeled by DiI injections. Axons in untreated (B) and control-injected embryos (C) had crossed the floor plate and turned rostrally into the longitudinal axis. In contrast, injection and electroporation of a Math1-driven miRNA construct targeting calsyntenin1 (D; miCst1) or dsRNA derived from calsyntenin1 (E; dsCst1) resulted in axons stalling in the floor plate (white arrowhead) or axons failing to turn into the longitudinal axis (blue arrowhead). Pathfinding was quantified as detailed in the Experimental Procedures (F; Table 1). Control-treated embryos injected and electroporated with a miRNA construct targeting Luciferase had on average 75.0±8.5% normal injection sites. This value was not significantly different from the percentage of normal injection sites found in untreated embryos (71.1±5.1%). In contrast, only an average of 22.5±5.2 % of the injection sites showed normal axonal navigation after downregulation of Calsyntenin1 specifically in dI1 neurons with miCst1. This value was virtually identical for downregulation of Calsyntenin1 with dsRNA, where 27.7±2.8% of the DiI injection sites were normal. (G-K) Calsyntenin1 affects guidance not growth of commissural axons. Downregulation of Calsyntenin1 (G), Calsyntenin2 (H), or Calsyntenin3 (I) did not affect neurite length of dissociated commissural axons cultured on laminin compared to control-treated axons, injected and electroporated with miLuc (J). No significant differences between the conditions were found (K). Inserts in (C-E) show GFP expression as injection control. Bar: 50 µm (B-E), 100 µm (G-J). * $p<0.05$ for Math-miCst1 compared to control, ** $p<0.01$ for Math-miCst1 versus Math-miLuc and dsCst1 versus both control groups. n.s. not significant. Values are given ± SEM.

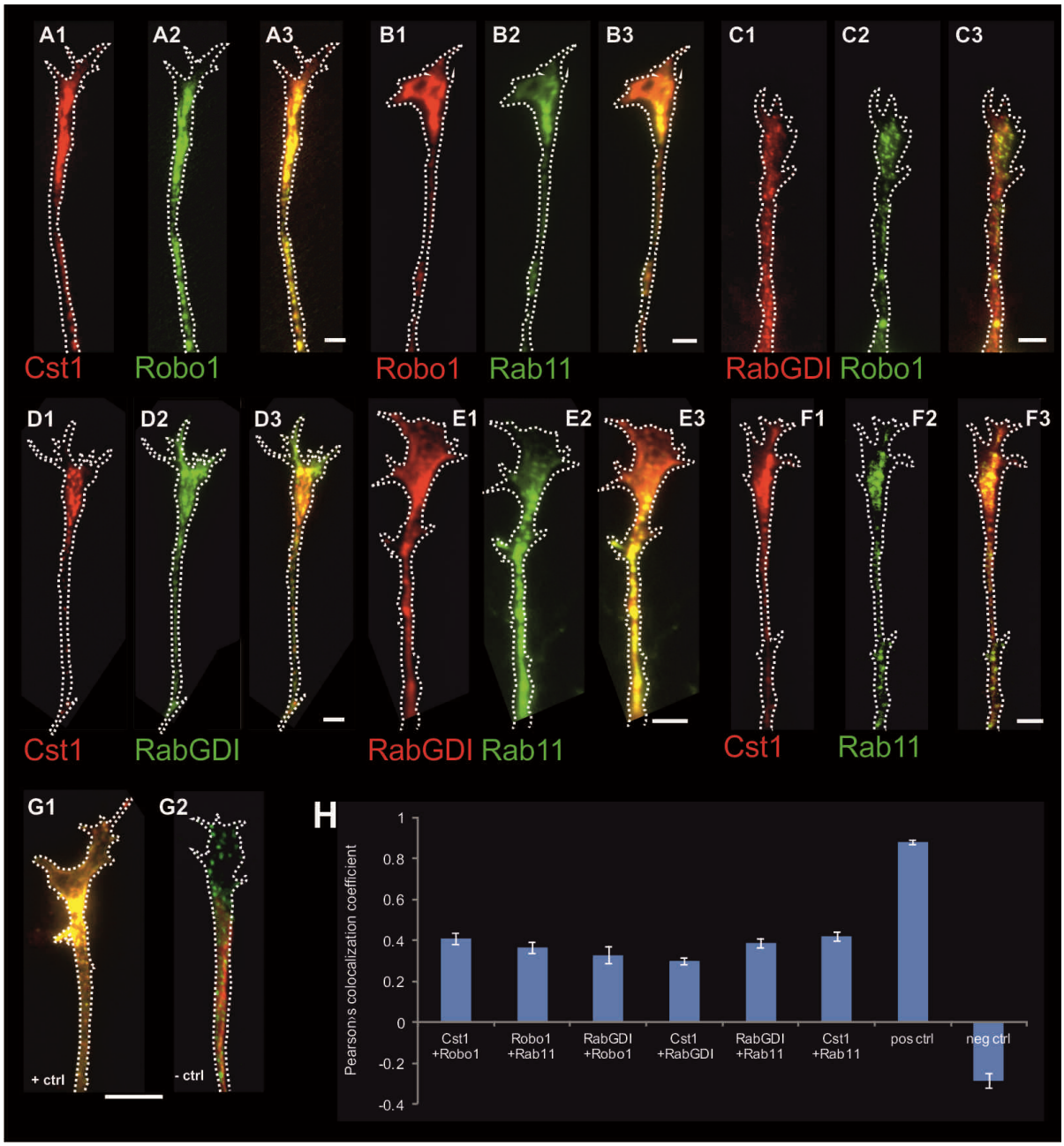

Figure 2: Calsyntenin1, RabGDI and Rab11 partially co-localize with Robo1-positive vesicles. Commissural neurons were dissected at HH25 from embryos injected and transfected with either mCherry-Calsyntenin1, RabGDI, Rab11, or Robo1. After 24-36 hours in vitro, axons were fixed and stained with anti-tag antibodies. Confocal image analysis followed by deconvolution indicated partial overlap between immunoreactivities for Calsyntenin1 and Robo1 (A), Robo1 and Rab11 (B), RabGDI and Robo1 (C), Cst1 and RabGDI (D), RabGDI and Rab11 (E), Calsyntenin1 and Rab11 (F). Co-localization coefficients are given in (H). As positive control, we stained double-tagged Robo1 with antibodies against both tags (for total

overlap; G1; H), and we stained neurofilament (red) and γ-tubulin (green) as a negative control, showing no overlap (G2; H). Values are given ± SEM. Bar: 5 µm.

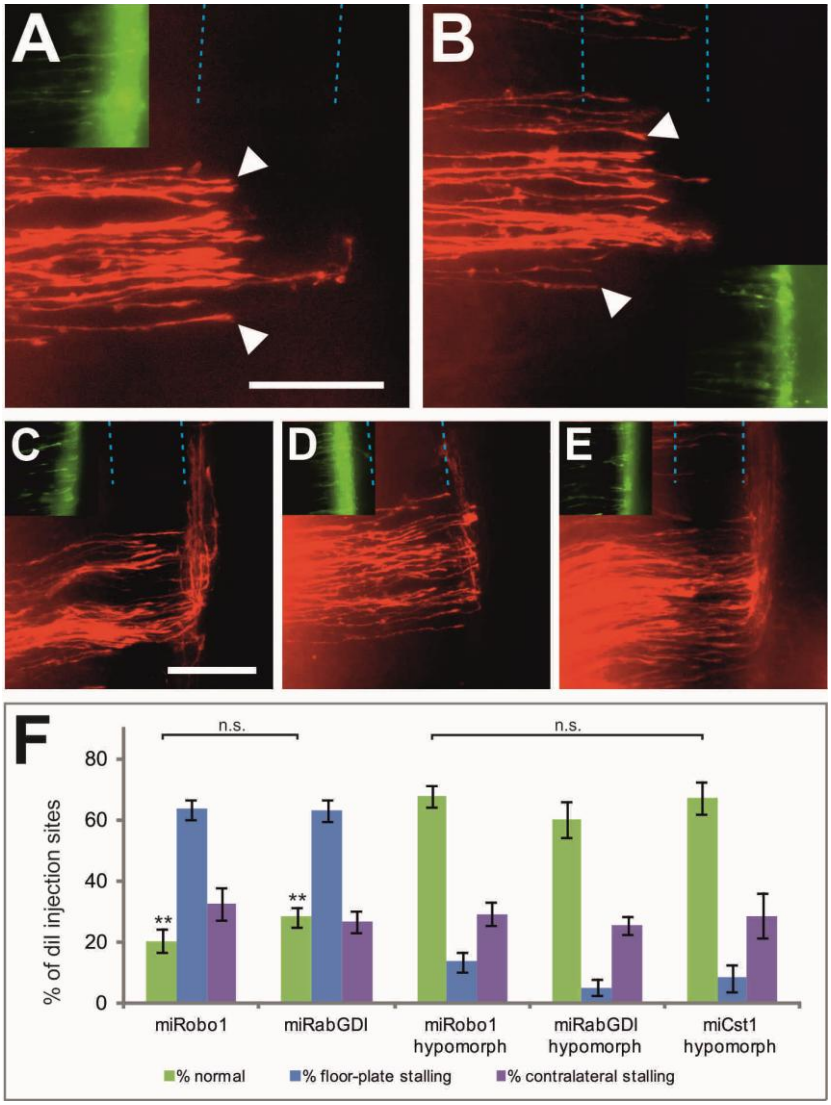

Figure 3: Downregulation of Robo1 and RabGDI reproduces the axon stalling phenotype observed in the absence of Calsyntenin1. Downregulation of Robo1 (A) or RabGDI (B) with miR constructs resulted in axonal stalling in the floor plate, as observed previously (Philipp et al., 2012). In the absence of Robo1, only 20.6±3.7% of the injection sites showed normal axonal pathfinding (F). In the absence of RabGDI, 28.4±3.3% of the injection sites showed normal axonal navigation. (C-E) Lowering the injected amount of the miR constructs to 300 ng/µl (miRobo1; C) or 350 ng/µl (miRabGDI (D); miCst1 (E)), respectively, did not significantly interfere with axon guidance, as normal axonal pathfinding was observed at 67.7±3.5%,

60.2±5.6%, and 67.0±5.20% of the injection sites (F). Inserts in (A-E) show GFP expression as injection control. Bar: 50 µm. n.s. not significant. ** p<0.01 compared to hypomorphic conditions and control groups (see Figure 1F). Values are given ± SEM.

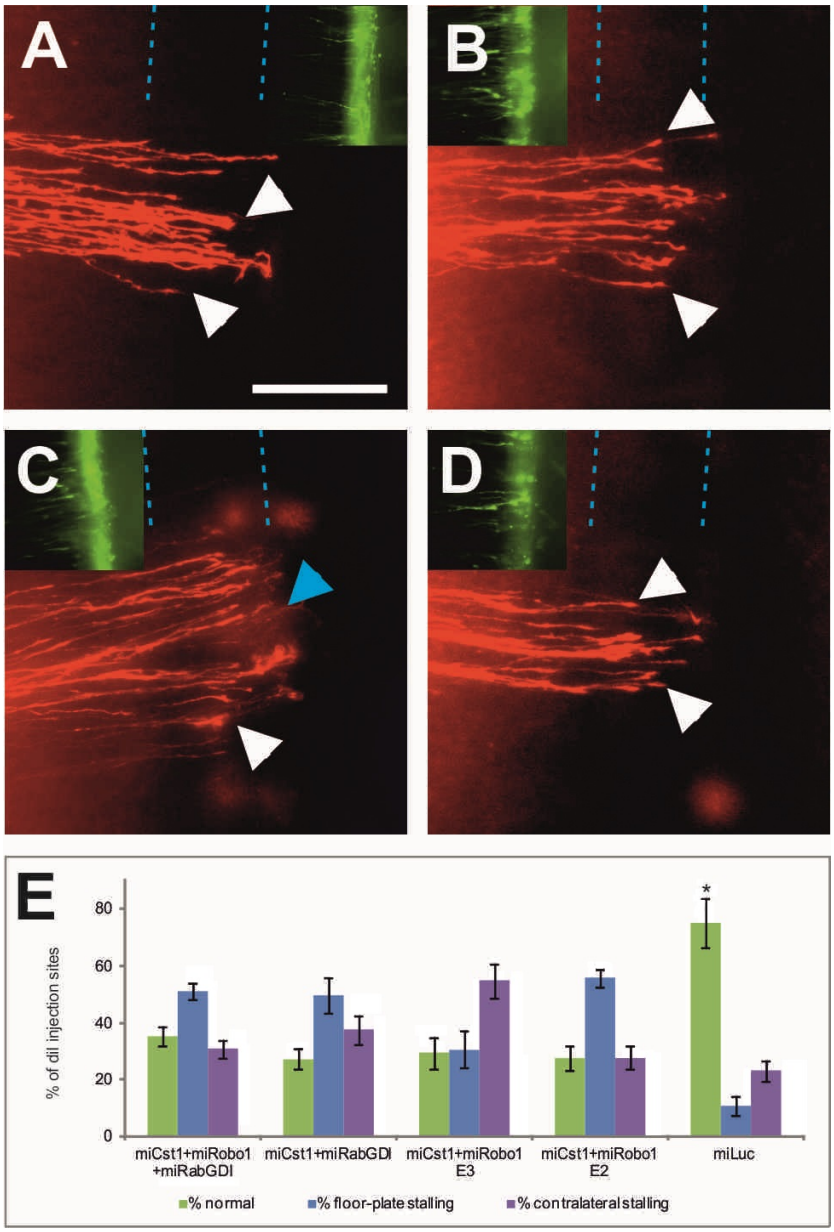

Figure 4: Calsyntenin1 and RabGDI cooperate in the regulation of Robo1 expression. Co-injection of low doses of miCst1, miRabGDI and miRobo1 results in axonal stalling in the floor plate (A; white arrowheads). Similarly, injection of low doses of only miCst1 and miRabGDI (B) also interfered with axonal pathfinding (E). Co-injection of miCst1 and miRobo1 at E3 (C) did interfere with axon guidance but resulted in a different phenotype, as axons were mainly stalling at the contralateral

floor-plate exit site (blue arrowhead). In contrast, injection and electroporation at E2 (D) reproduced the floor-plate stalling phenotypes seen in the absence of both Calsyntenin1 and RabGDI. This is also reflected in (E), where the quantitative analysis of the different groups miCst1/miRobo1/miRabGDI, miCst1/miRabGDI, miCst1/miRobo1 (E2) was virtually identical. * $p<0.05$ miLuc versus all other groups. Inserts in (A-D) show GFP expression as injection control. Values are given ± SEM.Bar: 50 µm.

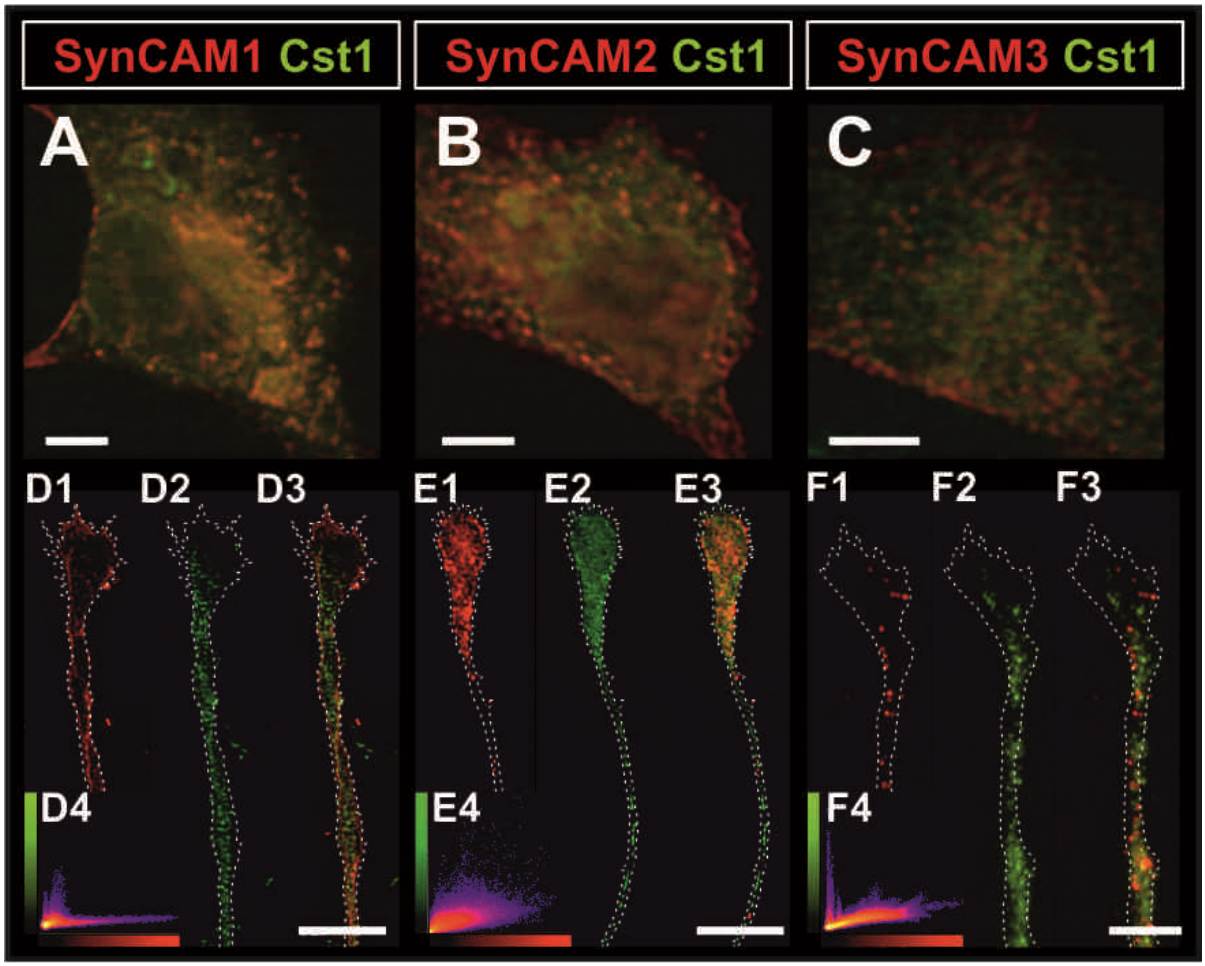

Figure 5: SynCAMs do not co-localize with Calsyntenin1. Expression of SynCAM1 (A; red), SynCAM2 (B; red), or SynCAM3 (C; red) did not result in co-localization with EGFP-Calsyntenin1 (green) in COS7 cells. Similarly, as indicated by the Scatter plot in the inserts, no overlap was found, when SynCAM1 (D; red), SynCAM2 (E; red), or SynCAM3 (F: red) were co-expressed with EGFP-Calsyntenin1 (green) in commissural neurons. Bar: 5 µm.

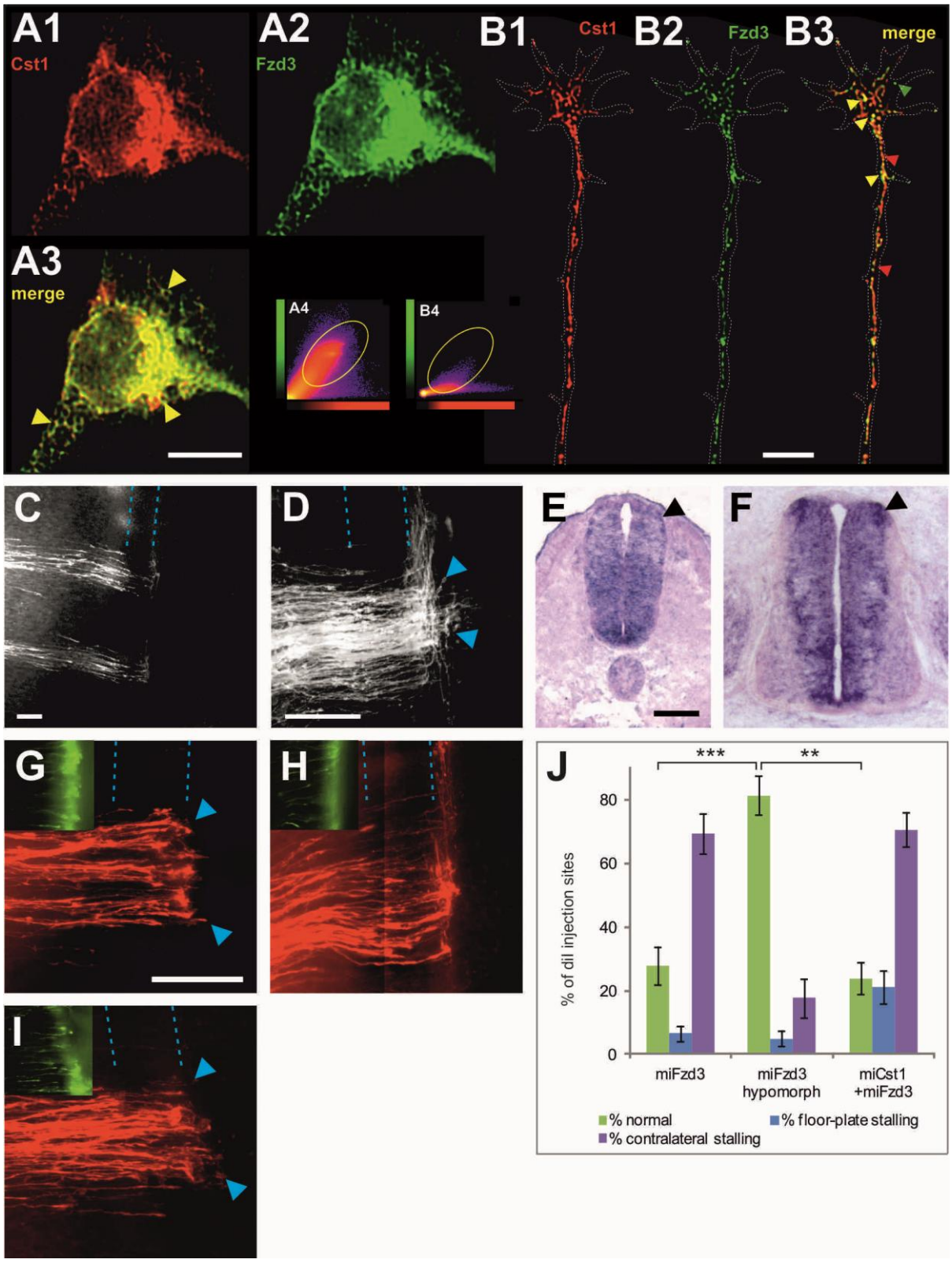

Figure 6: Calsytenin1 is required for Frizzled3 trafficking. Calsyntenin1 and Frizzled3 co-localize in COS7 cells (A) and in commissural axons and growth cones (B). The Pearson's coefficient was 0.75 in COS7 cells (A4) and 0.56 in commissural axons (B4). (C) Downregulation of Frz3 at E3 did not perturb commissural axon

guidance, whereas injection and electroporation of dsFrz3 at E2 did interfere with commissural axon guidance (D). Axons failed to turn into the longitudinal axis at the contralateral floor-plate border (blue arrowheads). This is in line with the expression pattern of Frz3, as we found mRNA in dI1 neurons already at HH18 (E; arrowhead). Strong Fzd3 expression in dI1 commissural neurons (arrowhead, F) was observed at HH24, when post-crossing commissural axons turn into the longitudinal axis. (G) miFrz3 injection and electroporation at E2 reproduced the Frz3 phenotype obtained with dsFrz3. (H) Injection and electroporation of a low dose of miFrz3 did not affect axon guidance. (I) In contrast, co-injection of low doses of miCst1 and miFrz3 together resulted in the failure of axonal turning at the exit site at 70.6±5.5% of the injection sites (J). This is similar to the value observed after perturbation of Fzd3 at the effective dose, where aberrant turning was observed at 69.3±6.2% of the injection sites. Injection and electroporation of only a low dose of miFzd3 interfered with axonal turning at the exit site at only 28.3±8.7% of the injection sites. Inserts in (G-I) show GFP expression as injection control. Bar: 5 µm (A,B), 50 µm (C,D,G,H,I), 100 µm (E,F). ** $p<0.01$, *** $p<0.0001$. Values are given ± SEM.

Figure 7 (next page)**: Robo1- and Fzd3-positive vesicles are transported by distinct mechanisms.** (A, B) Co-injection of low doses of miRabGDI and miFzd3 (A) or miRobo1 and miFzd3 (B) did not result in axon guidance defects (C). Normal pathfinding was observed at 65.9±1.5% of the injection sites for miRabGDI/miFzd3, at 55.7±3.2% of the injection sites for miRobo1/miFzd3. This is not different from control groups (see Figure 1), where we observed normal pathfinding at 75.0±8.5% for miLuc and 71.1±5.1% for untreated controls. This is in line with the observation that Robo1-positive vesicles (D) did barely overlap with Fzd3-positive vesicles (E), see (F) for merged image, where Robo1-positive vesicles are indicated by red arrowheads, Fzd3 with green arrowheads, and double-stained vesicles with yellow arrowheads. (G) Scatter plot indicating poor overlap between Robo1 and Fzd3. This is also reflected by the Pearson's coefficient (H). Values for positive and negative controls are taken from Figure 2H. The sparse overlap is confirmed in studies where we compared the co-localization of Calsyntenin1 immunoreactivity (I) with Fzd3 (J) and Robo1 (K). (L) merged image. Inserts in (A,B) show GFP expression as injection control. Bar: 50 µm (A,B), 5 µm (D-F), 3 µm (I-L). Boxed area in (I) is shown at higher magnification as insert in (I-L). n.s. not significant. Values are given ± SEM.

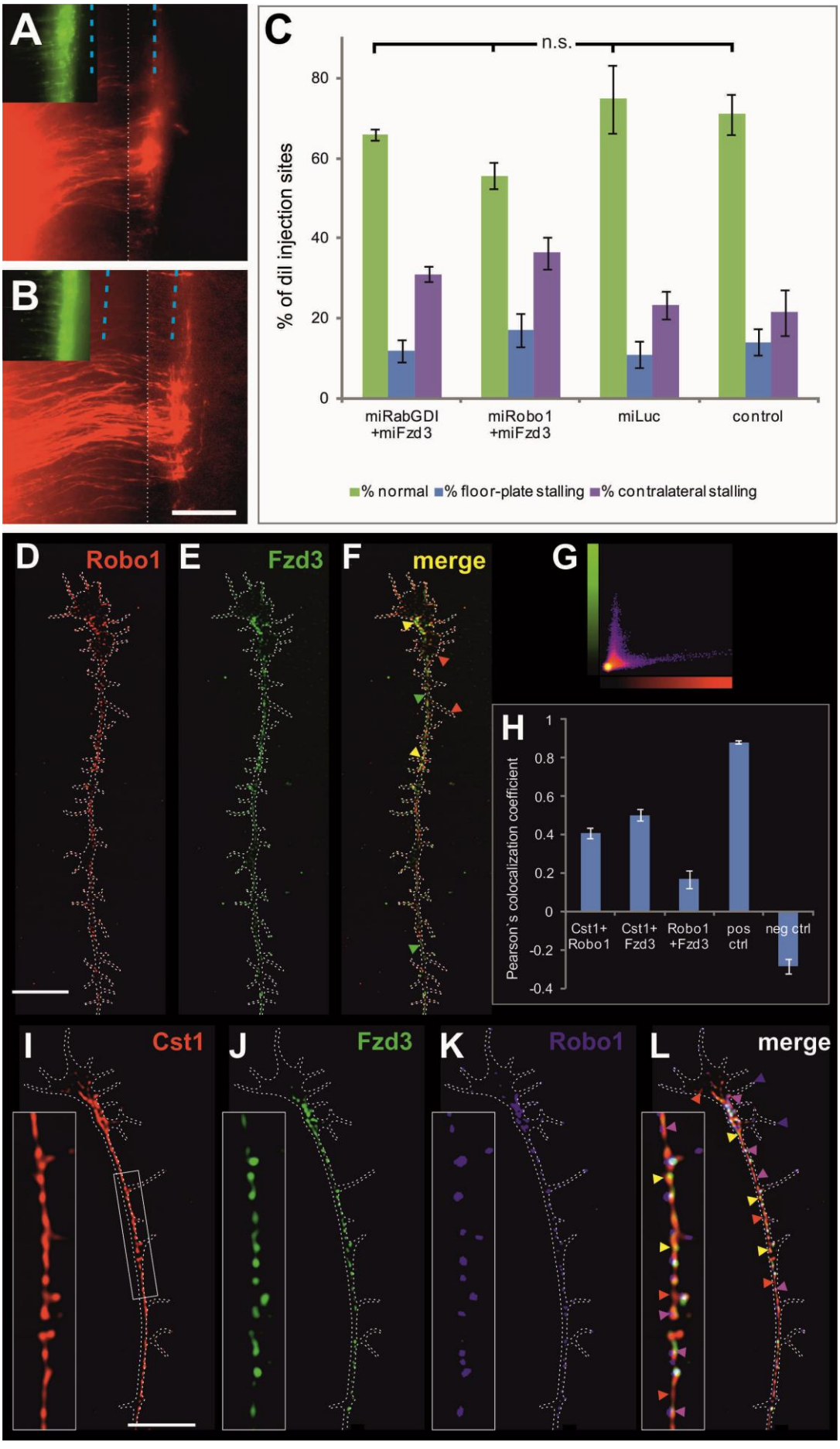
A
B
C
n.s.
% of dil injection sites
80
60
40
20
0
miRabGDI +miFzd3
miRobo1 +miFzd3
miLuc
control
% normal
% floor-plate stalling
% contralateral stalling
D Robo1
E Fzd3
F merge
G
H
Pearson's colocalization coefficient
1
0.8
0.6
0.4
0.2
0
-0.2
-0.4
Cst1+ Robo1
Cst1+ Fzd3
Robo1 +Fzd3
pos ctrl
neg ctrl
I Cst1
J Fzd3
K Robo1
L merge

Figure 7

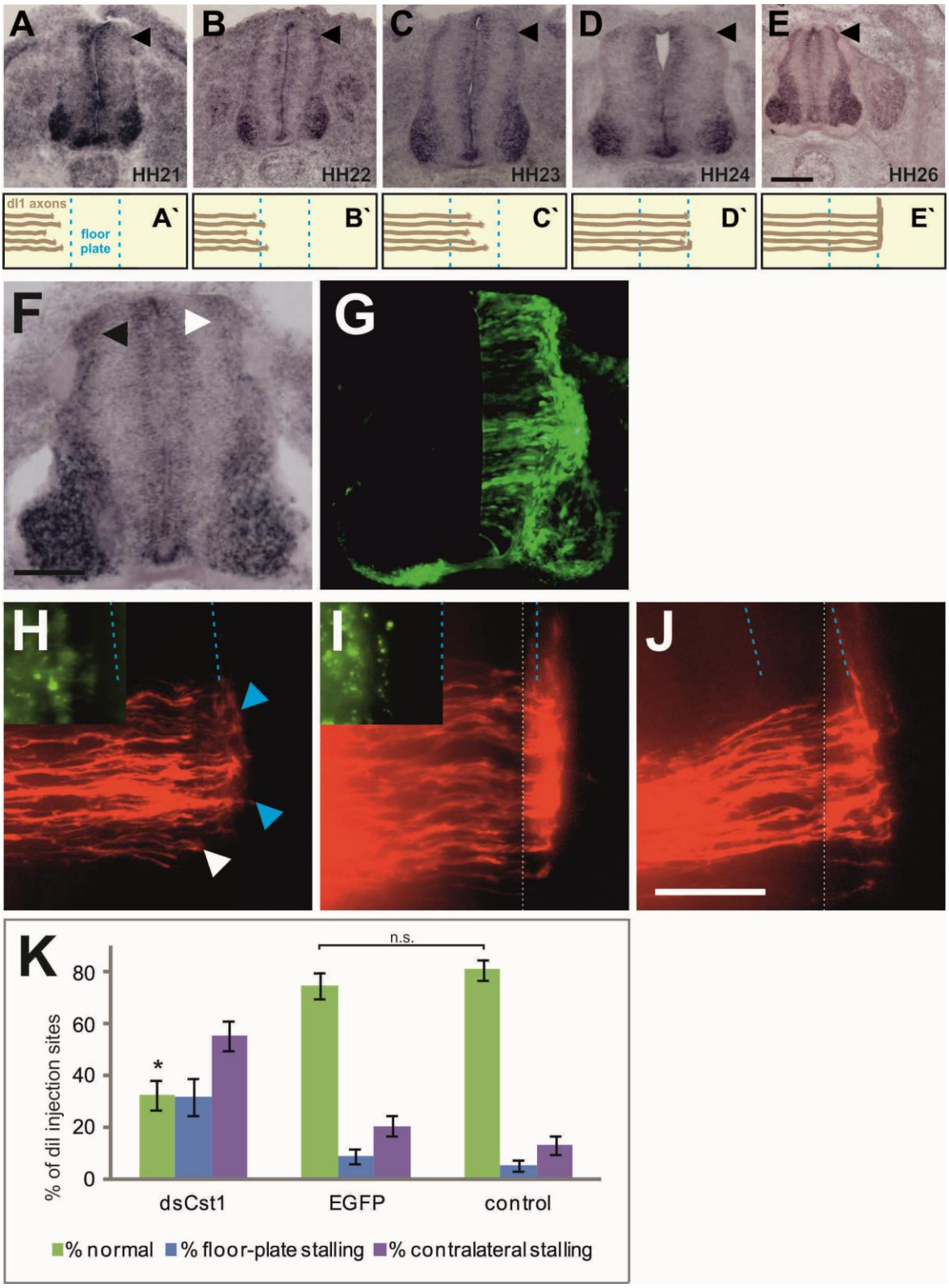

Supplementary Figure 1: Calsyntenin1 is required for commissural axon guidance in line with its expression pattern in dI1 neurons. (A-E) Calsyntenin1 is expressed in dI1 neurons (arrowhead) when their axons grow toward the floor plate at HH21 (A, A'). Expression is maintained during floor-plate entry HH22 (B;B'). At

HH23, commissural axons are in the floor plate crossing the midline (C,C'). At HH24, commissural axons turn into the longitudinal axis at the contralateral floor-plate exit site (D,D'). Calsyntenin1 expression is maintained after midline crossing and growth along the longitudinal axis at HH26 (E,E'). Silencing Calsyntenin1 with miCst1 efficiently and specifically downregulates Calsyntenin1 mRNA levels on the injected (white arrowhead) compared to the control side (black arrowhead) by 37.9% (F, G, Supplementary Table 1). (H-K) Silencing Calsyntenin1 did not perturb growth but affected guidance of dI1 axons. Open-book preparations of spinal cords taken from embryos at HH28, one day later than what we usually used, still had a majority of injection sites with axons stalling in the floor plate (white arrowhead) or failing to turn into the longitudinal axis (blue arrowheads) after downregulation of Calsyntenin1 (H,K). Control-treated embryos (I) did not differ from untreated controls (J). An average of 32.8±5.5% of the injection sites per embryo showed aberrant axonal navigation in the absence of Calsyntenin1, whereas 75.0±4.9% of the injection sites where normal in control-treated embryos (Table 1). This is not different from untreated control embryos, where 81.0±3.8% of the injections sites were normal. Values in (K) are shown ± SEM. Inserts in (H,I) show GFP expression as injection control. Bar: 100 µm. * $p<0.05$ for dsCst1 versus both control groups. n.s. not significant.

Supplementary Figure 2 (next page)**: Partial co-localization of Calsyntenins with Robo1, Robo2, RabGDI, and Rab11.** Ectopic expression of Calsyntenin1 (A-D) with Robo1 (A), or Robo2 (B), RabGDI (C), Rab11 (D) showed partial co-localization of all combinations, as quantified in (T). Similar level of co-localization were found for RabGDI and Robo1 (E), RabGDI and Robo2 (F), RabGDI and Rab11 (G), as well as Robo1 (H) and Robo2 (I) with Rab11. Comparative values were also found for Calsyntenin2 (T) with the exception of Calsyntenin2 and Rab11 (J, J') which showed hardly any co-localization. Calsyntenin3 values were also similar. Highest values for co-localization was shown for Calsyntenin3 and Robo1 (K,K'). As a positive control we used a double-tagged version of Robo1, HA-Robo1-myc and used antibodies against the tags to set maximal values for overlap (L-S). In (L-O) we used a goat anti-mouse Cy3 antibody to stain for the myc-tag (L) and a donkey anti-rabbitAlexa488

(M). The merged image is shown in (N) and the Scatter plot in (O). For (P-S) the colors were swapped. PC Pearson's coefficient. Values in (T) are shown ± SEM. Bar: 10 µm.

Supplementary Figure 2

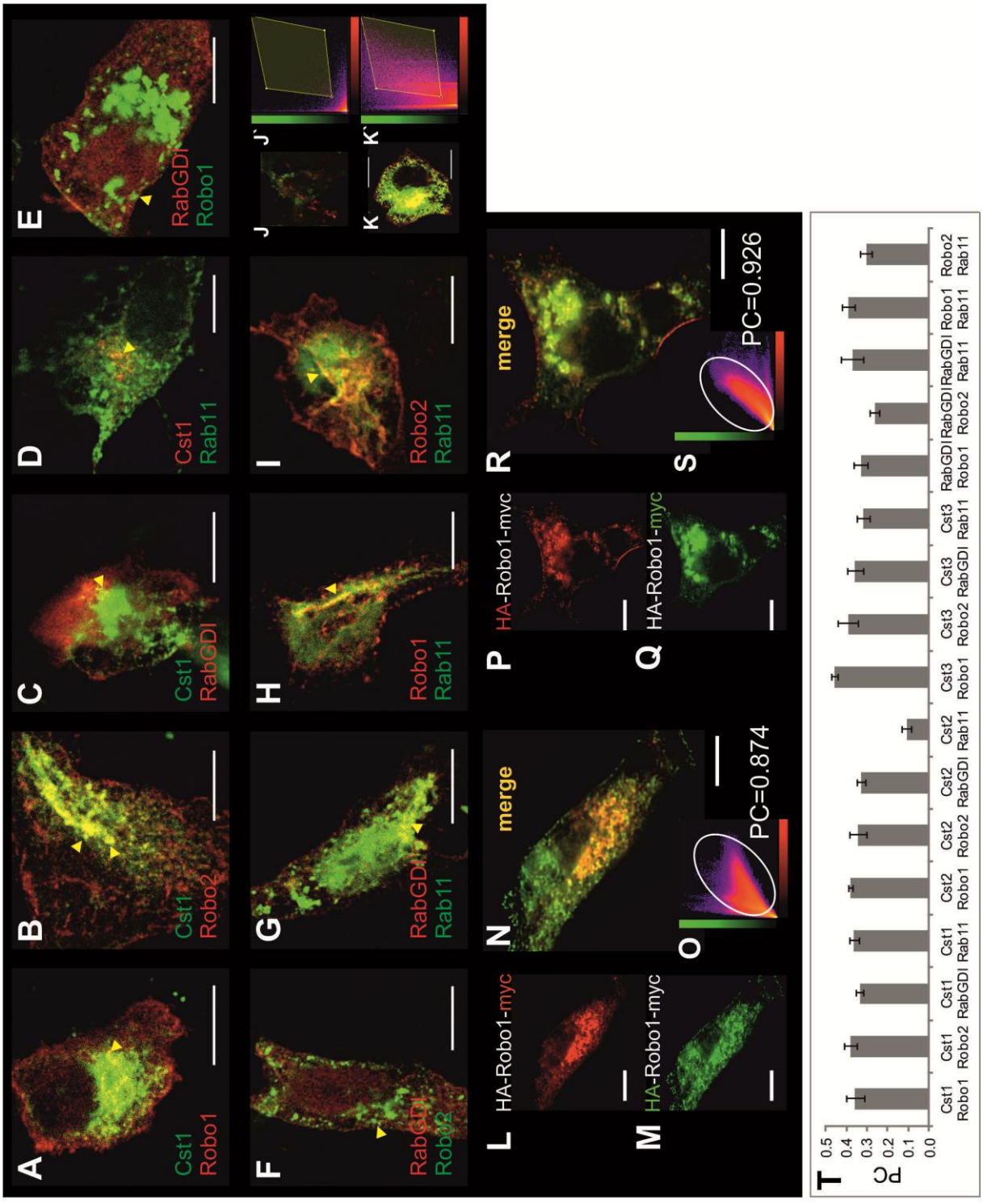

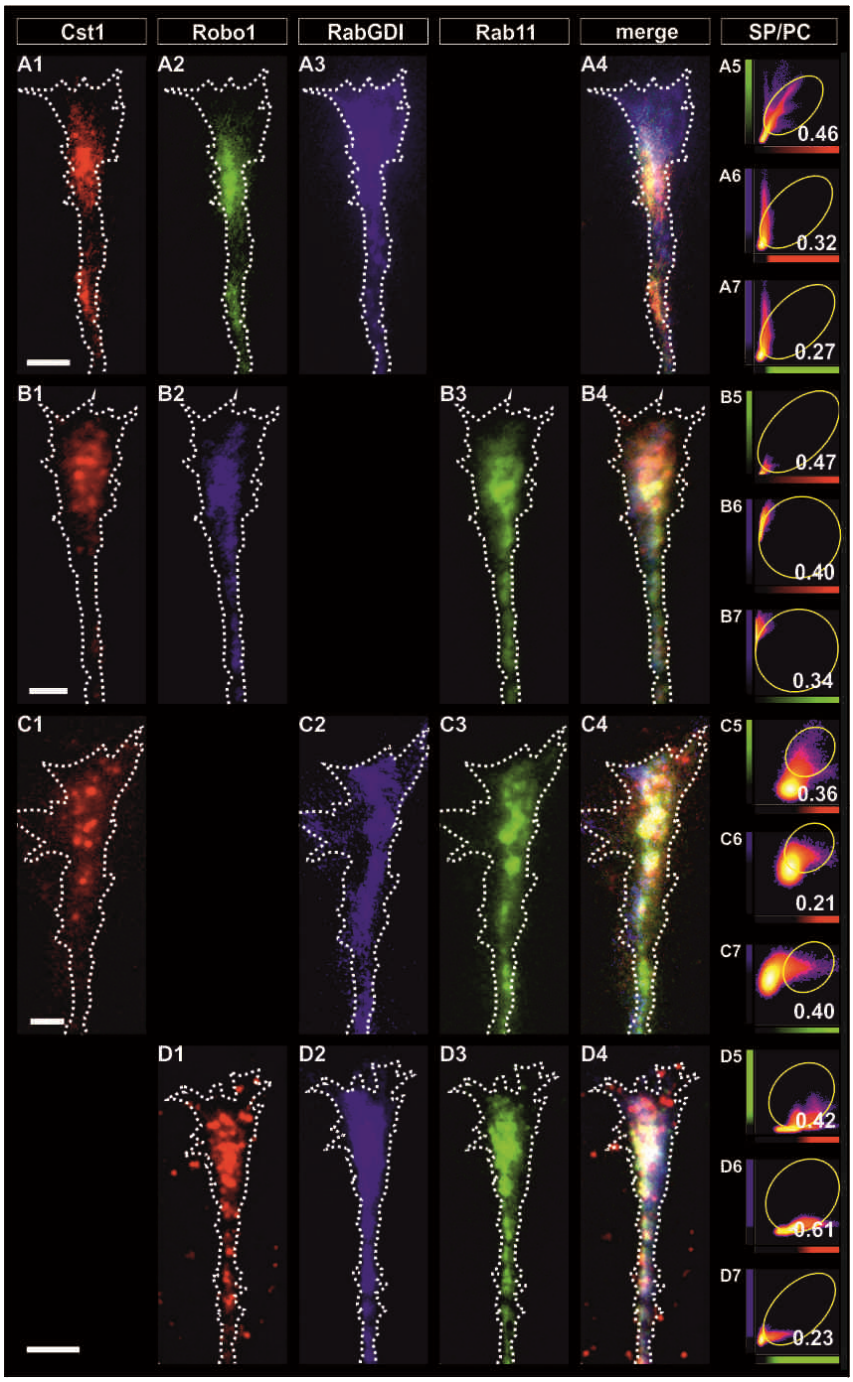

Supplementary Figure 3: Triple staining of Calsyntenin1, Robo1, RabGDI and Rab 11 confirms partial co-localization. Expression of mCherry-Calsyntenin1 (red in A1, B1, C1) with Robo1-myc (green in A2, blue in B2, red in D1) and RabGDI-HA (blue in A3, C2, D2) or Rab11-EGFP (green in B3,C3,D3) confirms partial co-localization between Calsyntenin1, Robo1, and RabGDI (A4-A7). Similarly, co-localization was found for Calsyntenin1 with Robo1 and Rab11 (B4-B7), Calsyntenin1, RabGDI and Rab11 (C4-C7), as well as for Robo1, RabGDI, and

Rab11 (D4-D7). Bar: 5 µm (A, D), 2 µm (B,C). SP Scatter plot, PC Pearson's coefficient.

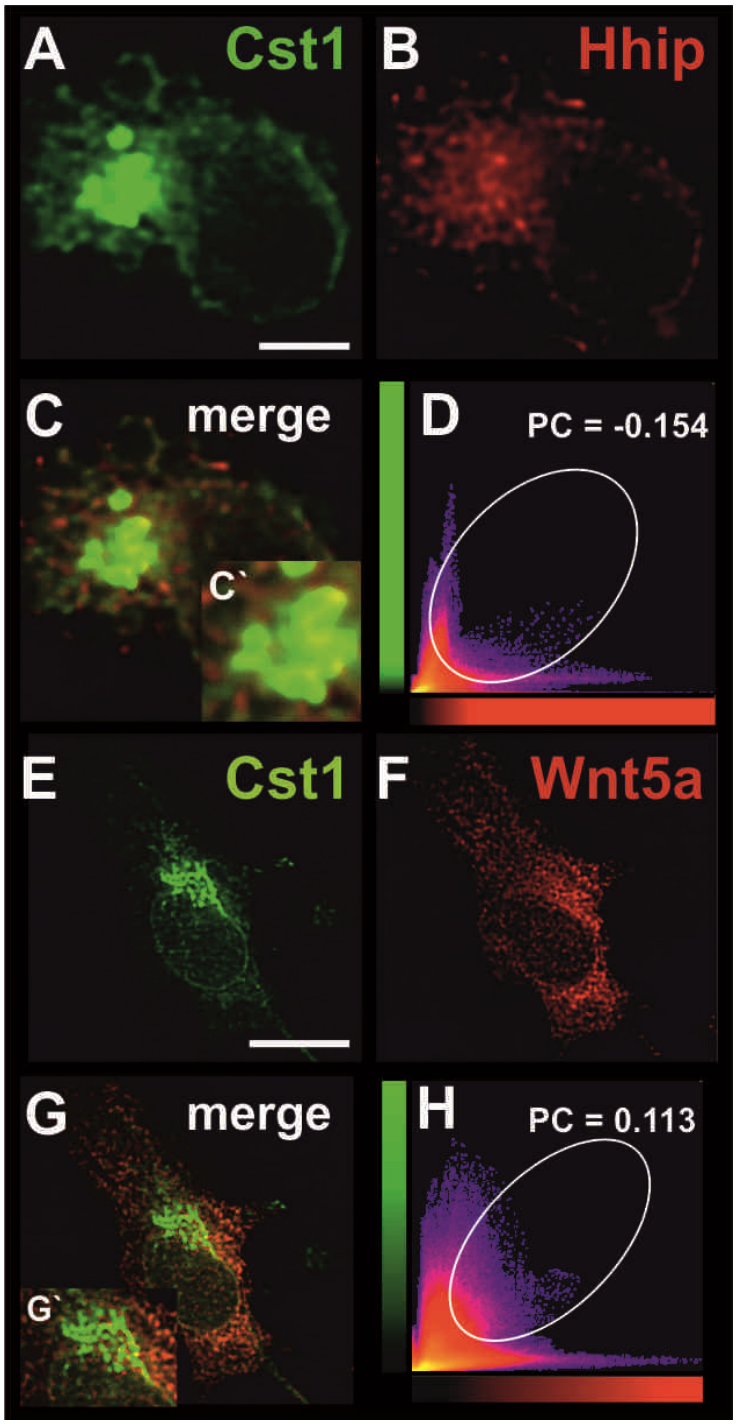

Supplementary Figure 4: Calsyntenin1 does not overlap with Hhip and Wnt5a. Immunoreactivity for Calsyntenin1 (green; A) did not overlap with Hhip (red; B). Merged image shown in (C), Scatter plot in (D). Similarly, no overlap was detected between Calsyntenin1 (green; E) and Wnt5a (red; F), see (G) for merged image and (H) for Scatter plot. Bar: 5 µm (A-C), 10 µm (E-G). PC Pearson's coefficient.

Table 1: Values of the open-book quantification.

	normal injection sites		floor-plate stalling		contralateral stalling	
Injected construct(s)	%	S.E.M	%	S.E.M	%	S.E.M
miCst1	22.5	5.2	30.2	4.3	65.9	7.5
miCst2	72.0	4.4	12.7	3.6	19.5	4.4
miCst3	46.7	4.0	19.1	4.1	44.8	5.2
miFzd3	27.7	6.1	6.6	2.3	69.3	6.2
miRobo1	20.6	3.7	63.5	3.0	32.5	5.3
miRabGDI	28.4	3.3	63.4	3.5	26.8	3.6
miCst1 hypomorph	67.0	5.2	8.5	4.3	28.7	7.5
miFzd3 hypomorph	67.0	8.5	10.4	3.9	28.3	8.7
miRobo1 hypomorph	67.7	3.5	13.7	3.3	29.4	3.8
miRabGDI hypomorph	60.2	5.6	5.4	2.4	25.8	2.9
miCst1+miFzd3	23.9	5.1	21.1	5.3	70.6	5.5
miCst1+miRobo1+miRabGDI	35.2	3.1	50.9	2.8	30.8	3.1
miCst1+miRabGDI	27.3	3.7	49.6	6.2	37.4	4.8
miCst1+miRobo1 E3	29.3	5.7	30.7	7.0	54.7	6.3
miCst1+miRobo1 E2	27.8	4.3	55.6	3.3	27.8	3.9
miRobo1+miFzd3	55.7	3.2	17.1	4.2	36.4	4.0
miRabGDI+miFzd3	65.9	1.5	11.9	2.7	31.1	1.9
miLuc control	75.0	8.5	10.9	3.3	23.2	3.5
untreated control	71.1	5.1	14.1	3.3	21.5	5.8
dsRNA-injected embryos (HH25/26)						
dsCst1	27.7	2.8	38.6	3.7	62.4	5.4
dsCst2	56.2	9.3	21.9	6.5	30.5	7.2
dsCst3	63.0	8.4	15.1	8.7	27.4	6.5
EGFP control	77.7	6.1	15.5	2.9	23.4	3.8
dsRNA-injected embryos (HH28)						
dsCst1	32.8	5.5	32.0	6.9	55.5	5.8
EGFP control	75.0	4.9	9.4	2.7	20.8	4.0
untreated control	81.0	3.8	5.4	2.1	13.5	3.6

Supplementary Table 1: Confirmation of downregulation.

	intensity (%)	p-value	S.E.M.
uninjected Cst1	100	0.000	4.29
miCst1	62.11		4.11
uninjected miLuc	100	0.632	4.38
miLuc	102.51		4.75
uninjected Cst2	100	0.000	3.11
miCst2	55.83		3.85
uninjected miLuc	100	0.539	7.34
miLuc	103.03		7.25
uninjected Cst3	100	0.002	3.44
miCst3	67.38		5.36
uninjected miLuc	100	0.740	5.92
miLuc	101.97		5.83
uninjected Robo1	100	0.000	1.37
miRobo1	85.86		0.51
uninjected miLuc	100	0.149	1.96
miLuc	104.14		1.88
uninjected RabGDI	100	0.000	2.19
miRabGDI	68.93		2.28
uninjected miLuc	100	0.790	4.01
miLuc	101.40		3.38
uninjected Fzd3	100	0.000	2.23
miFzd3	77.62		2.46
uninjected miLuc	100	0.297	0.26
miLuc	99.38		0.50

Supplementary Table 2: Target sequences and vector insertion sites for miRNAs used in this study.

Name	Gene	Target sequence
miLuc	Firefly luciferase	CGTGGATTACGTCGCCAGTCAA
miCst1	Chicken calsyntenin-1	AACACGCTAATCACATAGCTG
miCst2	Chicken calsyntenin-2	AAGGCTGTGATCGTGAAACCT
miCst3	Chicken calsyntenin-3	AACCTCGAACAACAACATTGA
miRobo1	Chicken roundabout 1	AAGCTGAAGCATCGGCAACTC
miFzd3	Chicken frizzled 3	AATATGTACTTCCGGCGTGAA
miRabGDI	Chicken Rab GDI	AAGATCGGCTGTTGGTCACAA

Supplementary Table 3: Plamids used for overexpression in COS7 cell cultures and in commissural neurons.

plasmid	promoter	used in	expression of
EGFPmmCST1	CMV	COS7	EGFP full-length mmCst1
EGFPmmCST2	CMV	COS7	EGFP full-length mmCst2
EGFPmmCST3	CMV	COS7	EGFP full-length mmCst3
mCherrymmCST1	CMV	COS7 and CN	mCherry full-length mmCst1
EGFPmmCST1	β-actin	COS7 and CN	EGFP full-length mmCst1
hsRabGDI-HA	β-actin	COS7 and CN	full-length hsRabGDI
hsRobo1-myc	β-actin	COS7 and CN	full-length hsRobo1
HA-hsRobo1-myc	β-actin	COS7 and CN	full-length hsRobo1
hsRobo2-myc	β-actin	COS7 and CN	full-length hsRobo2
pEGFP-hsRab11	CMV	COS7 and CN	full-length hsRab11
EGFP	β-actin	COS7 and CN	GFP
pEGFP-N2.1-ggFzd3	β-actin	COS7 and CN	full-length ggFzd3-GFP
myc-SynCAM1	β-actin	COS7 and DRGs	full-length ggSynCAM1
HA-SynCAM2	β-actin	COS7 and DRGs	full-length ggSynCAM2
HA-SynCAM3	β-actin	COS7 and DRGs	full-length ggSynCAM3
pcDNA-Wnt5a-myc	β-actin	COS7	full-length ggWnt5a
pcDNA-myc-Hhip	CMV	COS7	full-length mmHhip

5. Supplementary data

5.1. Supplementary results

Whole-mount in situ hybridization with focus on the head: early cranial Calsyntenin expression

We carried out whole-mount in situ hybridization as another approach to analyze Calsyntenin mRNA expression in the young chicken embryo. In the developing head (Figure 22 and 23), we found Cst1 mRNA expressed in the eye starting at HH14 (Figure 22A and 23A). This expression persisted and became stronger at HH17. Starting at this stage, Cst1 mRNA was also detected in the otic vesicle (Figure 22B) and between E3 and 4 there was a transient expression in the geniculate ganglion (Figure 22B and 23C). For Cst2, we also detected mRNA expression starting at HH18.5 in the geniculate ganglion and in the eye. Like in the spinal cord, Cst3 mRNA expression was similar to the Cst1 mRNA expression in the head at early stages of development. However, the transient Cst1 expression in the geniculate ganglion between E3 and 4 was not found for Cst3. In addition, Cst2 was expressed in somites and in the dermomyotome (see manuscript 4.1. Figure 2 and Figure 23B,D,E). We used Pax7 antibody staining to confirm the expression in the somites and their derivatives (Figure 23F,G' and H).

Figure 22 (next page)**: Calsyntenins are expressed in the developing head.** Expression of Cst1 (A-E), Cst2 (G-K) and Cst3 (M-Q) in the heads of embryonic whole-mount embryos (HH14-HH23). (F,L and R) are whole-mount embryos hybridized with sense probes. Tel, telencephalon; Di, diencephalon; Me, metencephalon; arrow, eye; red arrowhead, otic (auditory) vesicle; light blue arrowhead, geniculate ganglion. Bar: 0.5 mm for A, G and M, 1 mm for all others.

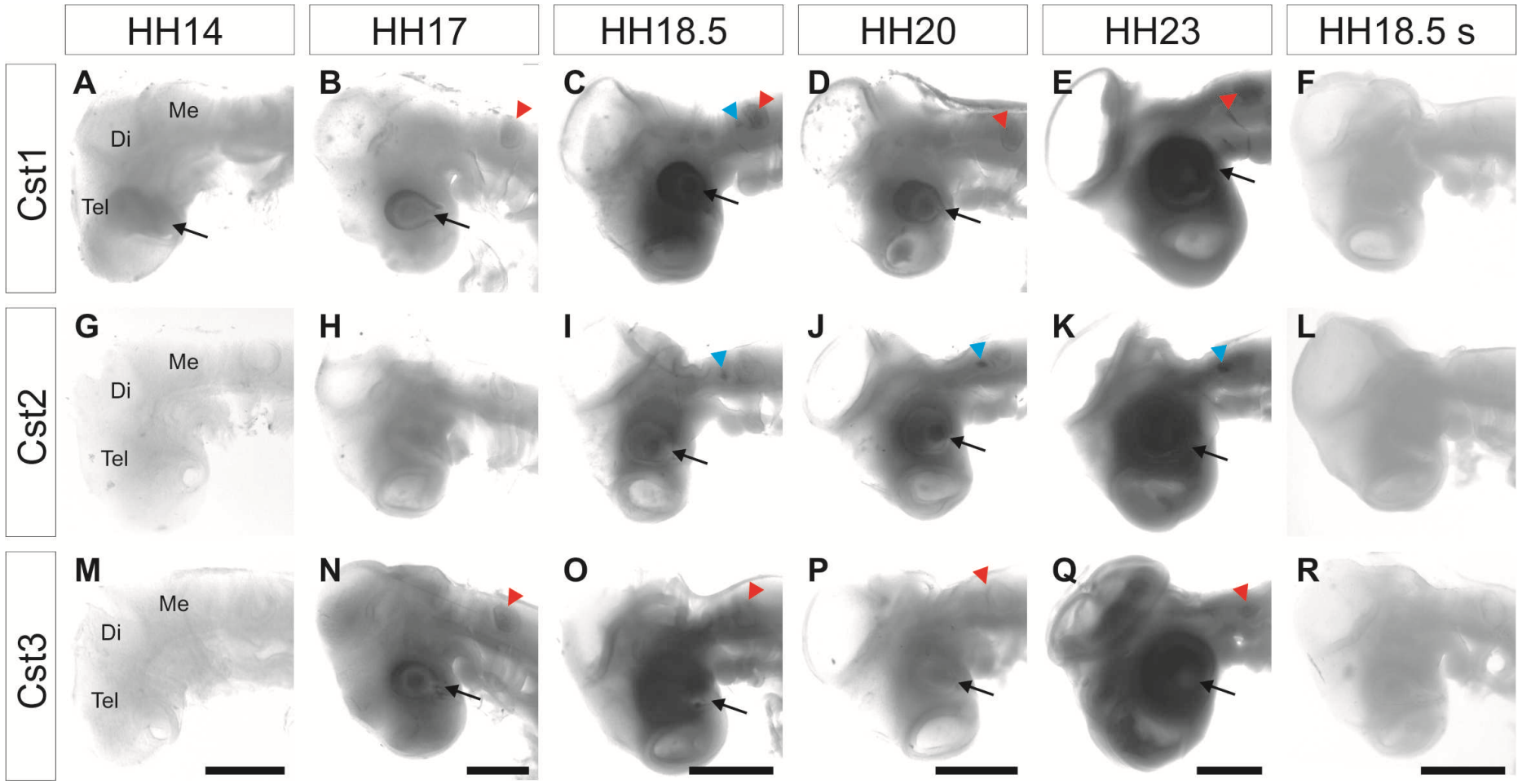
HH14
HH17
HH18.5
HH20
HH23
HH18.5 s
Cst1
Cst2
Cst3
A
B
C
D
E
F
G
H
I
J
K
L
M
N
O
P
Q
R
Me
Di
Tel

Figure 22

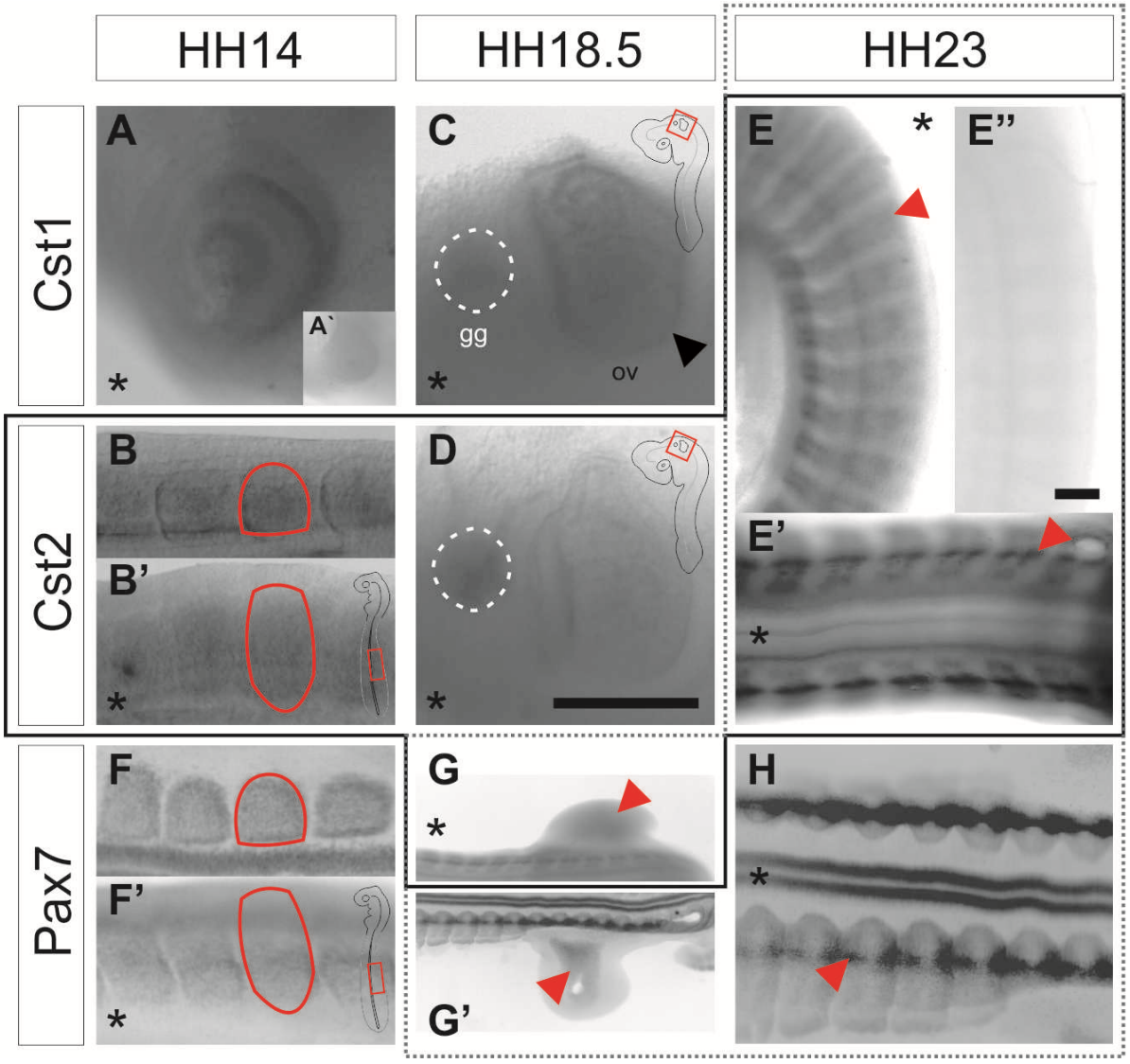

Figure 23: Expression of Calsyntenin1 and 2 in particular structures of embryonic whole-mount in situ preparations. At HH14, Calsyntenin1 is expressed in the eye (A; sense control A'). Calsyntenin2 is expressed in the somites (B dorsal view, B' lateral view; red circles) which was confirmed using Pax7 antibody staining (F dorsal view, F' lateral view; red circles). The orientation is indicated by the schematic drawing in (B') and (F'). At HH18.5, Calsyntenin1 is expressed in the otic vesicle (C; black arrowhead) and both Calsyntenin1 and -2 in the geniculate ganglion (C,D; white dashed circle). At HH23 (indicated by the gray dashed line), Calsyntenin2 is expressed in the derivatives of the somites (E lateral view, E' dorsal view; red arrowhead) and in the limb (G; red arrowhead), indicated by the Pax7 staining (G',H; red arrowheads). The solid black line indicates the images showing the Calsyntenin2 expression. (E'') is the sense control to (E). The black asterisk indicates rostral. Bar: 250 µm. gg geniculate ganglion, ov otic vesicle.

Confirmation of downregulation using plasmids encoding miRNA

To proof the efficiency and specificity of the miRNAs, we performed in situ hybridization on tissue sections of embryos expressing miRNAs under the control of the β-actin promoter (Figure 24; Supplementary Table 1 in manuscript 4.2.). In all experimental conditions, we found a highly significant decrease in mRNA signal intensity on the experimental halves of the spinal cord. In contrast, control-treated embryos showed equal mRNA expression levels on the miLuc injected and uninjected spinal cord halves.

Figure 24 (next page)**: miRNA-based knockdown of Calsyntenins, Robo1, RabGDI and Fzd3 is successful and leads to a significant reduction of mRNA expression.** In situ hybridization of Cst1 (A,B) , Cst2 (C,D), Cst3 (E,F), Robo1 (G,H), RabGDI (I,J) and Fzd3 (K,L). The injected miRNA-constructs are indicated in the box on the left side of the pictures. (A2-L2) shows the EGFP signal derived from the plasmid encoding the miRNA operon. (B1, D1, F1, H1, J1 and L1) are miLuc-injected controls. The black arrowheads indicate the uninjected, the white arrowhead the injected spinal-cord halves. The in situ signal intensities are decreased on miCst1-, miCst2-, miCst3-, miRobo1-, miRabGDI- and miFzd3-injected, but not on the control injected sites. Quantification (see manuscript 4.2., Supplementary Table 1) revealed the highly significant reduction of in situ signal intensities on the injected sites compared to the uninjected sites ($p < 0.0001$; t-test; $N = 3$ with $n = 2$-3 sections each). Bar: 100 µm.

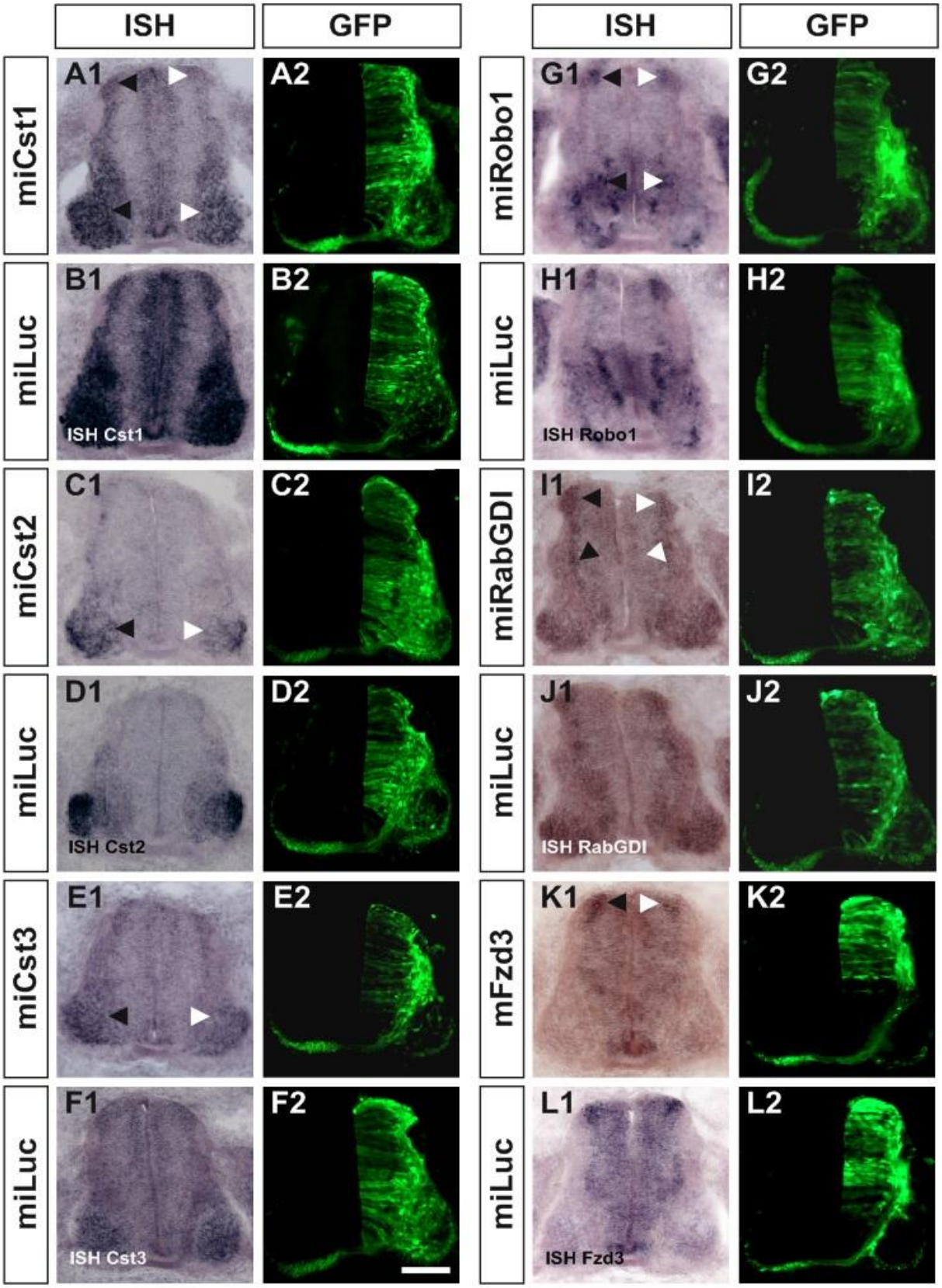
ISH
GFP
ISH
GFP
miCst1
A1
A2
miRobo1
G1
G2
miLuc
B1
ISH Cst1
B2
miLuc
H1
ISH Robo1
H2
miCst2
C1
C2
miRabGDI
I1
I2
miLuc
D1
ISH Cst2
D2
miLuc
J1
ISH RabGDI
J2
miCst3
E1
E2
mFzd3
K1
K2
miLuc
F1
ISH Cst3
F2
miLuc
L1
ISH Fzd3
L2

Figure 24

Spinal cord patterning is not altered by miRNA-based Calsyntenin, Robo1, RabGDI or Fzd3 downregulation

The injection of plasmids encoding miRNAs could result in aberrant patterning rather than having a direct effect on axonal wiring. In order to make sure that the miRNA treatment is not critical for patterning, we stained for patterning markers on sections of embryos treated with plasmid encoding miRNAs. Figure 25 indicates that our miRNAs and dCst1 do not alter patterning and can be used for specific downregulation. The antibodies used for this assay are described in the methods part in manuscript 4.2.

Figure 25 (next page)**: Patterning of the spinal cord is not altered due to miRNA expression.** (A1-H1) show the EGFP signal derived from the plasmid encoding the miRNA operon. (A2-H2) shows staining for the homeobox protein Nkx2.2 which characteristically is found the area around the floor plate. The distribution of transcription factors Isl1 in (A3-G3) (staining of motor neurons) and Pax6 in (A4-H4) (staining of precursor cells) were not different in experimental compared to control embryos. Additionally, the axonin-1 expression in (A5-H5) visualizes the commissural axons, which properly migrate from the dorsal to the ventral spinal cord. Bar: 100 µm.

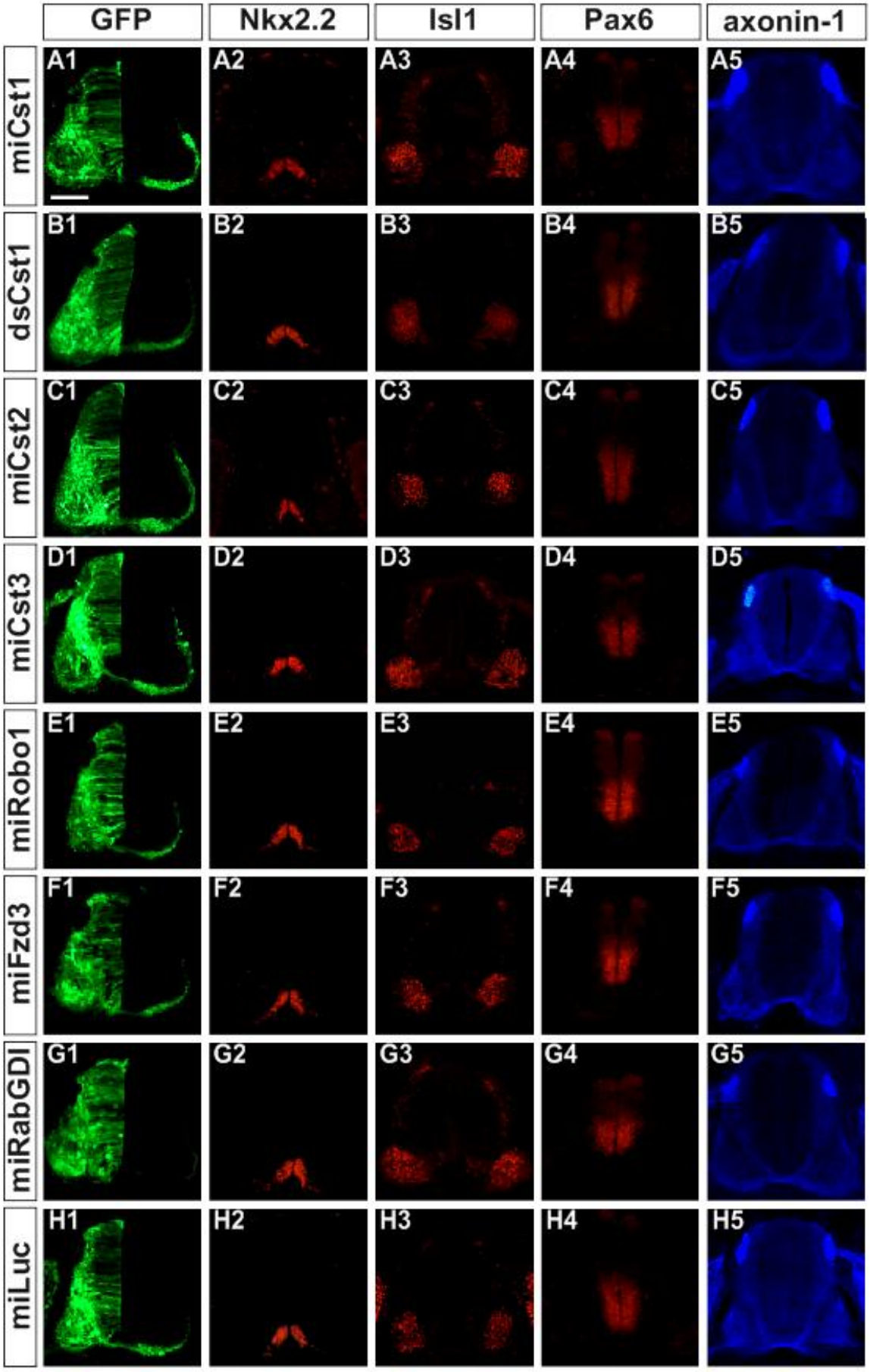
GFP
Nkx2.2
Isl1
Pax6
axonin-1
miCst1
dsCst1
miCst2
miCst3
miRobo1
miFzd3
miRabGDI
miLuc
A1
A2
A3
A4
A5
B1
B2
B3
B4
B5
C1
C2
C3
C4
C5
D1
D2
D3
D4
D5
E1
E2
E3
E4
E5
F1
F2
F3
F4
F5
G1
G2
G3
G4
G5
H1
H2
H3
H4
H5

Figure 25

Calsyntenins play a role in proper DRG and epaxial nerve formation

The prominent Calsyntenin expression in the DRGs and motor neurons as well as preliminary data of my Master thesis suggested a role for the Calsyntenins in the formation of the DRGs and peripheral nerves. After silencing Calsyntenins using dsRNA, we found previously defects in DRG, epaxial and sciatic nerve formation (Tobias Alther, Master Thesis). We repeated these whole-mount experiments using miRNA-based gene silencing. With respect to the peripheral nerves (sciatic, crural and LFCt), we did not find quantitative differences between embryos lacking Cst1, 2 or 3 and control embryos. However, we found changes in the formation of the DRGs and epaxial nerves in the experimental compared to control groups (Figure 26). In our quantitative analysis of the DRGs, we focused on 5 lumbosacral DRGs that have been targeted with miRNA-encoding plasmids (Figure 26 A3-D3). We observed in all conditions aberrantly small and abnormally shaped DRGs and DRGs with misarranged roots. When 2-3 of the DRGs were aberrant, the phenotype was considered weak, when more than 3 aberrant DRGs were found, we scored it as a strong phenotype. With respect to the epaxial nerves, we observed defasciculation in embryos lacking Cst1 or Cst3. For quantitative analysis, we again considered 2-3 abnormal epaxial nerves as weak, and more than 3 as strong phenotype.

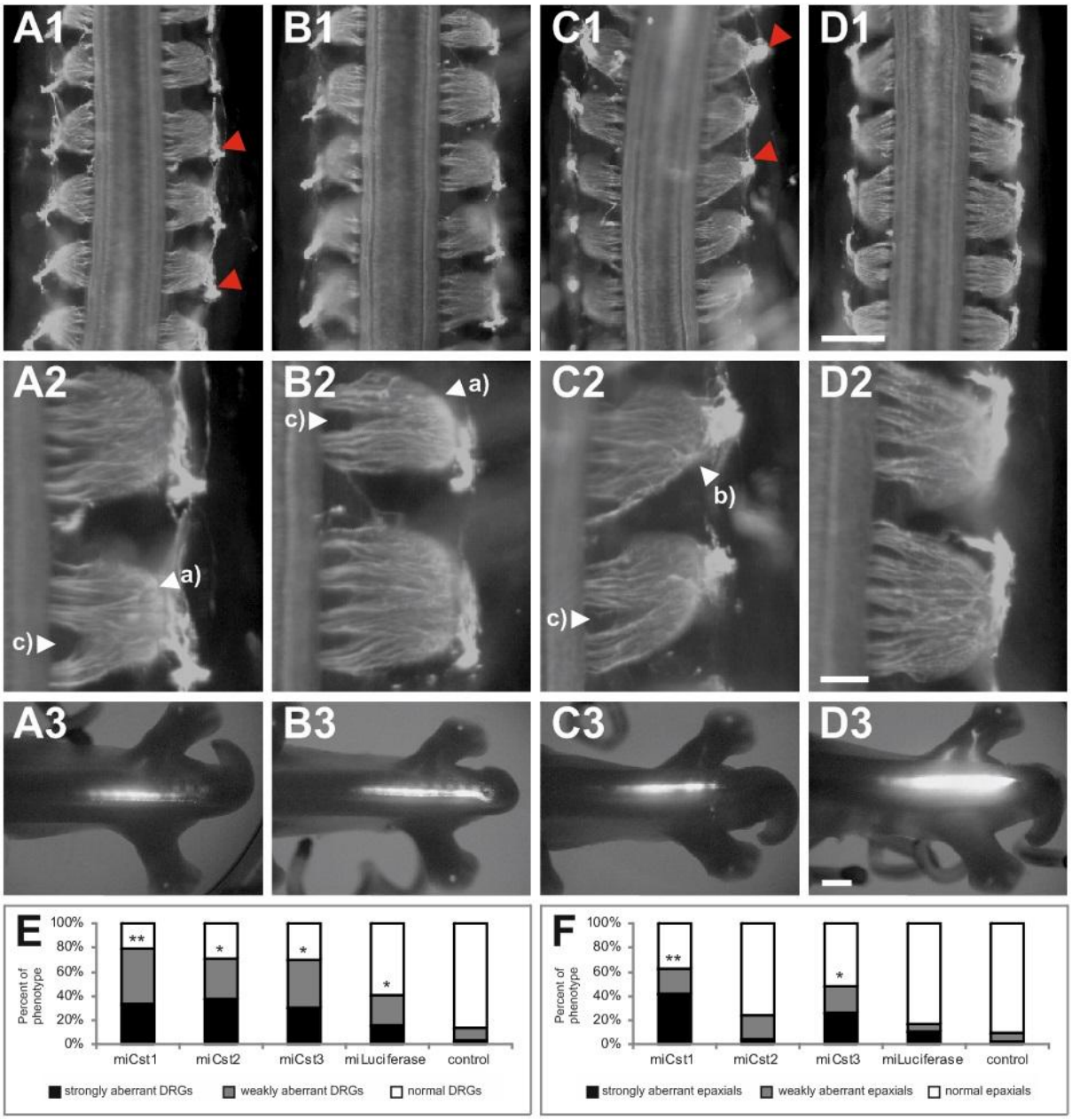

Figure 26: Embryos lacking Calsyntenin display aberrant DRGs and epaxial nerves. (A1-D1) Overview on the lumbosacral spinal cord with DRGs. The red arrowheads indicate the aberrant epaxial phenotype (defasciculated nerve bundles). (A2-D2) display higher magnifications of (A1-D1). The white arrowheads indicate the observed aberrant DRG phenotypes, i.e. a) aberrantly small DRGs, b) aberrantly shaped DRGs and c) DRGs with misarranged roots. (A3-D3) show the EGFP signal derived from the plasmid encoding the miRNA operon. The values of the quantification of the strong and weak whole-mount phenotypes (E and F) are statistically analyzed using the Fisher's exact test (vassarstats.net). The significances refer to the untreated control. All experimental knock-down conditions are also significant (*) to the miLuc control group, except for miCst2 in (F). The controls and miCst2 are not significant among each other in F; * $p \leq 0.05$, ** $p \leq 0.01$. Total number of embryos was 10-13 per condition. The p-values are given in the appendix. Bar: 250 µm for (A1-D1), 100 µm for (A2-D2), 1 mm for (A3-D3).

Calsyntenin downregulation does not affect growth of DRG axons

Based on the results of our in vivo experiments demonstrating a role of Cst1 and Cst3 on DRG formation, we analyzed DRG explants of embryos lacking Cst1, 2 and 3 and compared the average outgrowth and size (area and fluorescent intensity) to injected and uninjected control embryos (Figure 27). We did not find any statistical differences. We additionally analyzed cultured dissociated DRG neurons of embryos lacking Calsyntenins. However, when assessing the average length, we found significantly shorter neurites in the experimental knock-down conditions with respect to the untreated control, but not to the miLuc control injected neurites. We also looked at neurite branching, where we compared the number of branching neurites compared to the total number of neurons. In this case, we did not find any significant differences between downregulated and control conditions (not shown).

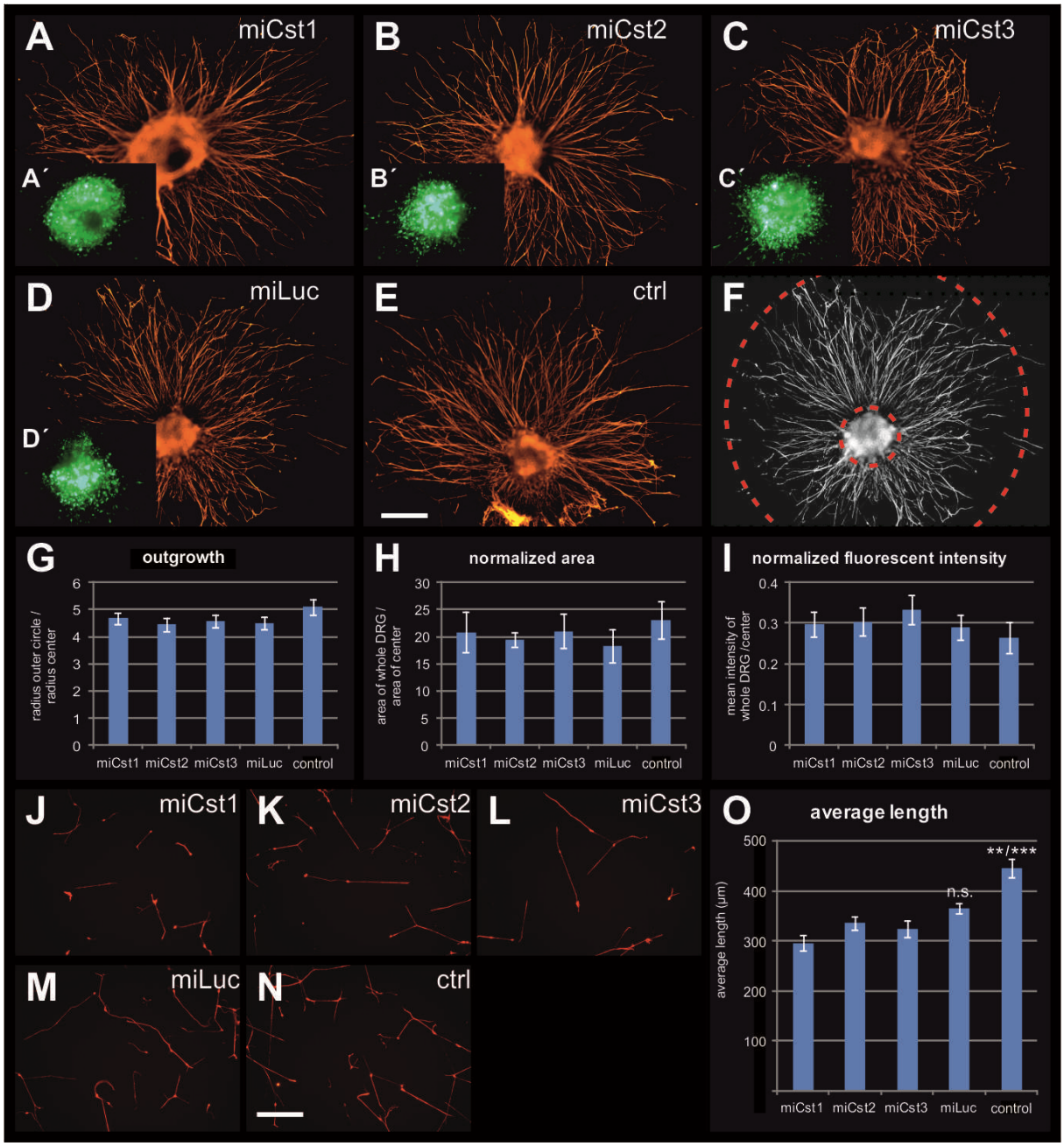

Figure 27: Neurite outgrowth of DRG explants and dissociated DRG neurons of embryos lacking Calsyntenin does not differ from control conditions. DRG explants of embryos treated with plasmids encoding miRNAs against Cst1 (A), Cst2 (B), Cst3 (C) or luciferase (D) were grown on laminin for 36h. (E) shows an explant of an untreated control embryo (ctrl). (F) indicates the way of quantification (center circle and outer circle) for (G-I). (G-I) show different ways of assessing the DRG behavior. (J-N) dissociated DRG neurons from embryos lacking Cst1 (J), Cst2 (K), Cst3 (L) or control injected (M) embryos untreated control embryos (N). O shows the quantification of the average neurite length. The untreated control (ctrl) is significant (**) to the miLuc control and significant (***) to miCst1, 2 and 3; one way ANOVA; ** $p \leq 0.01$, *** $p \leq 0.0001$. Values are given ± SEM. Total number of embryos = 4 per condition, numbers of neurites measured = 45-55 (per condition). The p-values are given in the appendix. Bar: 200 µm for (A-F), 100 µm for (J-N).

Floor-plate specific Calsyntenin downregulation results in axon guidance defects

The use of plasmid encoding miRNAs allows for the use of tissue-specific promoters. In the previously discussed open-book preparations, we primarily used Math1-driven plasmids which particularly drive miRNA expression in the dI1commissural neurons. Because Cst1 and 3 are also expressed in the floor plate and because Hoxa1, a floor-plate specific enhancer, was available in our lab (Wilson and Stoeckli, 2011), we wanted to learn more about the role of Calsyntenins in the floor plate. We injected plasmids encoding EGFP and miRNAs against Cst1-3 or luciferase as described previously and carried out open-book preparations (Figure 28). The floor-plate specific lack of Cst1 resulted in a significant decrease of normal injection sites, an increase in floor-plate and contralateral stalling and additionally in caudal turns. This phenotype has only rarely been observed during my previous experiments and therefore was a very interesting observation. The lack of Cst2 and Cst3 specifically in the floor plate did not have an effect on commissural axon guidance.

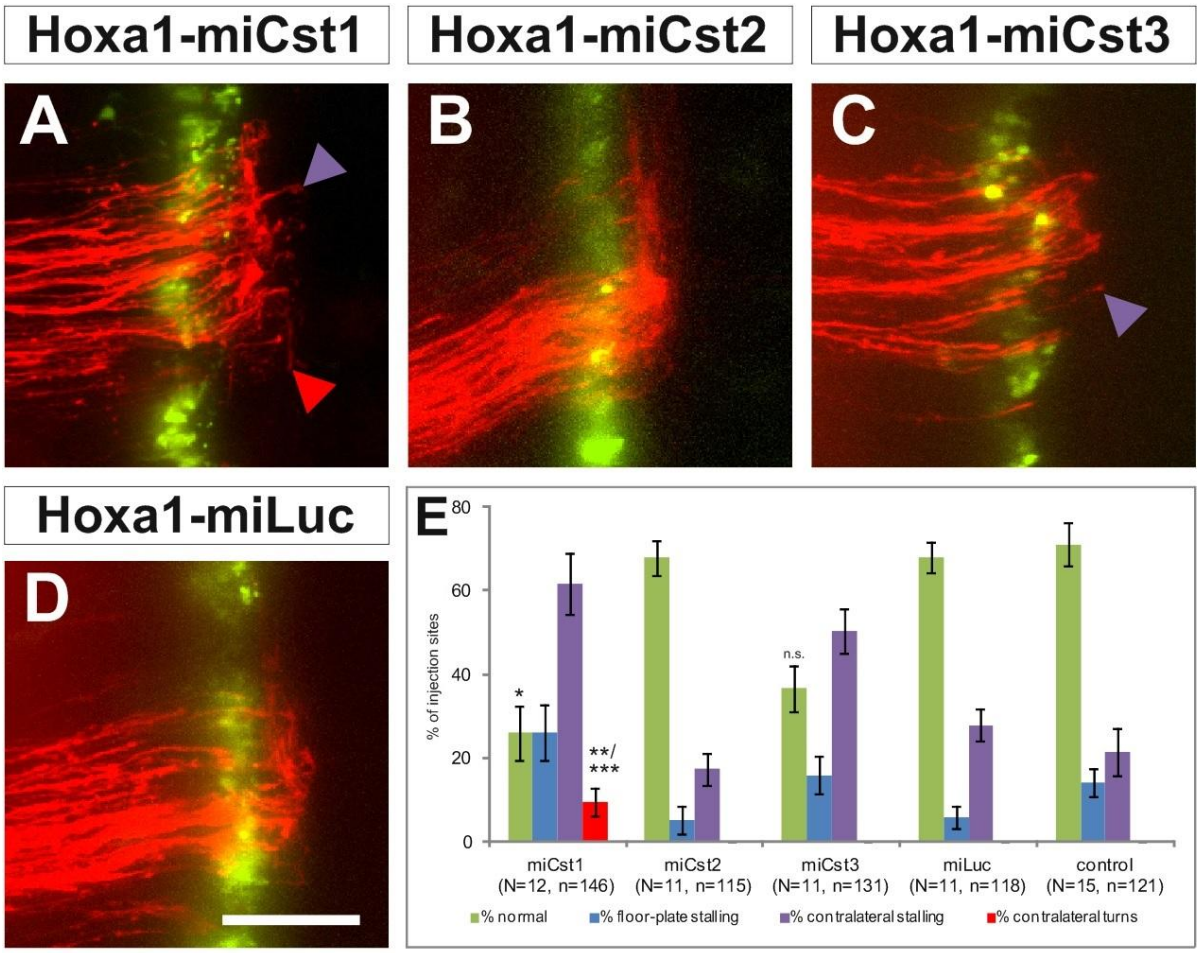

Figure 28: Floor-plate specific Calsyntenin1 downregulation leads to axon guidance defects. (A) When Cst1 was silenced in the floor plate (in green), we observed an increase of non-turning axons (violet arrowhead) and caudal turns (red arrowhead), whereas the floor-plate specific knock down of Cst2 (B) was not different controls. (C) The injection of a Hoxa1-driven plasmid encoding a miRNA against Cst3 resulted in an increase of contralateral stalling (violet arrowhead). The p values of the Hoxa1 open-book quantification are shown in the appendix. The values of the quantification of the open-book phenotypes (E) represent mean ± SEM; n.s. = not significant, * $p \leq 0.05$, ** $p \leq 0.01$, *** $p \leq 0.0001$; one way ANOVA; N = 10-15 with $n \geq 100$ per condition. The p-values are given in the appendix. Bar: 50 µm.

Calsyntenins are not expressed in a caudal to rostral gradient in the floor plate

In both mice and chicken morphogens are expressed in a gradient (Lyuksyutova et al., 2003 and Dominitskaya et al., 2010). In order to test for a potential role of Calsyntenins in the gradient expression of floor-plate associated molecules, we assessed Calsyntenin expression. Whole-mount in situ hybridization of open-book

explants confirmed that Cst1 was expressed strongly, whereas Cst3 was only very weakly expressed in the floor plate (Figure 29). Cst2 was not expressed at all. This experiment was carried out twice with 2 open books per gene. For Cst1 we found an inhomogeneous expression along the midline. To analyze the alternating expression levels in more detail, we cut two wild-type embryos at HH25 and collected every single section for in situ hybridization. We found that Cst1 is not expressed in a clear caudal to rostral gradient in the floor plate but we confirmed the alternating stronger and weaker floor-plate expression of Cst1.

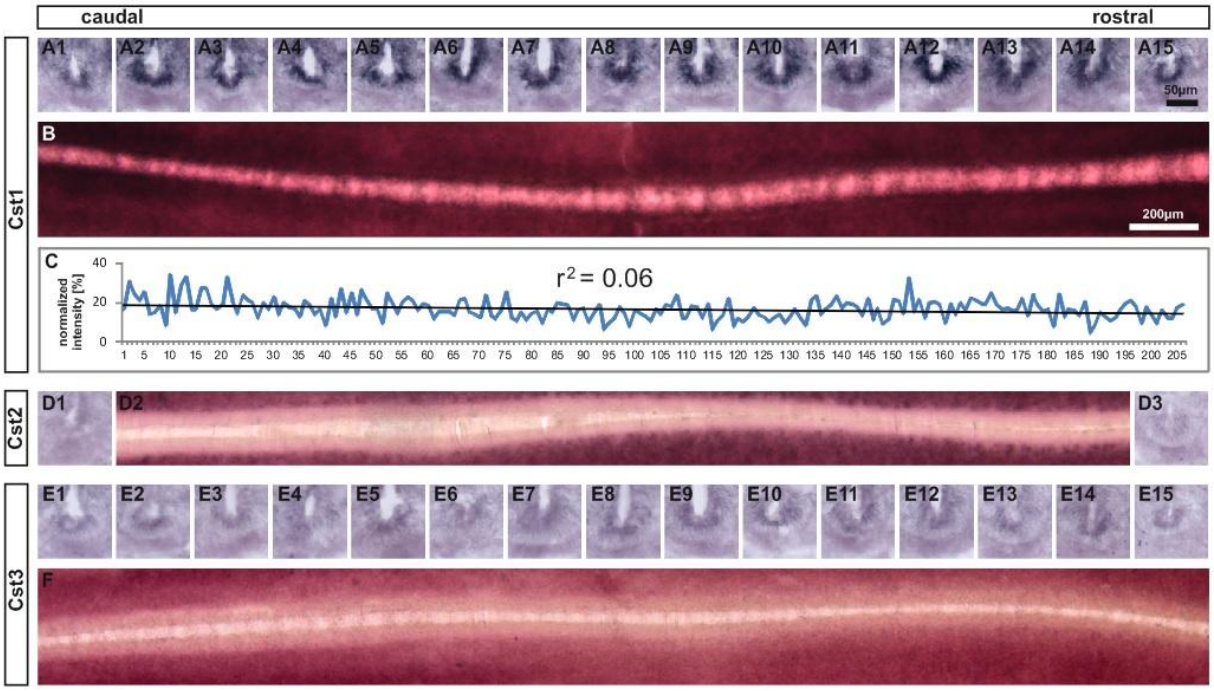

Figure 29: **Calsyntenin expression in the floor plate at HH25.** (A) Floor-plate sections from caudal (1) to rostral (15) stained for Cst1 expression. The sections correspond roughly to the level shown in (B). (C) Indicates the intensities of the in situ signal (normalized to the sense control; sense control is not shown) of every floor-plate section of a wild-type embryo and indicates the weaker and stronger expression of Cst1 in the midline. The regression line is almost horizontal (r^2 = 0.06 in the shown experiment and 0.04 the other assay) and indicates that there is no Cst1 gradient in the floor plate. (D, E and F) show the same for Cst2 and 3 but without graphical expression diagram. Bar: 50 µm for (A, D1,D3 and E), 100 µm for (B, D2 and F).

5.2. Supplementary methods

In situ hybridization of whole-mount embryos

Embryos were dissected and fixed as described in 4.1., methods part. Additionally, body cavities that could trap the probe were opened. Embryos were rinsed in PBT (PBS + 0.1% TritonX) twice for 10 min, then dehydrated in a graded methanol series diluted in PBT (25%, 50%, 75% methanol in PBT, 10 min each) and rinsed twice in pure methanol. Embryos were rehydrated by washing for 10 min each in the graded methanol series diluted in PBT (75%, 50%, 25% methanol in PBT) and then twice in PBT. Embryos were treated with 20 µg/ml proteinase K (Promega) for 5 min and refixed in 4% PFA in PBT for 20 min. After washing twice in PBT, embryos were incubated in prehybridization buffer at 56°C overnight (Mauti et al., 2006). Hybridization with 400 ng/ml in situ probe in hybridization buffer was carried out at 56°C for 72 h. Embryos were washed three times in 2x SSC, 0.1% CHAPS, then three times in 0.2x SSC, 0.1% CHAPS (at 56°C for 20 min each). After rinsing in KTBT (100 mM Tris-HCl, 150 mM NaCl, 1% TritonX, pH 7.5) at room temperature for 10 min, embryos were incubated in 10% FCS in KTBT for 3 h at RT and then incubated with the anti-DIG antibody (Roche) diluted 1:2000 in FCS/KTBT at 4°C overnight. Embryos were washed twice in NTMT (100 mM Tris-HCl, 50 mM MgCl2, 100 mM NaCl, 0.1% TritonX, pH 9.5) and incubated in the dark in NTMT containing 0.4 mM nitroblue tetrazolium (NBT; Roche), 0.4 mM 5-bromo-4-chloro-3-indoyl phosphate (BCIP; Roche), and 0.1 mM levamisole (Sigma). Signals for all Calsyntenins were visible after a few minutes of incubation. The enzymatic reaction was stopped after 40 min by incubating the embryos in TE buffer (Mauti et al., 2006) for two times 30 min. Embryos were stored in PBS containing 0.1% sodium azide. All steps were performed with constant shaking.

Pax7 staining of whole-mount embryos

Embryos (E2-E4, stages HH14-23) were dissected and fixed as described in 4.1., methods part. Embryos were washed in PBS, and then permeabilized with 1% Triton-X (in PBS) for 1 h. After incubation in 20 mM lysine in 0.1 M sodium phosphate buffer (pH 7.4) and 3 washes in PBS for 10 min each, the tissues were blocked in 10% FCS (in PBS) for 2 h. Embryos were incubated with anti-Pax7 antibody (Developmental

Studies) (diluted 1:1000 in 10% FCS in PBS) at 4°C for 48 h. After thoroughly washing (5x 10 min) in PBS, the embryos were blocked for 2 h before incubation with a goat anti-mouse Cy3 (Jackson ImmunoResearch) antibody (diluted 1:250 in 10% FCS in PBS) in the dark at 4°C o/n. The embryos were washed 5 times in PBS and analyzed with a stereobinocular microscope equipped with fluorescence optics (OLYMPUS SZX12).

Neurofilament staining of whole-mount embryos

Experimental or wild type embryos (E5, stages HH25-26) were dissected and fixed as described in 4.1., methods part. Embryos were briefly washed in PBS, and then permeabilized with 1% Triton-X (in PBS) for 1 h. After incubation in 20 mM lysine in 0.1 M sodium phosphate buffer (pH 7.4) and 3 washes in PBS for 10 min each, the tissues were blocked in 10% FCS (in PBS) for 2 h. Embryos were incubated with anti neurofilament antibody (RMO270) (diluted 1:1500 in 10% FCS in PBS) at 4°C for 48-72 h. After thoroughly washing (5x 10 min) in PBS, the embryos were blocked for 2 h before incubation with a goat anti-mouse IgG-Cy3 (Sigma) antibody (diluted 1:250 in 10% FCS in PBS) in the dark at 4°C o/n. The embryos were washed again 5 times in PBS and the GFP signal was imaged before embryos were dehydrated in a methanol series (25%, 50%, 75%, 2x 100%) for 10 min each. To clear the tissue, embryos were immersed in benzyl benzoate:benzyl alcohol (BB:BA) (2:1) and analyzed with a stereobinocular microscope equipped with fluorescence optics (OLYMPUS SZX12).

Cloning miRNAs under Hoxa1 specific promoter

The cloning of miRNAs is described in manuscript 4.2. in Table 1. We used the miRNA plasmid backbones as described in Wilson and Stoeckli (Wilson and Stoeckli, 2011) and inserted the hairpin-loop structure containing the miRNAs using NheI and MluI (both NEB) to create Hoxa1 RNA-polymerase II driven plamids.

6. Discussion and outlook

The analysis of the Calsyntenins in the chicken embryo revealed insights into the expression of these genes during development and provide new aspects of their function in commissural axon guidance during neural circuit formation. We showed that intracellular trafficking is a crucial regulatory mechanism in axon guidance as it delivers guidance cues to the growth cone surface. We describe for the first time the importance of this mechanism in commissural axon guidance. We found a contribution of Cst1 to the regulation of floor-plate exit and the contralateral turning decision of dorsal commissural axons as Cst1 is involved in controlling surface levels of Robo1 and Fzd3. Moreover, we could show that the absence of Calsyntenin in the DRGs also resulted in axon guidance defects. These findings reveal that Calsyntenins play an important role in axon guidance.

6.1. Calsyntenins are expressed in a distinct and partially overlapping pattern during development

We investigated the Calsyntenin mRNA expression in the chicken embryo with a special focus on the lumbosacral spinal cord. We found all Calsyntenins expressed in neural and non-neural tissue from already at early stages. All Calsyntenins are expressed in precursor cells suggesting a role in the rapid turnover of proliferating, newly born cells. Cst2 is strongly expressed in the somites and their derivatives, indicating that Cst2 may contribute to the formation of these structures. To reveal the particular functions of Cst2 in these cells, further studies are necessary. Cst1 and Cst3 are expressed in dI1 neurons and in the floor plate and we could show that both of them play a role in commissural axon guidance. Notably, expression patterns of Cst1 and Cst3 were similar in the spinal cord, whereas Cst2 turned up in a more distinct pattern. In contrast, the expression patterns of Cst2 and Cst3 were similar in the brain and Cst1 was expressed differently. This is particularly interesting considering that the protein domain structures of Cst1 and 2 are more similar to each other than to Cst3 (Hintsch et al., 2002). Due to the similarity of the Calsyntenins among each other, one could expect redundancy between them. However, our functional studies do not support this point of view as the downregulation of a single

Calsyntenin, e.g. in the DRG, resulted in axon guidance defects, no matter if the other two remaining Calsyntenins were still present. It would be interesting to see if double or triple Calsyntenin knockdowns would enhance the effects on axon guidance.

6.2. Vesicular trafficking: a way to regulate guidance cue surface expression and a role for Cst1 in commissural axon guidance

During neural circuit formation, axons must find their correct targets. The growth cones at the outgrowing axons' tips are constantly subject to a set of different guidance cues that must be recognized and correctly understood. Therefore, growth cones need to display the right combination of receptors at their plasma membrane in order to appropriately respond to the changing environment. During the wiring of dorsal commissural axons, the floor plate acts as an intermediate target for the axons, attracting pre-crossing, and repelling crossing and post-crossing axons. This switch between attraction and repulsion requires careful regulation of receptors for guidance cues on the surface. Generally, the surface expression of guidance cues can be regulated in four different ways: at the transcriptional or the translational level, at the level of protein stabilization or at the level of vesicular trafficking (Figure 30).

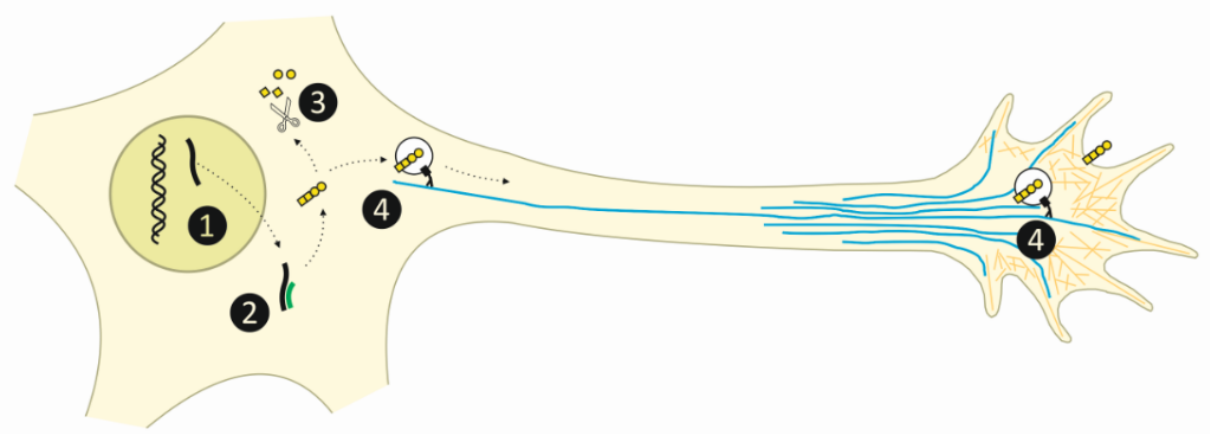

Figure 30: Four mechanisms to regulate guidance cue surface expression. 1) Regulation at transcriptional level. Only if a gene is transcribed, a certain protein can appear in the cellular system. 2) Regulation at translational level, e.g. by the inhibition of translation by miRNAs. 3) Once a protein is synthesized, it can be prevented from being exposed at the

cellular surface by cleavage (regulation at the level of protein stabilization), or (4) by the failure of specific vesicular transport (regulation by intracellular trafficking). If parts of the machinery that delivers vesicles to the plasma membrane are not active, proteins cannot be inserted into the cell membrane.

Bourikas and colleagues described a regulation of guidance cue expression at the transcriptional level (Bourikas et al., 2005). Only if a gene is transcribed, the protein can eventually be expressed in the cell. They showed that Hhip is expressed transiently by commissural neurons during the time when their axons turn into the longitudinal axis. Later it was found that Hhip transcription is induced by Shh in a glypican1- and patched-dependent manner, thus triggering the repulsive response to Shh in post-crossing axons (Wilson and Stoeckli, 2013). Another regulatory mechanism for the surface expression of guidance receptors or guidance cues respectively can be achieved by preventing translation of the messenger RNA, most likely based on miRNAs. This posttranscriptional mechanism was described for semaphorin signaling (Baudet et al., 2012), where Sema3A sensitivity to NRP1 is controlled by miR-124 in navigating retinal growth cones. However, in cases where the mRNA message is already present in the cell before the protein is required for axon guidance, posttranslational mechanisms must regulate guidance receptor surface expression. Also for that kind of regulation, there is an example from semaphorin signaling: plexin-A1 (PA1) is kept at low levels in pre-crossing axons due to proteolytic cleavage by calpain1 (Nawabi et al., 2010). Only upon floor-plate contact, signals derived from the floor plate (NrCAM) inhibit the calpain-1-mediated processing of PA1, resulting in PA1 stabilization and inducing sensitivity to the negative guidance cues at the floor plate. Furthermore, we recently introduced a regulatory mechanism depending on intracellular trafficking. RabGDI, a gene linked to human mental retardation (D'Adamo et al., 1998), is an important component of the vesicle fusion machinery (see Figure 3). In dorsal commissural axons it regulates surface expression of Robo1 (Philipp et al., 2012). Before crossing, Robo1 is detected inside the axons and rarely at the surface (Mambetisaeva et al., 2005, Chen et al., 2008). Only during floor-plate crossing, RabGDI is up-regulated and induces Robo1 surface expression which mediates the Slit-dependent repulsion from the midline. We showed that Robo1 trafficking is dependent on Cst1- and Rab11-positive vesicles. Because Cst1 and Rab11 are located in the same vesicular populations

(Steuble et al., 2010) and because commissural neuron-specific downregulation of Cst1 resulted in partial floor-plate stalling of commissural axons (see Figure 1, manuscript 4.2.) – the same phenotype as seen after RabGDI or Robo1 downregulation (Philipp et al., 2012), we concluded that Cst1 and Rab11 co-operate in Robo1 trafficking. This was supported by co-localization experiments in COS7 cells and commissural growth cones which revealed that Cst1 partially overlaps with Robo1, Rab11 and RabGDI-positive vesicles, indicating that they could work in the same pathway. In embryos treated with hypomorphic doses of miRNAs against Robo1 and Cst1, we found different commissural axon guidance defects depending on the time point of injection/electroporation. E3-injected embryos showed more defects at the contralateral site, whereas in E2.5-injected embryos, floor-plate stalling was the most prominent phenotype. This demonstrates the importance of timing during commissural axon guidance at the midline. Only when interfering with Robo1 expression before the protein has been made, the combinatorial knockdown of Cst1 and Robo1 at sub-threshold levels causes floor-plate stalling. When Robo1 protein is present, the remaining Cst1 actively transports Robo1-positive vesicles to the growth-cone surface, where it binds the negative guidance cue Slit to push the axons out of the midline. Taken together, our results confirm that for proper midline crossing, commissural axons need all three proteins: Cst1, Robo1, and RabGDI.

In addition to floor-plate stalling, we also detected a considerable number of axons stalling at the contralateral floor-plate exit site in open-book preparations of embryos lacking Cst1. We favored Fzd3 as potential cargo of Cst1-positve vesicles since Fzd3 is known to play a role in contralateral commissural axon guidance (Lyuksyutova et al., 2003). In addition, like Cst1, Fzd3 also localizes to Rab11-positive vesicles (Purvanov et al., 2010). We found a strong overlap of Cst1- and Fzd3-positive vesicles in COS7 cells and commissural growth cones. Intriguingly, dsRNA-based knockdown of Fzd3 at E3 did not lead to axon guidance defects (see Figure 6, manuscript 4.2.). Only when injecting dsRNA before Fzd3 expression starts, we found randomly turning axons and contralateral stalling after midline crossing. Similar to what was observed for Robo1, timing of intervention is important. Interfering with Fzd3 expression must precede protein accumulation. The injection and electroporation of plasmids encoding miRNAs against Fzd3 at E2.5 resulted also in contralateral axon guidance defects similar to those seen in embryos lacking Cst1.

We showed that the combinatorial knockdown of Cst1 and Fzd3 at sub-threshold levels mimicked the main phenotype seen after the single downregulation of either Cst1 or Fzd3. In contrast to the regulation of Robo1, the surface expression of Fzd3 is not RabGDI-dependent as a combinatorial knockdown of Fzd3 and RabGDI at sub-threshold levels did not result in axon guidance defects at the midline. Thus, like Robo1, Fzd3 regulation is dependent on vesicular trafficking rather than transcription. However, our results from the co-injection experiments indicate that Fzd3 expression is independent of RabGDI, in contrast to Robo1 trafficking that depends on Cst1 and RabGDI.

In this thesis, we describe a role for Cst1 in dorsal commissural axon guidance by co-regulating the levels of Robo1 and Fzd3 surface expression. We showed that the absence of Cst1 results in floor-plate stalling and contralateral stalling of commissural axons. We found that Cst1 is involved in the transport of distinct sets of vesicles, which are positive for Robo1 or Fzd3 and possibly for additional cargo. We further confirmed that Robo1 surface expression is regulated by RabGDI (Philipp et al., 2012) in combination with Cst1 and found that Fzd3 surface expression is regulated independently of RabGDI, but depending on Cst1. With these findings we introduce a new modulating mechanism for receptor surface expression and show that Cst1 is regulating intracellular trafficking in a specific manner.

6.3. A role for Calsyntenins in the floor plate?

As Cst1 and Cst3 are expressed in the midline, we investigated their role by floor-plate specific mRNA knockdown (Figure 28). Interestingly, we also found axon guidance defects when silencing them in the intermediate target. For both Cst1 and Cst3 we found increased contralateral stalling, for Cst1 additionally some contralateral caudal turns. However, only the floor-plate specific loss of Cst1 led to a significant decrease of normal injection sites, not when Cst2 or Cst3 were knocked down. Due to this finding, we considered a function for Cst1 in the transport of guidance cues that are necessary for the rostral turning decision of commissural axons. We carried out a couple of co-localization essays in COS7 cells and in floor-

plate cells (with Wnt5a (see manuscript 4.2., Supplementary Figure 4) and PlexinA2 (not shown)), but could not detect any convincing overlap of vesicles positive for Cst1 and either one of them. Other candidates such as Wnt7a or Shh have not yet been tested. There are guidance cues in the floor plate that are expressed in gradients (Lyuksyutova et al., 2003 and Dominitskaya et al., 2010). We checked if this was also the case for the Calsyntenins. However, we did not find any gradients, but rather a patchy expression for Cst1 (Figure 29). Thus, Calsyntenin function in the midline remains unclear and will have to be further investigated. Taken together, our results suggest that Cst1 plays a role in the floor plate during the formation of commissural circuits and points to the fact that Calsyntenins have multi-purpose functions in the formation of the nervous system.

6.4. Calsyntenins are required for proper neural circuit formation outside the CNS

As Calsyntenins are expressed in both sensory and motor neurons, we investigated whole-mount embryos lacking Calsyntenins to gain insights into their function in the formation of peripheral nerves. All Calsyntenins are already expressed in DRGs from early stages and persists throughout the entire embryonic development. Whole-mount embryos lacking any Calsyntenin display aberrant DRGs (Figure 26) indicating a role for them in DRG formation. We analyzed DRG explants and dissociated DRG neurons (Figure 27) looking at growth and branching but did not find statistical differences when compared to the injected control. These results suggest that the aberrant DRG phenotypes observed in the whole mounts are probably not caused by decreased DRG growth or incorrect branching capability. Our findings rather suggest that Calsyntenins have a function in DRG formation. Future experiments that focus on axon guidance are required to test this. With respect to the peripheral nerves in the limbs, we were not able to detect axon guidance defects. However, when focusing on the epaxial nerves, we found aberrations in fasciculation and bundling in the absence of either Cst1 or Cst3. The knockdown of Cst2 did not have an influence in epaxial nerve formation, which is in line with its expression. Cst1 and Cst3 are both expressed in the medial, whereas Cst2 is restricted to the lateral motor columns. The

epaxial nerves originate from neurons located close to the ventricular zone (Shirasaki et al., 2002), where we find expression of Cst1 and 3, but not of Cst2. Altogether, these preliminary data suggest that Calsyntenins play a role in proper PNS formation and indicate that they are required for correct axon guidance beyond their function as regulator for guidance cue transport in dorsal commissural neurons.

6.5. Calsyntenin as linker protein between kinesin and vesicles and its function synaptic plasticity

We showed that Cst1 is regulating vesicular trafficking in a highly specific manner, thus mediating proper axon guidance. Several studies from the lab of Peter Sonderegger reported earlier that Cst1 plays a role in the transport of vesicles required for synapse formation (Steuble et al., 2010 and 2012). Investigating Cst1-positive vesicles derived from cortical neurons of juvenile mice, they detected proteins required for synapse formation, synaptic maintenance and plasticity. Studies in the mature nervous system indicate that Calsyntenins also play a role in the maintainance of neurons, as patients suffering from different forms of dementia show altered Calsyntenin leves or cleavage products in the cerebrospinal fluid (Yin et al., 2009; Ringman et al., 2012; Uchida et al., 2013; Dieks et al., 2013). Taken together, these and our studies nicely illustrate the importance of Cst1 during both neural development and homeostasis in mature neurons which is in fact not too surprising as there are many parallels between axon guidance and synaptic plasticity. In both cases, vesicular trafficking and specific delivery of receptors into the cell membrane are crucial. It looks like nature uses the same Calsyntenin-dependent mechanism for protein delivery to the cell surface during both neuronal development and synaptic plasticity. During neural circuit formation, Cst1 delivers axon guidance molecules to the plasma membrane to ensure proper axon guidance. When axon guidance is complete, the same mechanism is involved in synapse formation and probably also in maintaining synaptic plasticity as Cst1 is involved in the correct transport a set of proteins required at the mature synapse, such as recycling membrane proteins, membrane transport proteins, SNAREs and many others (Steuble et al., 2010). Direct effects on synaptic plasticity have been demonstrated in vivo by Ikeda et al., where

they showed that the Cst2 ortholog CASY-1 is essential for learning in C. elegans (Ikeda et al., 2008). CASY-1 mutants showed impairments in learning capacity which can be explained by decreased synaptic plasticity.

6.6. A role for Calsyntenin in brain disorders?

Neurodevelopmental brain disorders such as schizophrenia, autism spectrum disorders or intellectual disability have in common that neural circuits do not function correctly due to aberrant formation during development (Stoeckli, 2012). At the other end of the spectrum, neurodegenerative diseases such as Alzheimer's or Parkinson's disease are rather associated with insufficient maintenance of neural circuits. My work provides further evidence that these diseases could be caused by a combination of both aberrant development and aberrant maintenance of neural circuits. Many neurodevelopmental genes have been identified as candidate disease genes in both neurodevelopmental and neurodegenerative disorders (Lesnick et al., 2007; Engle, 2010; Mitchell, 2011). For instance, the Robo1 gene has been suggested as a candidate for causing developmental dyslexia (Hannula-Jouppi et al., 2005). This provides a link to Cst1 that is involved in Robo1 transport, and supports the idea that proper vesicular distribution during neural circuit formation is required in order to prevent neurodevelopmental diseases. Calsyntenins have also been linked to neurodegenerative diseases (Yin et al., 2009; Ringman et al., 2012; Dieks et al., 2013), as altered Calsyntenin levels have been observed in the cerebrospinal fluid of patients suffering from Alzheimer's disease, Parkinson's disease or dementia with Lewy bodies. It remains to be shown how aberrant Calsyntenin expression affects neurological function, but it may well be a link between development and maintenance of the mature nervous system. Cst1 is a nice example of a protein that is required for axon guidance and in maintaining synaptic plasticity, as it illustrates the importance of vesicular trafficking during neuronal development and synaptic plasticity.

7. References

Adams RH, Wilkinson GA, Weiss C, Diella F, Gale NW, Deutsch U, Risau W, Klein R (1999) Roles of ephrinB ligands and EphB receptors in cardiovascular development: demarcation of arterial/venous domains, vascular morphogenesis, and sprouting angiogenesis. Genes Dev. 13:295–306.

Almeida R, Allshire RC (2005) RNA silencing and genome regulation. Trends Cell Biol 15:251–258.

Araki Y, Miyagi N, Kato N, Yoshida T, Wada S, Nishimura M, Komano H, Yamamoto T, Strooper B de, Yamamoto K, Suzuki T (2004) Coordinated metabolism of Alcadein and amyloid beta-protein precursor regulates FE65-dependent gene transactivation. J. Biol. Chem. 279:24343–24354.

Araki Y, Tomita S, Yamaguchi H, Miyagi N, Sumioka A, Kirino Y, Suzuki T (2003) Novel cadherin-related membrane proteins, Alcadeins, enhance the X11-like protein-mediated stabilization of amyloid beta-protein precursor metabolism. J. Biol. Chem. 278:49448–49458.

Armelin HA (1973) Pituitary extracts and steroid hormones in the control of 3T3 cell growth. Proc. Natl. Acad. Sci. U.S.A. 70:2702–2706.

Attisano L, Wrana J (2002) Signal transduction by the TGF-beta superfamily. Science 296:1646–1647.

Augsburger A, Schuchardt A, Hoskins S, Dodd J, Butler S (1999) BMPs as mediators of roof plate repulsion of commissural neurons. Neuron 24:127–141.

Avilés EC, Wilson NH, Stoeckli ET (2013) Sonic hedgehog and Wnt: antagonists in morphogenesis but collaborators in axon guidance. Front Cell Neurosci 7:86.

Baeriswyl T, Mauti O, Stoeckli ET (2008) Temporal control of gene silencing by in ovo electroporation. Methods Mol. Biol. 442:231–244.

Baeriswyl T, Stoeckli ET (2006) In ovo RNAi opens new possibilities for temporal and spatial control of gene silencing during development of the vertebrate nervous system. J RNAi Gene Silencing 2:126–135.

Bartkowska K, Paquin A, Gauthier AS, Kaplan DR, Miller FD (2007) Trk signaling regulates neural precursor cell proliferation and differentiation during cortical development. Development 134:4369–4380.

Baudet M, Zivraj KH, Abreu-Goodger C, Muldal A, Armisen J, Blenkiron C, Goldstein LD, Miska EA, Holt CE (2012) miR-124 acts through CoREST to control onset of Sema3A sensitivity in navigating retinal growth cones. Nat. Neurosci 15:29–38.

Ben-Yair R, Kalcheim C (2008) Notch and bone morphogenetic protein differentially act on dermomyotome cells to generate endothelium, smooth, and striated muscle. The Journal of Cell Biology 180:607–618.

Bernstein E, Denli AM, Hannon GJ (2001) The rest is silence. RNA 7:1509–1521.

Bianchi V, Gambino F, Muzio L, Toniolo D, Humeau Y, D'Adamo P (2012) Forebrain deletion of αGDI in adult mice worsens the pre-synaptic deficit at cortico-lateral amygdala synaptic connections. PLoS ONE 7:e29763.

Bleuming SA, He XC, Kodach LL, Hardwick JC, Koopman FA, Kate FJ ten, van Deventer SJH, Hommes DW, Peppelenbosch MP, Offerhaus GJ, Li L, van den Brink GR (2007) Bone morphogenetic protein signaling suppresses tumorigenesis at gastric epithelial transition zones in mice. Cancer Res. 67:8149–8155.

Bottcher RT (2005) Fibroblast Growth Factor Signaling during Early Vertebrate Development. Endocrine Reviews 26:63–77.

Bourikas D, Pekarik V, Baeriswyl T, Grunditz A, Sadhu R, Nardó M, Stoeckli ET (2005) Sonic hedgehog guides commissural axons along the longitudinal axis of the spinal cord. Nat. Neurosci 8:297–304.

Brinkman R, Martin AH (1973) A cytoarchitectonic study of the spinal cord of the domestic fowl Gallus gallus domesticus. I. Brachial region. Brain Res. 56:43–62.

Brose K, Bland KS, Wang KH, Arnott D, Henzel W, Goodman CS, Tessier-Lavigne M, Kidd T (1999) Slit proteins bind Robo receptors and have an evolutionarily conserved role in repulsive axon guidance. Cell 96:795–806.

Brunger AT (2005) Structure and function of SNARE and SNARE-interacting proteins. Q. Rev. Biophys. 38:1–47.

Buckingham M, Montarras D (2008) Skeletal muscle stem cells. Curr. Opin. Genet. Dev. 18:330–336.

Burden-Gulley SM, Payne HR, Lemmon V (1995) Growth cones are actively influenced by substrate-bound adhesion molecules. J. Neurosci. 15:4370–4381.

Butler SJ, Dodd J (2003) A role for BMP heterodimers in roof plate-mediated repulsion of commissural axons. Neuron 38:389–401.

Carrodeguas JA, Rodolosse A, Garza MV, Sanz-Clemente A, Pérez-Pé R, Lacosta AM, Domínguez L, Monleón I, Sánchez-Díaz R, Sorribas V, Sarasa M (2005) The chick embryo appears as a natural model for research in beta-amyloid precursor protein processing. Neuroscience 134:1285–1300.

Charron F, Stein E, Jeong J, McMahon AP, Tessier-Lavigne M (2003) The morphogen sonic hedgehog is an axonal chemoattractant that collaborates with netrin-1 in midline axon guidance. Cell 113:11–23.

Chédotal A (2011) Further tales of the midline. Curr. Opin. Neurobiol. 21:68–75.

Chen Z, Gore BB, Long H, Le Ma, Tessier-Lavigne M (2008) Alternative splicing of the Robo3 axon guidance receptor governs the midline switch from attraction to repulsion. Neuron 58:325–332.

Cheng HJ, Flanagan JG (1994) Identification and cloning of ELF-1, a developmentally expressed ligand for the Mek4 and Sek receptor tyrosine kinases. Cell 79:157–168.

Christ B, Scaal M (2008) Formation and differentiation of avian somite derivatives. Adv Exp Med Biol 638:1–41.

Cinnamon Y (2006) Differential effects of N-cadherin-mediated adhesion on the development of myotomal waves. Development 133:1101–1112.

Colamarino SA, Tessier-Lavigne M (1995) The axonal chemoattractant netrin-1 is also a chemorepellent for trochlear motor axons. Cell 81:621–629.

D'Adamo P, Menegon A, Lo Nigro C, Grasso M, Gulisano M, Tamanini F, Bienvenu T, Gedeon AK, Oostra B, Wu SK, Tandon A, Valtorta F, Balch WE, Chelly J, Toniolo D (1998) Mutations in GDI1 are responsible for X-linked non-specific mental retardation. Nat. Genet. 19:134–139.

Davey MG, Tickle C (2007) The chicken as a model for embryonic development. Cytogenet. Genome Res. 117:231–239.

Dessaud E, McMahon AP, Briscoe J (2008) Pattern formation in the vertebrate neural tube: a sonic hedgehog morphogen-regulated transcriptional network. Development 135:2489–2503.

Dickson BJ (2002) Molecular mechanisms of axon guidance. Science 298:1959–1964.

Dieks J, Gawinecka J, Asif AR, Varges D, Gmitterova K, Streich J, Dihazi H, Heinemann U, Zerr I (2013) Low-abundant cerebrospinal fluid proteome alterations in dementia with lewy bodies. J. Alzheimers Dis. 34:387–397.

Domanitskaya E, Wacker A, Mauti O, Baeriswyl T, Esteve P, Bovolenta P, Stoeckli ET (2010) Sonic hedgehog guides post-crossing commissural axons both directly and indirectly by regulating Wnt activity. J. Neurosci. 30:11167–11176.

Eberhart J (2004) Ephrin-A5 Exerts Positive or Inhibitory Effects on Distinct Subsets of EphA4-Positive Motor Neurons. Journal of Neuroscience 24:1070–1078.

Engle EC (2010) Human Genetic Disorders of Axon Guidance. Cold Spring Harbor Perspectives in Biology 2:a001784.

Fire A, Xu S, Montgomery MK, Kostas SA, Driver SE, Mello CC (1998) Potent and specific genetic interference by double-stranded RNA in Caenorhabditis elegans. Nature 391:806–811.

Gale NW, Holland SJ, Valenzuela DM, Flenniken A, Pan L, Ryan TE, Henkemeyer M, Strebhardt K, Hirai H, Wilkinson DG, Pawson T, Davis S, Yancopoulos GD (1996) Eph receptors and ligands comprise two major specificity subclasses and are reciprocally compartmentalized during embryogenesis. Neuron 17:9–19.

Gao WQ, Shinsky N, Armanini MP, Moran P, Zheng JL, Mendoza-Ramirez JL, Phillips HS, Winslow JW, Caras IW (1998) Regulation of hippocampal synaptic plasticity by the tyrosine kinase receptor, REK7/EphA5, and its ligand, AL-1/Ephrin-A5. Mol. Cell. Neurosci. 11:247–259.

Geraldo S, Gordon-Weeks PR (2009) Cytoskeletal dynamics in growth-cone steering. J. Cell. Sci. 122:3595–3604.

Gordon MD (2006) Wnt Signaling: Multiple Pathways, Multiple Receptors, and Multiple Transcription Factors. Journal of Biological Chemistry 281:22429–22433.

Gospodarowicz D (1974) Localisation of a fibroblast growth factor and its effect alone and with hydrocortisone on 3T3 cell growth. Nature 249:123–127.

Guthrie S (2004) Axon guidance: mice and men need Rig and Robo. Curr. Biol. 14:R632-4.

Hallonet ME, Le Douarin NM (1993) Tracing neuroepithelial cells of the mesencephalic and metencephalic alar plates during cerebellar ontogeny in quail-chick chimaeras. Eur. J. Neurosci. 5:1145–1155.

Hamburger V and Hamilton HL (1951) A series of normal stages in the development of the chick embryo. J. Morph. 88:49-92.

Hannula-Jouppi K, Kaminen-Ahola N, Taipale M, Eklund R, Nopola-Hemmi J, Kääriäinen H, Kere J (2005) The axon guidance receptor gene ROBO1 is a candidate gene for developmental dyslexia. PLoS Genet. 1:e50.

Hanson PI, Heuser JE, Jahn R (1997) Neurotransmitter release - four years of SNARE complexes. Curr. Opin. Neurobiol. 7:310–315.

Hata S, Fujishige S, Araki Y, Kato N, Araseki M, Nishimura M, Hartmann D, Saftig P, Fahrenholz F, Taniguchi M, Urakami K, Akatsu H, Martins RN, Yamamoto K, Maeda M, Yamamoto T, Nakaya T, Gandy S, Suzuki T (2009) Alcadein Cleavages by Amyloid -Precursor Protein (APP) - and -Secretases Generate Small Peptides, p3-Alcs, Indicating Alzheimer Disease-related -Secretase Dysfunction. Journal of Biological Chemistry 284:36024–36033.

Hatten ME, Heintz N (1995) Mechanisms of Neural Patterning and Specification in the Development Cerebellum. Annu. Rev. Neurosci. 18:385–408.

Hedgecock EM, Culotti JG, Hall DH (1990) The unc-5, unc-6, and unc-40 genes guide circumferential migrations of pioneer axons and mesodermal cells on the epidermis in C. elegans. Neuron 4:61–85.

Hintsch G, Zurlinden A, Meskenaite V, Steuble M, Fink-Widmer K, Kinter J, Sonderegger (2002) The calsyntenins--a family of postsynaptic membrane proteins with distinct neuronal expression patterns. Mol. Cell. Neurosci 21:393–409.

Hoerndli FJ, Walser M, Fröhli Hoier E, Quervain D de, Papassotiropoulos A, Hajnal A (2009) A conserved function of C. elegans CASY-1 calsyntenin in associative learning. PLoS ONE 4:e4880.

Holland SJ, Peles E, Pawson T, Schlessinger J (1998) Cell-contact-dependent signalling in axon growth and guidance: Eph receptor tyrosine kinases and receptor protein tyrosine phosphatase beta. Curr. Opin. Neurobiol. 8:117–127.

Holmes GP, Negus K, Burridge L, Raman S, Algar E, Yamada T, Little MH (1998) Distinct but overlapping expression patterns of two vertebrate slit homologs implies functional roles in CNS development and organogenesis. Mech. Dev. 79:57–72.

Honig MG, Camilli SJ, Xue Q (2002) Effects of L1 blockade on sensory axon outgrowth and pathfinding in the chick hindlimb. Dev. Biol. 243:137–154.

Huminiecki L, Gorn M, Suchting S, Poulsom R, Bicknell R (2002) Magic roundabout is a new member of the roundabout receptor family that is endothelial specific and expressed at sites of active angiogenesis. Genomics 79:547–552.

Ikeda DD, Duan Y, Matsuki M, Kunitomo H, Hutter H, Hedgecock EM, Iino Y (2008) CASY-1, an ortholog of calsyntenins/alcadeins, is essential for learning in Caenorhabditis elegans. Proc. Natl. Acad. Sci. U.S.A. 105:5260–5265.

Islam SM, Shinmyo Y, Okafuji T, Su Y, Naser IB, Ahmed G, Zhang S, Chen S, Ohta K, Kiyonari H, Abe T, Tanaka S, Nishinakamura R, Terashima T, Kitamura T, Tanaka H (2009) Draxin, a repulsive guidance protein for spinal cord and forebrain commissures. Science 323:388–393.

Itoh A, Miyabayashi T, Ohno M, Sakano S (1998) Cloning and expressions of three mammalian homologues of Drosophila slit suggest possible roles for Slit in the formation and maintenance of the nervous system. Brain Res. Mol. Brain Res. 62:175–186.

Jacobsen LK, Picciotto MR, Heath CJ, Mencl WE, Gelernter J (2009) Allelic variation of calsyntenin 2 (CLSTN2) modulates the impact of developmental tobacco smoke exposure on mnemonic processing in adolescents. Biol. Psychiatry 65:671–679.

Kalil K, Szebenyi G, Dent EW (2000) Common mechanisms underlying growth cone guidance and axon branching. J. Neurobiol. 44:145–158.

Keleman K, Ribeiro C, Dickson BJ (2005) Comm function in commissural axon guidance: cell-autonomous sorting of Robo in vivo. Nat. Neurosci. 8:156–163.

Kennedy TE, Serafini T, La Torre JR de, Tessier-Lavigne M (1994) Netrins are diffusible chemotropic factors for commissural axons in the embryonic spinal cord. Cell 78:425–435.

Kidd T, Bland KS, Goodman CS (1999) Slit is the midline repellent for the robo receptor in Drosophila. Cell 96:785–794.

Kidd T, Brose K, Mitchell KJ, Fetter RD, Tessier-Lavigne M, Goodman CS, Tear G (1998) Roundabout controls axon crossing of the CNS midline and defines a novel subfamily of evolutionarily conserved guidance receptors. Cell 92:205–215.

Klaus A, Birchmeier W (2008) Wnt signalling and its impact on development and cancer. Nat Rev Cancer 8:387–398.

Kolodkin AL, Matthes DJ, Goodman CS (1993) The semaphorin genes encode a family of transmembrane and secreted growth cone guidance molecules. Cell 75:1389–1399.

Kolodkin AL, Matthes DJ, O'Connor TP, Patel NH, Admon A, Bentley D, Goodman CS (1992) Fasciclin IV: sequence, expression, and function during growth cone guidance in the grasshopper embryo. Neuron 9:831–845.

Konecna A, Frischknecht R, Kinter J, Ludwig A, Steuble M, Meskenaite V, Indermühle M, Engel M, Cen C, Mateos J, Streit P, Sonderegger P (2006) Calsyntenin-1 docks vesicular cargo to kinesin-1. Mol. Biol. Cell 17:3651–3663.

Krull CE, Koblar SA (2000) Motor axon pathfinding in the peripheral nervous system. Brain Res. Bull. 53:479–487.

Kullander K, Klein R (2002) Mechanisms and functions of eph and ephrin signalling. Nat. Rev. Mol. Cell Biol. 3:475–486.

Lance-Jones C, Landmesser L (1980) Motoneurone projection patterns in embryonic chick limbs following partial deletions of the spinal cord. J. Physiol. (Lond.) 302:559–580.

Lance-Jones C, Landmesser L (1980) Motoneurone projection patterns in the chick hind limb following early partial reversals of the spinal cord. J. Physiol. (Lond.) 302:581–602.

Landmesser L (1978) The development of motor projection patterns in the chick hind limb. J. Physiol. (Lond.) 284:391–414.

Landmesser L, Dahm L, Tang JC, Rutishauser U (1990) Polysialic acid as a regulator of intramuscular nerve branching during embryonic development. Neuron 4:655–667.

Landmesser L, Morris DG (1975) The development of functional innervation in the hind limb of the chick embryo. J. Physiol. (Lond.) 249:301–326.

Lasek RJ, Garner JA, Brady ST (1984) Axonal transport of the cytoplasmic matrix. J. Cell Biol. 99:212s-221s.

Lawrence CJ (2004) A standardized kinesin nomenclature. The Journal of Cell Biology 167:19–22.

Lee KJ, Jessell TM (1999) The specification of dorsal cell fates in the vertebrate central nervous system. Annu. Rev. Neurosci. 22:261–294.

Lesnick TG, Papapetropoulos S, Mash DC, Ffrench-Mullen J, Shehadeh L, Andrade M de, Henley JR, Rocca WA, Ahlskog JE, Maraganore DM (2007) A genomic pathway approach to a complex disease: axon guidance and Parkinson disease. PLoS Genet. 3:e98.

Lowery LA, van Vactor D (2009) The trip of the tip: understanding the growth cone machinery. Nat. Rev. Mol. Cell Biol. 10:332–343.

Ludwig A, Blume J, Diep T, Yuan J, Mateos JM, Leuthäuser K, Steuble M, Streit P, Sonderegger P (2009) Calsyntenins mediate TGN exit of APP in a kinesin-1-dependent manner. Traffic 10:572–589.

Luo Y, Raible D, Raper JA (1993) Collapsin: a protein in brain that induces the collapse and paralysis of neuronal growth cones. Cell 75:217–227.

Lyuksyutova AI, Lu C, Milanesio N, King LA, Guo N, Wang Y, Nathans J, Tessier-Lavigne M, Zou Y (2003) Anterior-posterior guidance of commissural axons by Wnt-frizzled signaling. Science 302:1984–1988.

Mallik R, Rai AK, Barak P, Rai A, Kunwar A (2013) Teamwork in microtubule motors. Trends Cell Biol.

Mambetisaeva ET, Andrews W, Camurri L, Annan A, Sundaresan V (2005) Robo family of proteins exhibit differential expression in mouse spinal cord and Robo-Slit interaction is required for midline crossing in vertebrate spinal cord. Dev. Dyn 233:41–51.

Manitt C, Kennedy TE (2002) Where the rubber meets the road: netrin expression and function in developing and adult nervous systems. Prog. Brain Res. 137:425–442.

Martin AH (1979) A cytoarchitectonic scheme for the spinal cord of the domestic fowl, Gallus gallus domesticus: lumbar region. Acta Morphol Neerl Scand 17:105–117.

Maruta C, Saito Y, Hata S, Gotoh N, Suzuki T, Yamamoto T (2012) Constitutive cleavage of the single-pass transmembrane protein alcadeinα prevents aberrant peripheral retention of Kinesin-1. PLoS ONE 7:e43058.

Mauti O, Sadhu R, Gemayel J, Gesemann M, Stoeckli ET (2006) Expression patterns of plexins and neuropilins are consistent with cooperative and separate functions during neural development. BMC Dev. Biol 6:32.

Mitchell KJ (2011) The genetics of neurodevelopmental disease. Curr. Opin. in Neurobiol. 21:197–203.

Müller BK, Bonhoeffer F, Drescher U (1996) Novel gene families involved in neural pathfinding. Curr. Opin. Genet. Dev. 6:469–474.

Nakamoto M, Cheng HJ, Friedman GC, McLaughlin T, Hansen MJ, Yoon CH, O'Leary DD, Flanagan JG (1996) Topographically specific effects of ELF-1 on retinal axon guidance in vitro and retinal axon mapping in vivo. Cell 86:755–766.

Napoli C, Lemieux C, Jorgensen R (1990) Introduction of a Chimeric Chalcone Synthase Gene into Petunia Results in Reversible Co-Suppression of Homologous Genes in trans. Plant Cell 2:279–289.

Nawabi H, Briançon-Marjollet A, Clark C, Sanyas I, Takamatsu H, Okuno T, Kumanogoh A, Bozon M, Takeshima K, Yoshida Y, Moret F, Abouzid K, Castellani V (2010) A midline switch of receptor processing regulates commissural axon guidance in vertebrates. Genes Dev 24:396–410.

Nawabi H, Castellani V (2011) Axonal commissures in the central nervous system: how to cross the midline? Cell. Mol. Life Sci. 68:2539–2553.

Niederkofler V, Baeriswyl T, Ott R, Stoeckli ET (2010) Nectin-like molecules/SynCAMs are required for post-crossing commissural axon guidance. Development 137:427–435.

Nielsen E, Severin F, Backer JM, Hyman AA, Zerial M (1999) Rab5 regulates motility of early endosomes on microtubules. Nat. Cell Biol. 1:376–382.

Nishimura N, Nakamura H, Takai Y, Sano K (1994) Molecular cloning and characterization of two rab GDI species from rat brain: brain-specific and ubiquitous types. J. Biol. Chem. 269:14191–14198.

Nusse R, Varmus HE (1982) Many tumors induced by the mouse mammary tumor virus contain a provirus integrated in the same region of the host genome. Cell 31:99–109.

Nüsslein-Volhard C, Wieschaus E (1980) Mutations affecting segment number and polarity in Drosophila. Nature 287:795–801.

Okada A, Charron F, Morin S, Shin DS, Wong K, Fabre PJ, Tessier-Lavigne M, McConnell SK (2006) Boc is a receptor for sonic hedgehog in the guidance of commissural axons. Nature 444:369–373.

Ornitz DM, Itoh N (2001) Fibroblast growth factors. Genome Biol. 2:REVIEWS3005.

Pan A, Chang L, Nguyen A, James AW (2013) A review of hedgehog signaling in cranial bone development. Front. Physiol. 4.

Pascuzzi RM, Roos KL, Louis ED, Fine EJ, Ionita CC, Lohr L (2002) The History of the Development of the Cerebellar Examination. Semin Neurol 22:375–384.

Paumet F, Rahimian V, Rothman JE (2004) The specificity of SNARE-dependent fusion is encoded in the SNARE motif. Proc. Natl. Acad. Sci. U.S.A. 101:3376–3380.

Payne HR, Lemmon V (1993) Glial cells of the O-2A lineage bind preferentially to N-cadherin and develop distinct morphologies. Dev. Biol. 159:595–607.

Pekarik V, Bourikas D, Miglino N, Joset P, Preiswerk S, Stoeckli ET (2003) Screening for gene function in chicken embryo using RNAi and electroporation. Nat. Biotechnol 21:93–96.

Perrin FE, Stoeckli ET (2000) Use of lipophilic dyes in studies of axonal pathfinding in vivo. Microsc. Res. Tech. 48:25–31.

Pettem KL, Yokomaku D, Luo L, Linhoff MW, Prasad T, Connor SA, Siddiqui TJ, Kawabe H, Chen F, Zhang L, Rudenko G, Wang YT, Brose N, Craig AM (2013) The Specific α-Neurexin Interactor Calsyntenin-3 Promotes Excitatory and Inhibitory Synapse Development. Neuron 80:113–128.

Pettitt J (2005) The cadherin superfamily. WormBook:1–9.

Pfeffer SR (2001) Rab GTPases: specifying and deciphering organelle identity and function. Trends Cell Biol. 11:487–491.

Pfeffer SR, Dirac-Svejstrup AB, Soldati T (1995) Rab GDP dissociation inhibitor: putting rab GTPases in the right place. J. Biol. Chem. 270:17057–17059.

Pfeffer S, Aivazian D (2004) Targeting Rab GTPases to distinct membrane compartments. Nat. Rev. Mol. Cell Biol. 5:886–896.

Philipp M, Niederkofler V, Debrunner M, Alther T, Kunz B, Stoeckli ET (2012) RabGDI controls axonal midline crossing by regulating Robo1 surface expression. Neural Dev 7:36.

Preuschhof C, Heekeren HR, Li S, Sander T, Lindenberger U, Bäckman L (2010) KIBRA and CLSTN2 polymorphisms exert interactive effects on human episodic memory. Neuropsychologia 48:402–408.

Purvanov V, Koval A, Katanaev VL (2010) A direct and functional interaction between Go and Rab5 during G protein-coupled receptor signaling. Sci Signal 3:ra65.

Raper JA (2000) Semaphorins and their receptors in vertebrates and invertebrates. Curr. Opin. Neurobiol. 10:88–94.

Reddi AH, Reddi A (2009) Bone morphogenetic proteins (BMPs): from morphogens to metabologens. Cytokine Growth Factor Rev. 20:341–342.

Reuss B, Bohlen und Halbach O von (2003) Fibroblast growth factors and their receptors in the central nervous system. Cell and Tissue Research 313:139–157.

Rindler MJ, Xu C, Gumper I, Cen C, Sonderegger P, Neubert TA (2008) Calsyntenins are secretory granule proteins in anterior pituitary gland and pancreatic islet alpha cells. J. Histochem. Cytochem. 56:381–388.

Ringman JM, Schulman H, Becker C, Jones T, Bai Y, Immermann F, Cole G, Sokolow S, Gylys K, Geschwind DH, Cummings JL, Wan HI (2012) Proteomic changes in cerebrospinal fluid of presymptomatic and affected persons carrying familial Alzheimer disease mutations. Arch. Neurol. 69:96–104.

Ringman JM, Schulman H, Becker C, Jones T, Bai Y, Immermann F, Cole G, Sokolow S, Gylys K, Geschwind DH, Cummings JL, Wan HI (2012) Proteomic changes in cerebrospinal fluid of presymptomatic and affected persons carrying familial Alzheimer disease mutations. Arch. Neurol. 69:96–104.

Roy S, Zhang B, Lee VM, Trojanowski JQ (2005) Axonal transport defects: a common theme in neurodegenerative diseases. Acta Neuropathol. 109:5–13.

Ruit KG, Elliott JL, Osborne PA, Yan Q, Snider WD (1992) Selective dependence of mammalian dorsal root ganglion neurons on nerve growth factor during embryonic development. Neuron 8:573–587.

Sabatier C, Plump AS, Le Ma, Brose K, Tamada A, Murakami F, Lee EYP, Tessier-Lavigne M (2004) The divergent Robo family protein rig-1/Robo3 is a negative regulator of slit responsiveness required for midline crossing by commissural axons. Cell 117:157–169.

Sánchez-Camacho C, Bovolenta P (2009) Emerging mechanisms in morphogen-mediated axon guidance. Bioessays 31:1013–1025.

Sasaki T, Kikuchi A, Araki S, Hata Y, Isomura M, Kuroda S, Takai Y (1990) Purification and characterization from bovine brain cytosol of a protein that inhibits the dissociation of GDP from and the subsequent binding of GTP to smg p25A, a ras p21-like GTP-binding protein. J. Biol. Chem. 265:2333–2337.

Schnitzer MJ, Block SM (1997) Kinesin hydrolyses one ATP per 8-nm step. Nature 388:386–390.

Seabra MC, Mules EH, Hume AN (2002) Rab GTPases, intracellular traffic and disease. Trends Mol Med 8:23–30.

Sedlacek Z, Shimeld SM, Münstermann E, Poustka A (1999) The amphioxus rab GDP-dissociation inhibitor (GDI) gene is neural-specific: implications for the evolution of chordate rab GDI genes. Mol. Biol. Evol. 16:1231–1237.

Seeger M, Tear G, Ferres-Marco D, Goodman CS (1993) Mutations affecting growth cone guidance in Drosophila: genes necessary for guidance toward or away from the midline. Neuron 10:409–426.

Serafini T, Kennedy TE, Galko MJ, Mirzayan C, Jessell TM, Tessier-Lavigne M (1994) The netrins define a family of axon outgrowth-promoting proteins homologous to C. elegans UNC-6. Cell 78:409–424.

Shirasaki R, Pfaff SL (2002) Transcriptional Codes and the Control of Neuronal Identity. Annu. Rev. Neurosci. 25:251–281.

Snider WD (1994) Functions of the neurotrophins during nervous system development: what the knockouts are teaching us. Cell 77:627–638.

Sosa LJ, Bergman J, Estrada-Bernal A, Glorioso TJ, Kittelson JM, Pfenninger KH, Xie Z (2013) Amyloid Precursor Protein Is an Autonomous Growth Cone Adhesion Molecule Engaged in Contact Guidance. PLoS ONE 8:e64521.

Sperry RW (1963) Chemoaffinity in the Orderly Growth of Nerve Fiber Patterns and Connections. Proc. Natl. Acad. Sci. U.S.A. 50:703–710.

Stein E, Tessier-Lavigne M (2001) Hierarchical organization of guidance receptors: silencing of netrin attraction by slit through a Robo/DCC receptor complex. Science 291:1928–1938.

Stenmark H (2009) Rab GTPases as coordinators of vesicle traffic. Nat. Rev. Mol. Cell Biol. 10:513–525.

Steuble M, Diep T, Schätzle P, Ludwig A, Tagaya M, Kunz B, Sonderegger P (2012) Calsyntenin-1 shelters APP from proteolytic processing during anterograde axonal transport. Biol Open 1:761–774.

Steuble M, Gerrits B, Ludwig A, Mateos JM, Diep T, Tagaya M, Stephan A, Schätzle P, Kunz B, Streit P, Sonderegger P (2010) Molecular characterization of a trafficking organelle: dissecting the axonal paths of calsyntenin-1 transport vesicles. Proteomics 10:3775–3788.

Stoeckli ET, Landmesser LT (1995) Axonin-1, Nr-CAM, and Ng-CAM play different roles in the in vivo guidance of chick commissural neurons. Neuron 14:1165–1179.

Stoeckli ET, Landmesser LT (1998) Axon guidance at choice points. Curr. Opin. Neurobiol. 8:73–79.

Stoeckli ET, Sonderegger P, Pollerberg GE, Landmesser LT (1997) Interference with axonin-1 and NrCAM interactions unmasks a floor-plate activity inhibitory for commissural axons. Neuron 18:209–221.

Stoeckli ET, Ziegler U, Bleiker AJ, Groscurth P, Sonderegger P (1996) Clustering and functional cooperation of Ng-CAM and axonin-1 in the substratum-contact area of growth cones. Dev. Biol. 177:15–29.

Stoeckli ET (2006) Dissection of Spinal Cords for Analysis of Axonal Pathfinding in dsRNA-Treated Avian Embryos. CSH Protoc 2006.

Stoeckli ET (2012) What does the developing brain tell us about neural diseases? European Journal of Neuroscience 35:1811–1817.

Strobl-Wildemann G, Kalscheuer VM, Hu H, Wrogemann K, Ropers H, Tzschach A (2011) Novel GDI1 mutation in a large family with nonsyndromic X-linked intellectual disability. Am. J. Med. Genet. A 155:3067–3070.

Sundaresan V, Mambetisaeva E, Andrews W, Annan A, Knöll B, Tear G, Bannister L (2004) Dynamic expression patterns of Robo (Robo1 and Robo2) in the developing murine central nervous system. J. Comp. Neurol. 468:467–481.

Tamada A, Kumada T, Zhu Y, Matsumoto T, Hatanaka Y, Muguruma K, Chen Z, Tanabe Y, Torigoe M, Yamauchi K, Oyama H, Nishida K, Murakami F (2008) Crucial roles of Robo proteins in midline crossing of cerebellofugal axons and lack of their up-regulation after midline crossing. Neural Dev 3:29.

Tamagnone L, Artigiani S, Chen H, He Z, Ming GI, Song H, Chedotal A, Winberg ML, Goodman CS, Poo M, Tessier-Lavigne M, Comoglio PM (1999) Plexins are a large family of receptors for transmembrane, secreted, and GPI-anchored semaphorins in vertebrates. Cell 99:71–80.

Tamagnone L, Comoglio PM (2000) Signalling by semaphorin receptors: cell guidance and beyond. Trends Cell Biol. 10:377–383.

Tessier-Lavigne M, Goodman CS (1996) The molecular biology of axon guidance. Science 274:1123–1133.

Trischler M, Stoorvogel W, Ullrich O (1999) Biochemical analysis of distinct Rab5- and Rab11-positive endosomes along the transferrin pathway. J. Cell. Sci. 112 (Pt 24):4773–4783.

Uchida Y, Gomi F, Murayama S, Takahashi H (2013) Calsyntenin-3 C-terminal fragment accumulates in dystrophic neurites surrounding aβ plaques in tg2576 mouse and Alzheimer disease brains: its neurotoxic role in mediating dystrophic neurite formation. Am. J. Pathol. 182:1718–1726.

Uchida Y, Gomi F, Murayama S, Takahashi H (2013) Calsyntenin-3 C-terminal fragment accumulates in dystrophic neurites surrounding aβ plaques in tg2576 mouse and Alzheimer disease brains: its neurotoxic role in mediating dystrophic neurite formation. Am. J. Pathol. 182:1718–1726.

Uchida Y, Nakano S, Gomi F, Takahashi H (2011) Up-regulation of calsyntenin-3 by β-amyloid increases vulnerability of cortical neurons. FEBS Lett. 585:651–656.

Ulloa F, Martí E (2010) Wnt won the war: antagonistic role of Wnt over Shh controls dorso-ventral patterning of the vertebrate neural tube. Dev. Dyn. 239:69–76.

Ullrich O, Reinsch S, Urbé S, Zerial M, Parton RG (1996) Rab11 regulates recycling through the pericentriolar recycling endosome. J. Cell Biol. 135:913–924.

Vagnoni A, Perkinton MS, Gray EH, Francis PT, Noble W, Miller CCJ (2012) Calsyntenin-1 mediates axonal transport of the amyloid precursor protein and regulates Aβ production. Hum. Mol. Genet 21:2845–2854.

Vagnoni A, Rodriguez L, Manser C, Vos KJ de, Miller CCJ (2011) Phosphorylation of kinesin light chain 1 at serine 460 modulates binding and trafficking of calsyntenin-1. J. Cell. Sci. 124:1032–1042.

Vale RD, Reese TS, Sheetz MP (1985) Identification of a novel force-generating protein, kinesin, involved in microtubule-based motility. Cell 42:39–50.

Vale RD, Schnapp BJ, Mitchison T, Steuer E, Reese TS, Sheetz MP (1985) Different axoplasmic proteins generate movement in opposite directions along microtubules in vitro. Cell 43:623–632.

van den Brink DM, Banerji O, Tear G (2013) Commissureless regulation of axon outgrowth across the midline is independent of Rab function. PLoS ONE 8:e64427.

van der Sluijs P, Hull M, Webster P, Mâle P, Goud B, Mellman I (1992) The small GTP-binding protein rab4 controls an early sorting event on the endocytic pathway. Cell 70:729–740.

Vargesson N, Luria V, Messina I, Erskine L, Laufer E (2001) Expression patterns of Slit and Robo family members during vertebrate limb development. Mech. Dev. 106:175–180.

Vogt L, Schrimpf SP, Meskenaite V, Frischknecht R, Kinter J, Leone DP, Ziegler U, Sonderegger P (2001) Calsyntenin-1, a proteolytically processed postsynaptic membrane protein with a cytoplasmic calcium-binding domain. Mol. Cell. Neurosci 17:151–166.

Voogd J, Glickstein M (1998) The anatomy of the cerebellum. Trends Neurosci 21:370–375.

Vult von Steyern F, Martinov V, Rabben I, Njå A, Lapeyrière O de, Lømo T (1999) The homeodomain transcription factors Islet 1 and HB9 are expressed in adult alpha and gamma motoneurons identified by selective retrograde tracing. Eur. J. Neurosci. 11:2093–2102.

Wang VY, Zoghbi HY (2001) Genetic regulation of cerebellar development. Nat Rev Neurosci 2:484–491.

Wilkinson DG (2001) Multiple roles of EPH receptors and ephrins in neural development. Nat. Rev. Neurosci. 2:155–164.

William CM, Tanabe Y, Jessell TM (2003) Regulation of motor neuron subtype identity by repressor activity of Mnx class homeodomain proteins. Development 130:1523–1536.

Wilson NH, Stoeckli ET (2011) Cell type specific, traceable gene silencing for functional gene analysis during vertebrate neural development. Nucleic Acids Res 39:e133.

Wilson NH, Stoeckli ET (2012) In ovo Electroporation of miRNA-based Plasmids in the Developing Neural Tube and Assessment of Phenotypes by DiI Injection in Open-book Preparations. J Vis Exp.

Wilson NH, Stoeckli ET (2013) Sonic hedgehog regulates its own receptor on postcrossing commissural axons in a glypican1-dependent manner. Neuron 79:478–491.

Wolf AM, Lyuksyutova AI, Fenstermaker AG, Shafer B, Lo CG, Zou Y (2008) Phosphatidylinositol-3-kinase-atypical protein kinase C signaling is required for Wnt attraction and anterior-posterior axon guidance. J. Neurosci. 28:3456–3467.

Wolpert L (1989) Positional information revisited. Development 107:3–12.

Wolpert L (2004) Much more from the chicken's egg than breakfast--a wonderful model system. Mech. Dev. 121:1015–1017.

Yam PT, Kent CB, Morin S, Farmer WT, Alchini R, Lepelletier L, Colman DR, Tessier-Lavigne M, Fournier AE, Charron F (2012) 14-3-3 proteins regulate a cell-intrinsic switch from sonic hedgehog-mediated commissural axon attraction to repulsion after midline crossing. Neuron 76:735–749.

Yin GN, Lee HW, Cho J, Suk K (2009) Neuronal pentraxin receptor in cerebrospinal fluid as a potential biomarker for neurodegenerative diseases. Brain Res. 1265:158–170.

Yuan W, Zhou L, Chen JH, Wu JY, Rao Y, Ornitz DM (1999) The mouse SLIT family: secreted ligands for ROBO expressed in patterns that suggest a role in morphogenesis and axon guidance. Dev. Biol. 212:290–306.

Zechel S, Werner S, Unsicker K, Bohlen und Halbach O von (2010) Expression and Functions of Fibroblast Growth Factor 2 (FGF-2) in Hippocampal Formation. The Neuroscientist 16:357–373.

Zerial M, McBride H (2001) Rab proteins as membrane organizers. Nat. Rev. Mol. Cell Biol. 2:107–117.

Zhang H, Kranzler HR, Poling J, Gruen JR, Gelernter J (2009) Cognitive flexibility is associated with KIBRA variant and modulated by recent tobacco use. Neuropsychopharmacology 34:2508–2516.

Zhou Y, Gunput RF, Pasterkamp RJ (2008) Semaphorin signaling: progress made and promises ahead. Trends Biochem. Sci. 33:161–170.

Zhou Z, Xie J, Lee D, Liu Y, Jung J, Zhou L, Xiong S, Mei L, Xiong W (2010) Neogenin regulation of BMP-induced canonical Smad signaling and endochondral bone formation. Dev. Cell 19:90–102.

8. Appendix

Statistical quantification of Figure 1 and Suppl. Figure 1, manuscript 4.2.

dependent variable		p-value
ctrl	miLuc	.331
	miCst1	**.019**
	dsCst1	**.006**
miLuc	ctrl	.331
	miCst1	**.003**
	dsCst1	**.003**
miCst1	ctrl	**.019**
	miLuc	**.003**
	dsCst1	1.000
dsCst1	ctrl	**.006**
	miLuc	**.003**
	miCst1	1.000

Post-hoc test Figure 1.

dependent variable		p-value
ctrl	GFP	.878
	dsCst1	**.042**
GFP	ctrl	.878
	dsCst1	**.035**
dsCst1	ctrl	**.042**
	GFP	**.035**

Post-hoc test Suppl. Figure 1.

Statistical quantification of Figure 3, manuscript 4.2.

dependent variable		p-value
miRobo1	miRabGDI	.399
	miC1hypo	.062
	miR1hypo	**.013**
	miRGhypo	**.000**
	miLuc	**.004**
	ctrl	**.001**
	miCst2	**.000**
miRabGDI	miRobo1	.399
	miC1hypo	.532
	miR1hypo	.157
	miRGhypo	**.019**
	miLuc	**.039**
	ctrl	.214
	miCst2	**.003**

dependent variable		p-value
miC1hypo	miRobo1	.062
	miRabGDI	.532
	miR1hypo	1.000
	miRGhypo	1.000
	miLuc	.998
	ctrl	1.000
	miCst2	1.000
miR1hypo	miRobo1	**.013**
	miRabGDI	.157
	miC1hypo	1.000
	miRGhypo	1.000
	miLuc	1.000
	ctrl	1.000
	miCst2	1.000

dependent variable		p-value
miRGhypo	miRobo1	**.000**
	miRabGDI	**.019**
	miC1hypo	1.000
	miR1hypo	1.000
	miLuc	1.000
	ctrl	.999
	miCst2	1.000
miLuc	miRobo1	**.004**
	miRabGDI	**.039**
	miC1hypo	.998
	miR1hypo	1.000
	miRGhypo	1.000
	ctrl	.847
	miCst2	1.000

dependent variable		p-value
ctrl	miRobo1	**.001**
	miRabGDI	.214
	miC1hypo	1.000
	miR1hypo	1.000
	miRGhypo	.999
	miLuc	.847
	miCst2	.783
miCst2	miRobo1	**.000**
	miRabGDI	**.003**
	miC1hypo	1.000
	miR1hypo	1.000
	miRGhypo	1.000
	miLuc	1.000
	ctrl	.783

Post-hoc tests Figure 3.

Statistical quantification of Figure 4, manuscript 4.2.

	dependent variable	p-value
miLuc	miC1+miR1+miRG	**.035**
	miC1+miRG	**.011**
	miC1+miR1_E2	**.017**
	miC1+miR1_E3	**.002**
miC1+miR1+miRG	miLuc	**.035**
	miC1+miRG	.554
	miC1+miR1_E2	.763
	miC1+miR1_E3	.067

	dependent variable	p-value
miC1+miRG	miLuc	**.011**
	miC1+miR1+miRG	.554
	miC1+miR1_E2	1.000
	miC1+miR1_E3	.967
miC1+miR1_E2	miLuc	**.017**
	miC1+miR1+miRG	.763
	miC1+miRG	1.000
	miC1+miR1_E3	.766

	dependent variable	p-value
miC1+miR1_E3	miLuc	**.002**
	miC1+miR1+miRG	.067
	miC1+miRG	.967
	miC1+miR1_E2	.766

Post-hoc tests Figure 4.

Statistical quantification of Figure 6, manuscript 4.2.

	dependent variable	p-value
miFzd3	miF3hyp	**.000**
	miLuc	**.044**
	ctrl	**.001**
	miC1+miF3	.999
	miCst2	**.026**
	miRG+miF3	**.006**
miF3hyp	miFzd3	**.000**
	miLuc	1.000
	ctrl	1.000
	miC1+miF3	**.006**
	miCst2	1.000
	miRG+miF3	1.000

	dependent variable	p-value
miLuc	miFzd3	**.044**
	miF3hyp	1.000
	ctrl	.755
	miC1+miF3	**.005**
	miCst2	1.000
	miRG+miF3	1.000
ctrl	miFzd3	**.001**
	miF3hyp	1.000
	miLuc	.755
	miC1+miF3	**.009**
	miCst2	.682
	miRG+miF3	.159

	dependent variable	p-value
miC1+miF3	miFzd3	.999
	miF3hyp	**.006**
	miLuc	**.005**
	ctrl	**.009**
	miCst2	**.000**
	miRG+miF3	**.000**
miCst2	miFzd3	**.026**
	miF3hyp	1.000
	miLuc	1.000
	ctrl	.682
	miC1+miF3	**.000**
	miRG+miF3	1.000

	dependent variable	p-value
miRG+miF3	miFzd3	**.006**
	miF3hyp	1.000
	miLuc	1.000
	ctrl	.159
	miC1+miF3	**.000**
	miCst2	1.000

Post-hoc tests Figure 6.

Statistical quantification of Figure 7, manuscript 4.2.

	dependent variable	p-value
miLuc	ctrl	.488
	miCst2	1.000
	miRG+miF3	1.000
	miR1+miF3	.570
ctrl	miLuc	.488
	miCst2	.420
	miRG+miF3	.079
	miR1+miF3	1.000

	dependent variable	p-value
miRG+miF3	miLuc	1.000
	ctrl	.079
	miCst2	1.000
	miR1+miF3	.060
miR1+miF3	miLuc	.570
	ctrl	1.000
	miCst2	.479
	miRG+miF3	.060

	dependent variable	p-value
miCst2	miLuc	1.000
	ctrl	.420
	miRG+miF3	1.000
	miR1+miF3	.479

Post-hoc tests Figure 7.

P-values of the growth-cone colocalization assays

dependent variable		p-val.	dependent variable		p-val.	dependent variable		p-val.	dependent variable		p-val.
Cst1+Robo1	Robo1+Rab11	1.000	pos ctrl	Cst1+Robo1	.000	RabGDI+Rab11	Cst1+Robo1	1.000	Cst1+SynCAM2	Cst1+Robo1	.000
	RabGDI+Robo1	.978		Robo1+Rab11	.000		Robo1+Rab11	1.000		Robo1+Rab11	.000
	Cst1+RabGDI	.717		RabGDI+Robo1	.000		RabGDI+Robo1	.999		RabGDI+Robo1	.001
	RabGDI+Rab11	1.000		Cst1+RabGDI	.000		Cst1+RabGDI	.902		Cst1+RabGDI	.002
	Cst1+Rab11	1.000		RabGDI+Rab11	.000		Cst1+Rab11	1.000		RabGDI+Rab11	.000
	Cst1+Fzd3	.726		Cst1+Rab11	.000		Cst1+Fzd3	.214		Cst1+Rab11	.000
	pos ctrl	.000		Cst1+Fzd3	.000		pos ctrl	.000		Cst1+Fzd3	.000
	neg ctrl	.000		neg ctrl	.000		neg ctrl	.000		pos ctrl	.000
	R1+F3	.000		R1+F3	.000		R1+F3	.000		neg ctrl	.000
	C1+S1	.000		C1+S1	.000		C1+S1	.000		R1+F3	.803
	C1+S2	.000		C1+S2	.000		C1+S2	.000		C1+S1	1.000
	C1+S3	.000		C1+S3	.000		C1+S3	.000		C1+S3	.996
	C1+PA2	.000		C1+PA2	.000		C1+PA2	.000		C1+PA2	.996
Robo1+Rab11	Cst1+Robo1	1.000	neg ctrl	Cst1+Robo1	.000	Cst1+Rab11	Cst1+Robo1	1.000	Cst1+SynCAM3	Cst1+Robo1	.000
	RabGDI+Robo1	1.000		Robo1+Rab11	.000		Robo1+Rab11	.999		Robo1+Rab11	.000
	Cst1+RabGDI	.992		RabGDI+Robo1	.000		RabGDI+Robo1	.934		RabGDI+Robo1	.000
	RabGDI+Rab11	1.000		Cst1+RabGDI	.000		Cst1+RabGDI	.555		Cst1+RabGDI	.000
	Cst1+Rab11	.999		RabGDI+Rab11	.000		RabGDI+Rab11	1.000		RabGDI+Rab11	.000
	Cst1+Fzd3	.104		Cst1+Rab11	.000		Cst1+Fzd3	.876		Cst1+Rab11	.000
	pos ctrl	.000		Cst1+Fzd3	.000		pos ctrl	.000		Cst1+Fzd3	.000
	neg ctrl	.000		pos ctrl	.000		neg ctrl	.000		pos ctrl	.000
	R1+F3	.003		R1+F3	.000		R1+F3	.000		neg ctrl	.000
	C1+S1	.000		C1+S1	.000		C1+S1	.000		R1+F3	.082
	C1+S2	.000		C1+S2	.000		C1+S2	.000		C1+S1	.996
	C1+S3	.000		C1+S3	.000		C1+S3	.000		C1+S2	.996
	C1+PA2	.002		C1+PA2	.000		C1+PA2	.000		C1+PA2	.524
RabGDI+Robo1	Cst1+Robo1	.978	Robo1+Fst3	Cst1+Robo1	.000	Cst1+Fzd3	Cst1+Robo1	.726	Cst1+PlexinA2	Cst1+Robo1	.000
	Robo1+Rab11	1.000		Robo1+Rab11	.003		Robo1+Rab11	.104		Robo1+Rab11	.002
	Cst1+RabGDI	1.000		RabGDI+Robo1	.118		RabGDI+Robo1	.030		RabGDI+Robo1	.057
	RabGDI+Rab11	.999		Cst1+RabGDI	.220		Cst1+RabGDI	.001		Cst1+RabGDI	.111
	Cst1+Rab11	.934		RabGDI+Rab11	.000		RabGDI+Rab11	.214		RabGDI+Rab11	.000
	Cst1+Fzd3	.030		Cst1+Rab11	.000		Cst1+Rab11	.876		Cst1+Rab11	.000
	pos ctrl	.000		Cst1+Fzd3	.000		pos ctrl	.000		Cst1+Fzd3	.000
	neg ctrl	.000		pos ctrl	.000		neg ctrl	.000		pos ctrl	.000
	R1+F3	.118		neg ctrl	.000		R1+F3	.000		neg ctrl	.000
	C1+S1	.001		C1+S1	.820		C1+S1	.000		R1+F3	1.000
	C1+S2	.001		C1+S2	.803		C1+S2	.000		C1+S1	.997
	C1+S3	.000		C1+S3	.082		C1+S3	.000		C1+S2	.996
	C1+PA2	.057		C1+PA2	1.000		C1+PA2	.000		C1+S3	.524
Cst1+RabGDI	Cst1+Robo1	.717	Cst1+SynCAM1	Cst1+Robo1	.000						
	Robo1+Rab11	.992		Robo1+Rab11	.000						
	RabGDI+Robo1	1.000		RabGDI+Robo1	.001						
	RabGDI+Rab11	.902		Cst1+RabGDI	.002						
	Cst1+Rab11	.555		RabGDI+Rab11	.000						
	Cst1+Fzd3	.001		Cst1+Rab11	.000						
	pos ctrl	.000		Cst1+Fzd3	.000						
	neg ctrl	.000		pos ctrl	.000						
	R1+F3	.220		neg ctrl	.000						
	C1+S1	.002		R1+F3	.820						
	C1+S2	.002		C1+S2	1.000						
	C1+S3	.000		C1+S3	.996						
	C1+PA2	.111		C1+PA2	.997						

Post-hoc tests of the growth-cone colocalization assays (see manuscript 4.2.).

Statistical quantification of Figure 26

Quantification using the Fisher's exact test, p-values

DRGs:

miC1 to miC2 **0.44535**	miC1 to miC3 **0.76483**	miC1 to miLuc **0.00646**	miC1 to ctrl **0.00024**
	miC2 to miC3 **0.86761**	miC2 to miLuc **0.04781**	miC2 to ctrl **0.01249**
		miC3 to mi Luc **0.04357**	miC3 to ctrl **0.01028**
			miLuc to ctrl **0.04943**

Epaxial nerves:

miC1 to miC2 **0.00019**	miC1 to miC3 **0.15468**	miC1 to miLuc **0.00015**	miC1 to ctrl **0.00011**
	miC2 to miC3 **0.03761**	miC2 to miLuc **0.31754**	miC2 to ctrl **0.26481**
		miC3 to mi Luc **0.004731**	miC3 to ctrl **0.00773**
miC1=miCst1			miLuc to ctrl **0.79133**
miC2=miCst2			
miC3=miCst3			

Statistical quantification of Figure 27, O

	dependent variable		p-value	dependent variable		p-value
Tukey-HSD	miCst1	miCst2	.352	miLuc	miCst1	.080
		miCst3	.675		miCst2	.632
		miLuc	.080		miCst3	.293
		ctrl	**.000**		ctrl	**.001**
	miCst2	miCst1	.352	ctrl	miCst1	**.000**
		miCst3	.986		miCst2	**.000**
		miLuc	.632		miCst3	**.000**
		ctrl	**.000**		miLuc	**.001**
	miCst3	miCst1	.675			
		miCst2	.986			
		miLuc	.293			
		ctrl	**.000**			

Statistical quantification of Figure 28

normal injections sites			contralateral caudal turns		
dependent variable		p-value	dependent variable		p-value
ctrl	miLuc	.348	ctrl	miLuc	1.000
	miCst1	**.047**		miCst1	**.000**
	miCst2	.994		miCst2	1.000
	miCst3	.822		miCst3	1.000
miLuc	ctrl	.777	miLuc	ctrl	1.000
	miCst1	**.035**		miCst1	**.001**
	miCst2	.997		miCst2	1.000
	miCst3	.096		miCst3	1.000
miCst1	ctrl	**.047**	miCst1	ctrl	**.000**
	miLuc	**.035**		miLuc	**.001**
	miCst2	.094		miCst2	**.000**
	miCst3	.981		miCst3	**.001**
miCst2	ctrl	.994	miCst2	ctrl	1.000
	miLuc	.997		miLuc	1.000
	miCst1	.094		miCst1	**.000**
	miCst3	.257		miCst3	1.000
miCst3	ctrl	.822	miCst3	ctrl	1.000
	miLuc	.096		miLuc	1.000
	miCst1	.981		miCst1	**.001**
	miCst2	.257		miCst2	1.000

Post-hoc tests Figure 28.

Solutions and reagents

In situ hybridization

10% PFA (ca. 100 ml)	10 g Paraformaldehyde 100 ml DEPC-treated PBS 100 µl 1 M NaOH Heated at 65°C till completely dissolved, filtrated through 0.22 µm filter and aliquoted, stored at -20°C
4% PFA (200 ml)	80 ml 10% PFA Adjusted to a volume of 200 ml with DEPC-treated PBS
20x SSC (1 l)	175 g NaCl 88.3 g Tri-sodium citrate dihydrate pH adjusted to pH 7.0, adjusted to a volume of 1 l, 1 ml DEPC added, stirred overnight, autoclaved
20x PBS (1 l)	160 g NaCl 4 g KCl

	28.8 g Na_2HPO_4 * $2H_2O$ 4 g KH_2PO_4 adjusted to a volume of 1 l, 1 ml DEPC added, stirred overnight, then autoclaved
10x Detection buffer (1 l)	87.7 g NaCl 121.1 g Tris-base pH adjusted to 7.5, adjusted to a volume of 1 l, autoclaved
1x Blocking buffer	3% milkpowder in 1x detection buffer
10x AP buffer (1 l)	58.4 g NaCl 121.1 g Tris-base pH adjusted to 9.5, adjusted to a volume of 1 l, autoclaved
10x TE buffer (1 l)	12.1 g Tris-base 3.72 g EDTA (pH 8.0) Adjusted to a volume of 1 l, autoclaved
NBT (MW: 818 g)	75 mg/ml in dimethylformamide
BCIP (MW: 433.64 g)	50 mg/ml in dimethylformamide
Levamisole (MW: 240 g)	24 mg/ml in AP buffer
Development solution (10 ml)	100 µl Levamisole 45 µl NBT (blue) 35 µl BCIP Adjusted to a volume of 10 ml with AP buffer + 1 M $MgCl_2$
50x Denhardt solution (100 ml)	1 g Ficoll 1 g Polyvinylpyrrolidone 1 g BSA Solved in 100 ml DEPC-treated H_2O, heated for solving, filtrated trough 0.45 µm filter and aliquoted
(Pre)Hybridization buffer (15 ml)	7.5 ml Formamide 3.75 ml 20x SSC 1.5 ml 50x Denhardt's solution 375 µl 10 mg/ml ytRNA (yeast total RNA) 375 µl 20 mg/ml hsDNA (herring sperm DNA) Adjusted to a volume of 15 ml with DEPC-treated H_2O

Explants and dissociated neurons:

DRG medium	500 µl Albumax (4 mg/ml), Invitrogen 250 µl N3 (1x, see below) 50 µl NGF (20 ng/ml), Invitrogen 24.2 ml MEM + Glutamax, Invitrogen

Commissural neuron medium	400 µl Albumax (4 mg/ml), Invitrogen 200 µl N3 (1x, see below) 200 µl Pyruvate (1mM), Sigma 19.2 ml MEM + Glutamax, Invitrogen
N3 (100x)	1 ml transferrin (100 mg/ml), Gibco 1 ml Albumax (10 mg/ml), Gibco 400 µl putrescine (500 mM), Sigma 1 ml Na-Selenit (60 µM), Sigma 100 µl triiodothyronine (200 µg/ml), Sigma 400 µl insulin (25 mg/ml), Sigma 100 µl progesterone (400 µM), Sigma 100 µl corticosteron (2 mg/ml), RdH 5.9 ml PBS

Whole-mount staining

0.2 M sodium phosphate buffer (1 l)	5.52 g NaH_2PO_4 * H_2O 28.48 g Na_2HPO_4 * $2H_2O$ pH adjusted to 7.4, adjusted to a volume of 1 l with ddH_2O, autoclaved
20 mM lysine in 0.1 M sodium phosphate buffer	2.92 g L-lysine dissolved in 500 ml 0.2 M sodium phosphate buffer (pH 7.4), adjusted to 1 l with ddH_2O

Solutions for Minipreparation of plasmid DNA

Solution 1	50 mM Glucose 10 mM Ethylenediaminetetraacetic (EDTA) 25 mM Tris-HCl (pH=8.0) 100 µg/ml RNAseA (Roche)
Solution 2	1 ml 2 M Sodium hydroxide (NaOH) 1 ml Sodium dodecyl sulfate (SDS) 8 ml ddH2O
Solution 3	60 ml 5 M Potassium acetate 11.5 ml Glacial acetic acid 28.5 ml H2O
RNaseA	10 mg/ml (10 mM Tris pH=7.5, 15 mM NaCl)

9. Acknowledgments

I am very grateful to Prof. Dr. Esther T. Stoeckli, who gave me the opportunity to do my PhD in her lab. Her experience, enthusiasm and great support were crucial for the completion of my dissertation.

I also want to thank my thesis committee members Prof. Dr. Jean-Marc Fritschy and Prof. Dr. Dieter Zimmermann for giving me helpful input and advice.

Special thanks also go to Dr. Nicole Wilson, Dr. Vera Niederkofler and Dr. Beat Kunz. Their instructions and help concerning cell culture and cloning were indispensable for my work. Thanks also to Dr. Tu-My Diep for providing gene constructs, and to all former and present Stoeckli lab members for the great atmosphere in and around the lab.

I am also very grateful for the company and support of my fiancée Tanja Gurtner, my parents, family and friends. Thanks especially to my sister Esther Brown for proofreading. Without their support and patience I would not have been able to finish my studies.

10. Curriculum vitae

Name	ALTHER
Surname	Tobias Andreas
Date of birth	15.09.1985
Hometown	St.Gallen SG

Education

03.2010 – 02.2014	**Institute of Molecular Life Sciences, University of Zurich** PhD thesis *„Calsyntenin1-Dependent Vesicular Trafficking is an Important Regulator of Axonal Behavior at Choice Points"* under supervision of Prof. Dr. Esther Stoeckli
08.2008 – 01.2010	**Institute of Zoology, University of Zurich** Master of Science in Biology, Master thesis *„The Role of Calsyntenin in Neural Circuit Formation"* under supervision of Prof. Dr. Esther Stoeckli
10.2005 – 08.2008	**University of Zurich** Bachelor of Science in Biology (major subject biology, minor subject biochemistry)
08.2001-07.2005	**Kantonsschule Wattwil SG**, Matura Typus B

Publications

● Melanie Philipp, Vera Niederkofler, Marc Debrunner, **Tobias Alther**, Beat Kunz, and Esther T. Stoeckli (2012). *RabGDI controls axonal midline crossing by regulating Robo1 surface expression*. Neural Dev. 2012 Nov 9;7:36. doi: 10.1186/1749-8104-7-36.

● **Tobias Alther**, Diego Geering and Esther T. Stoeckli (submitted). *Calsyntenins and APP are Expressed in a Dynamic and Similar Manner in the Chicken Embryo*.

● **Tobias Alther**, Elena Domanitskaya and Esther T. Stoeckli (submitted). *Calsyntenin1-Mediated Trafficking of Axon Guidance Receptors Regulates the Switch in Axonal Responsiveness at Choice Points*.

Abstracts

● *Downregulation of Calsyntenin Leads to Axonal Pathfinding Errors in Chicken Embryo*, ZNZ Symposium 2009, Zurich.

● *Calsyntenin-Mediated Vesicle Trafficking is Required for Neural Circuit Formation*, NCCR Meeting 2011, Ittingen.

● *Calsyntenin-Mediated Trafficking: Distribution of Vesicles for Proper Neural Circuit Formation,* ZNZ Symposium 2012, Zurich.

● *Selective trafficking of guidance receptors as a mechanism to change a growth cone`s responsiveness at intermediate targets,* Wiring the Brain 2013, Cold Spring Harbor, New York.

● *Calsyntenin1-Mediated Trafficking of Axon Guidance Receptors Regulates the Switch in Axonal Responsiveness at Choice Points,* SSN Meeting 2014, Berne.

11. Plagiarism disclaimer

I hereby confirm that this dissertation is entirely my own work and that all sources used have been correctly identified within the text and the bibliography.

January 2014 Tobias Alther